DEVELOPMENT OF A COLUMN MODEL TO PREDICT

MULTICOMPONENT MIXED BED ION

EXCHANGE BREAKTHROUGH

By

RAMESH BULUSU

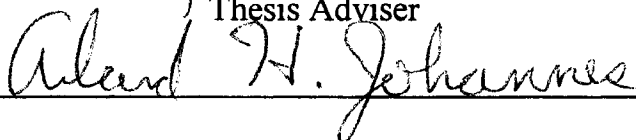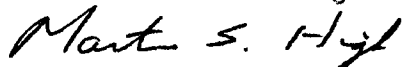Bachelor of Technology

Andhra University

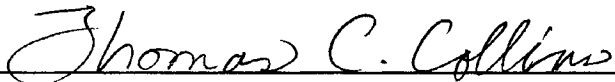Visakhapatnam, AP, India

1992

Submitted to the Faculty of the
Graduate College of the
Oklahoma State University
in partial fulfillment of
the requirements for
the Degree of
MASTER OF SCIENCE
December, 1994

DEVELOPMENT OF A COLUMN MODEL TO PREDICT

MULTICOMPONENT MIXED BED ION

EXCHANGE BREAKTHROUGH

Thesis Approved:

_____
Thesis Adviser

_____

_____

_____
Dean of the Graduate College

PREFACE

Multicomponent mixed bed ion exchange simulations are studied in this work. A general column model is developed which can predict column effluent for a multicomponent system of ions with arbitrary valences. The model is tested for a five component system of ions and for a wide range of conditions. A carbonate equilibrium subroutine is developed to include carbonic species in the system of ions.

I wish to express my deepest appreciation to my major advisor, Dr. Gary L. Foutch, for his guidance, inspiration, patience and invaluable helpfulness throughout my masters program. Grateful acknowledgment is also extended to Dr. Arland H. Johannes and Dr. Martin High for serving on my committee and for their helpful suggestions and technical assistance.

Special gratitude and appreciation are expressed to my parents and brothers for their encouragement, understanding and sacrifice. Particular thanks go to Vikram Chowdiah and Sudhir Pondugula for their help and suggestions throughout my study.

Financial assistance from School of Chemical Engineering at Oklahoma State University for completion of this study, is gratefully appreciated. I would like to express my special thanks to all my friends for their encouragement in completing this manuscript.

TABLE OF CONTENTS

LIST OF TABLES

LIST OF FIGURES

Figure   Page

NOMENCLATURE

A_i parameter of ion i

a_s interfacial area (L^2/L^3)

B_i parameter of ion i

C_i concentration of species i (meq/L^3)

C_i^* concentration of species i at the surface of the resin (meq/L^3)

C_i^* concentration of species i in the bulk solution (meq/L^3)

C_T total equivalent concentration (meq/L^3)

C_{Tc} total carbonic species concentration (meq/L^3)

d_p particle diameter (L)

D_i self-diffusivity of species i (L^2/T)

D_e effective diffusivity (L^2/T)

F Faradya's constant (coulombs/mole)

FR volumetric flowrate (L^3/T)

FAR fraction of anionic resin

FCR fraction of cationic resin

J_i flux of species i in the film $(meq/T.L^2)$

K representative mass transfer coefficient (L/T)

K_A^B resin selectivity coefficient for ion B in solution compared to A in the resin

K_w water dissociation equilibrium constant

K_1 first dissociation constant of CO_2

K_2 second dissociation constant of CO_2

m	number of coions
N_i	$\equiv -Z_i/Z_Y$ relative valence
n	number of counterions
P	exponent
q_i	concentration of species i in the resin (meq/L^3)
Q	capacity of the resin (meq/L^3)
R	universal gas constant $(atm.cm^3/mol.K)$
R_e	particle Reynolds number
Sc	Schmidt number
T	temperature $(°C)$
t	time (T)
u_s	superficial velocity in axial flow packed bed (L/T)
V	volume of the packed resin (L^3)
X_i	concentration fraction in liquid phase
Y_i	concentration fraction in the resin phase
Z_i	charge on species i
Z_j	charge on species j
Z_Y	mean coion valence

Greek Letters

δ	film thickness (L)
ε	bed void fraction
τ	dimensionless time coordinate
ξ	dimensionless space coordinate
ϕ	electric potential (ergs/coulomb)
μ	solution viscosity (cp)
ω	+1 for cations; -1 for anions
ρ	solution density (M/L^3)

λ ion conductivity (S.m/mole)

Suprescripts

bar   referes to resin phase

*   interfacial equilibrium condition

f   column feed condition

o   bulk phase condition

0   previous time value

Subscripts

A   ion leaving the resin phase

B   ion entering the resin phase

c   reference ion

i   counterion species

j   coion species

CHAPTER I

INTRODUCTION

Ion exchange is a branch of separation science concerned with the partition of charged species between different regions of an overall system, usually being separate phases. For the simplest case, ion exchange is a stoichiometric reaction that redistributes charged species between two phases, while the exchange capacity and overall electroneutrality of each phase is maintained constant. The industrial applications of ion exchange are widespread, ranging from water purification, bioseparations, and the treatment of valuable metals such as gold and uranium. The most common and largest application is in the purification of water. Although ion exchange was developed eighty years ago, improvements in products, techniques, economics and new applications are still continuing. The drive for these improvements is special needs such as ultrapure water, reduction of wastes and elimination of process problems.

Recent developments in water treatment by ion exchange usually followed evolutionary steps. Innovations in the ion exchangers and in process techniques are the result of the demand for purer water. To meet this need, limitations resulting from the following had to be reduced (Calmon, 1986).

1. The ion exchangers: Improvements are needed in selectivity, kinetics, physical stability, uniformity in bead sizes and reduction of organic fouling tendencies of anion and cation exchangers.

2.   Process techniques: Improvements in mixed bed separation, counter-flow operation, regenerant waste volume reduction, cleaning of fouled resins and better analytical procedures for trace of species are desired.

Mechanism of Ion Exchange

Ion exchange is stoichiometric and any ions which leave the resin are replaced by a charge equivalent amount of counter ions. The overall mechanism of ion exchange is essentially diffusion to the site followed by ion exchange. The rate process consists of the following steps:

1.   Diffusion of the counter ions from the bulk solution through a film outside the resin,

2.   Diffusion of the counter ions within the resin phase,

3.   Reaction between the counter ions and the exchange site,

4.   Diffusion of the displaced ions out of the resin, and

5.   Diffusion of the exchanged ions from the resin surface through the film into the bulk solution.

The slowest of these steps is the rate determining step. Helfferich (1962) discusses quantitative criteria for predicting the rate determining step.

Mixed Bed Ion Exchange

Mixed bed ion exchange (MBIE) is an intimate mixture of cationic and anionic resins in the same column, used to deionize a contaminated liquid stream. MBIE is used particularly in ultrapure water production. The idea of MBIE was conceived by Kunin (1951). In this, ion exchange is accompanied by a neutralization reaction, thereby reducing the bulk phase concentrations of hydrogen and hydroxide ions. MBIE is the

traditional method of eliminating the final traces of ionic material from ultrapure water. Typically, the resistivity of the output from a MBIE system ranges from 16 to 18.3 megaohms.

There is more than one cyclic operational choice for MBIE units. The hydrogen cycle (HOH cycle) uses cationic resin in the hydrogen form and anionic resin in the hydroxyl form to allow the water equilibrium reaction to consume excess hydrogen and hydroxide. Another choice, the ammonia (or amine) cycle involves the addition of ammonia to the feed water to increase the pH of the water for corrosion control. Sometimes the ammonia cycle can be operated with cationic resin in the ammonia form. Both the above cycles are used industrially. The purest form of water is produced in the HOH cycle. However, in some cases amine cycles are economical to operate and the pH additives are recycled rather than wastefully removed.

The Power generation and semi-conductor manufacturing are two industries where MBIE is of major importance. The Electrical Power Research Institute (EPRI) sets guidelines for ionic contaminants in boiler feed water for electric power plants. The American Society of Testing of Materials (ASTM) and Semi-conductor Manufacturers Institute (SEMI) set standards for semi-conductor grade ultrapure water. These guidelines become more stringent with improving technology and demands for greater quality.

Mixed Bed Ion Exchange Modeling

Haub and Foutch (1986 a, b) were the first to model mixed bed ion exchange systems at ultra low concentrations. Their model was for a hydrogen cycle MBIE with only two ions, sodium and chloride, considered for exchange with hydrogen and hydroxide respectively. The temperature was fixed at 25^oC. They were the first to accommodate water dissociation at these low concentrations, which allows water

3

equilibrium rather than assuming an irreversible reaction. A major improvement of this model is the separate material balance considerations for each resin. Previous work treated the mixture of cationic and anionic resin as a single salt removing substance. Divekar and Foutch (1987) extended this model to incorporate temperature effects. This required expressions as functions of temperature for all of the physical properties used within the model.

Zecchini (1990) extended the above model to handle a ternary system of ions. But this model could address only monovalent ions. Pondugula (1994) further extended this model to incorporate divalent ions. This model could predict the column effluent concentrations for a variety of industrial cases like bed heels and bed cleaning. The development of a model that can consider concentrations in this ultra low range for arbitrary number of species will allow for improvement in operation and design of MBIE units. It is the objective of this work to develop such a general column model.

Objective

The existing models for prediction of effluent concentrations from MBIE columns are confined to binary or ternary systems. These system of ions are restricted to univalent counter ions (Zecchini, 1990) or contain just one divalent ion (S.K. Pondugula, 1994). But in reality, any system of ions are multicomponent, with arbitrary valences. The main objective of this thesis is to develop a general MBIE column model which can handle multicomponent system of ions with arbitrary valences.

The model is tested for a ternary system of cations and a five component system of anions. The effect of various plant operating conditions on the effluent concentrations, are discussed in the following chapters. Actual plant input is supplied by Pennsylvania Power & Light. The results are analyzed and compared with plant experience.

4

CHAPTER II

LITERATURE REVIEW

An extensive literature review of ion exchange and mixed bed ion exchange

modeling has been carried out by Haub (1984), Yoon (1990) and Zecchini (1990). This

review concentrates on the objectives of this thesis.

Ion Exchange Equilibria

One of the controlling factors governing the use of ion-exchange separations is

the equilibrium distribution of ions between the resin and solution phases. Several

investigators have shown that for an ion exchange reaction at equilibrium, the distribution

of counter ions between the two phases is not equal. This gives rise to the concept of

selectivity. The experimentally observed selectivity shown by an exchanger is

represented by the value of the separation factor, α_b^a, which is defined as follows:

$$\alpha_B^A = \frac{\overline{C}_A C_B}{C_A \overline{C}_B}$$

(2-1)

A value of α_b^a greater than unity means that ion A is preferred by the exchanger. In

theoretical studies, selectivity is usually defined in terms of selectivity coefficient, which

is the mass action relationship for the reaction:

$$K_B^A = \frac{\overline{C_A^{Z_B}} C_B^{Z_A}}{\overline{C_B^{Z_A}} C_A^{Z_B}}$$

(2-2)

It is important to distinguish between the separation factor and selectivity coefficient for heterovalent ion exchange. Selectivity depends on the nature of the counterions, the nature of the fixed charges in the matrix, the degree of ion exchanger saturation, the total solution concentration, and external forces such as temperature and pressure. The ion exchanger prefers counterions that have the higher valence, smaller equivalent volume, greater polarity, and stronger association with fixed ionic groups in the matrix (Helfferich, 1962).

The following observations, made by Kunin (1960) are helpful in understanding ion exchange equilibria.

1.   At low concentrations and ordinary temperatures, the selectivity increases with increasing valence of the exchanging species:

$$Na^+ < Ca^{+2} < Al^{+3} < Th^{+4}$$
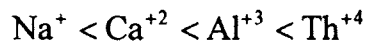
2.   At low concentrations, ordinary temperatures, and constant valence, selectivity increases with increasing atomic number of the exchanging species:

$$Li < Na < K < Rb < Cs; \quad Mg < Ca < Sr < Ba$$
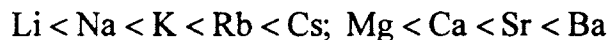
3.   Organic ions of high molecular weight and metallic anionic complexes exhibit high exchange potentials.

4.   Ions with higher activity coefficients have greater exchange potential.

5.   Decrease in the degree of crosslinking makes the exchange equilibrium constant approach unity.

Nearly all practical and important ion exchange processes deal with more than two exchangeable ions. However, most of our knowledge of the behavior of ion-exchange comes from the study of binary systems. Few systematic studies have been

6

done on multicomponent ion exchange because of the complexity of both experimental and theoretical multi-ionic systems.

Multicomponent Ion Exchange Equilibria

According to a study by De Lucas et al. (1992), methods for the prediction of multicomponent ion-exchange equilibria are classified into four main groups.

1. Models assuming ideality of the exchange equilibria (i.e., ideal solutions with negligible effect due to resin swelling and hydration) with a constant separation factor and activity coefficients of all components in the solid phase equal to unity.

2. Models assuming regular systems with a linear transformation between the separation factor and the composition in the solid phase.

3. Treating ion exchange as a phase equilibrium using standard procedures developed for solution thermodynamics. Surface effects are taken into account by introducing surface excess variables similar to those used to study adsorption from liquid mixtures on solids.

4. Theoretical Models which consider non ideal or real systems, that should be more accurate in predicting equilibrium behavior.

Smith and Woodburn (1978) developed a generalized model to predict multicomponent ion exchange equilibria from binary data. The binary systems used in their study are $SO_4^{2-} - Cl^-$, $SO_4^{2-} - NO_3^-$, and $Cl^- - NO_3^-$ on a strong base anion exchange resin. These systems exhibit non-ideal characteristics in both phases and the experimental characterization is based on the reaction equilibrium constants. Wilson's correlation's for the activity coefficients are used in the model.

Triay and Rundberg (1989) developed a method of deconvolution to determine the site-specific selectivity coefficients for divalent and trivalent exchange in relatively

rigid ion exchangers. The technique involved the measurement of ion exchange isotherms and the application of a numerical approach to effect deconvolution. This method can be applied to systems undergoing ion exchange by different mechanisms. de Bokx and Boots (1989) studied the ion-exchange equilibria of alkali-metal and alkaline-earth-metal ions by using surface-sulfonated polystyrene-divinylbenzene resins. They found that the equilibrium coefficient is independent of the concentration of the liquid phase, and therefore specificity in ion exchange is due solely to interactions in the resin phase. Equations were derived that relate the equilibrium coefficient to a product of the difference between two interaction parameters and a factor that is constant within a class of ions. It was shown that selectivity is determined by the interaction between adsorbed ions and not by the interaction of separate adsorbed ions with the resin. The same workers in 1990 introduced the term 'compensating mixture' to specify a mixture of components that belong to the same compensation class. They developed a compensating mixture model for multicomponent systems which is applicable to ion exchange.

Horst et al. (1990) proposed a different theoretical model of ion exchange equilibria on weak acid resins in which fixed sites and counterions are assumed to form surface complexes. According to this model, the electric charges of the fixed sites generate an electric field normal to the resin surface. Counterions are located in individual sorption layers which have a certain charge density. Due to the existence of one layer for each kind of counterions, the entire resin phase can be considered as a series of electric capacitors. For the exchange of protons with metal counterions, a set of two characteristic quantities are derived from experiments. By means of this set of quantities, the equilibrium is calculated for a broad range of initial conditions. They applied the relationships of a series of electric capacitors and predicted the multicomponent equilibria using the sets of binary exchange parameters. The assumption that all counterions are located in their characteristic layers led to a simplified mathematical method. This method provided an excellent agreement between experimental and predicted equilibria.

de Lucas et al. (1992) studied the cation-exchange equilibria between Amberlite IR-120 resin and aqueous solution of calcium, magnesium, potassium, and sodium chlorides and hydrochloric acid. Experimental data for ion-exchange equilibria of the ternary and quaternary systems are reported in this study. They also developed a model which allows the prediction of multicomponent ion-exchange equilibria from binary data. They concluded that the predictions of ternary and quaternary systems based solely on the binary data are in good agreement with the experimental results.

Multicomponent Ion Exchange Column Models

Studies on multicomponent system of ions in single resins began as early as 1958. In their study, Dranoff and Lapidus (1958) approximated the rate of exchange with a reaction kinetic model. The rate constants for the exchange process and the equilibrium constants were determined experimentally. The model predicted accurately the shallow bed operation for a wide range of process conditions but failed to describe the diffusion limited nature of the ion exchange process. In their later studies (Dranoff and Lapidus, 1961), they found that their model could handle only shallow bed systems. Moreover, the equilibrium constants determined in the model were substantially different from the published resin characteristics.

Klein et al (1967) developed a multicomponent ion exchange equilibrium theory in fixed beds. Equilibrium operation, uniform presaturation and constant feed composition were assumed in this analysis. The model predicted accurately the number of composition changes (transitions) between zones of constant composition (plateau zones). The model could handle variable separation factors as well. During the same time, Helfferich (1967) developed a generalized equilibrium theory for systems with constant separation factors in which the concept of 'coherence' was introduced. The

model could handle an arbitrary number of exchanging species. It predicted the intermediate plateau zones that other investigators have since observed.

Tondeur (1970) developed a theory for ion exchange columns in which he showed that multicomponent heterovalent systems governed by mass-action equilibria are not always ordered. The order of affinities of the various components for the resin may depend on composition, even with constant equilibrium constants. Consequences of these equilibrium properties on the solution of the column differential equations were considered in detail for ternary systems, which may display one or two inversions. According to this study, the dynamic behavior of the column may be qualitatively different from that of the earlier studies. Helffercih (1984) described a simple physical model which illustrates the concept of coherent waves (concentration waves) and their interferences in multicomponent ion exchange columns. Klein et al (1984) considered multicomponent fixed bed sorption systems with variable initial and feed compositions. A computer program was developed which predicts the local equilibrium behavior. The program could handle up to 11 ion exchange components.

More recently, Garcia et al. (1992) made a theoretical analysis of multicomponent ion exchange in fixed beds. The concentration profiles and the number of transitions between plateau zones were obtained for systems with an arbitrary number of exchanging species. Lopez et al. (1992) considered modeling and experimental behavior of multicomponent anion exchange with amberlite IRA-410. The equilibrium theory developed by Helfferich (1967) was used to predict the effluent concentration profiles. The order of selectivity of the anions was:

$$Fl^- < OH^- < HCO_3^- < Cl^- < SO_4^{2-}$$
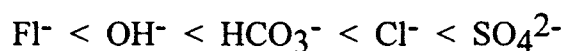
The most recent study on multicomponent ion exchange column dynamics is by Tan and Spinner (1994). Simple, model equations which consider different rate control mechanisms were formulated for fixed bed multicomponent ion exchange processes. The resulting equations were solved numerically for liquid phase, solid phase or combined

10

phase control. These algorithms were applicable to liquid adsorption as well. Several examples were discussed.

Particle Resistance Models

Bajpai et al. (1974) were the first to consider the diffusional limitations of ion exchange ever since it was discovered by Boyd et al. (1947). They conducted single particle studies on binary and ternary cation exchange kinetics. These studies were limited to the particle diffusion regime of ion exchange. Equations for ionic fluxes in the resin phase were derived using the Nernst-Planck model and were solved numerically. Particle diffusion in multicomponent systems has been further studied by Hwang and Helfferich (1987) and Yoshida and Kataoka (1987). Hwang and Helfferich extended the Nernst-Planck model to general multispecies systems with fast, reversible reactions at local equilibrium. The Nernst-Planck model and a reaction coefficient matrix are combined to determine the concentration profiles within the particle. However, this model has not been extended to film diffusion or to evaluate column performance. Yoshida and Kataoka developed a theory for a ternary system and showed how three ions diffuse within the particle. Comparisons were made between model predictions and experimental data for the mean resin phase concentration. The theory was once again based on the Nernst-Planck model.

Film Resistance Models

Schlogl and Helfferich (1957) were the first to apply Nernst-Planck equations to film diffusion controlled ion exchange. They compared the ion fluxes through a Nernst film with and without consideration of the electric field. The solution is restricted to binary systems with monovalent ions, however, selectivity of the resin was not

11

considered. An implicit solution for the function of conversion versus time was found. Copeland et al. (1967) expanded this solution to include selectivity. The implicit solutions of these two papers are only valid for the case of constant composition of the solution. Omatete et al. (1980 a, b) were the first to consider multicomponent film diffusion controlled ion exchange. They made comparisons between the Nernst-Planck model and Fick's law. The method also considered concentration dependent diffusion coefficients. In their later work (1980 b) they experimentally evaluated the column performance for ternary exchange. The intermediate plateau zones predicted by Helfferich (1967) were confirmed. The work had the disadvantage of determining experimentally the overall mass transfer coefficients. They considered only one set of data in their evaluation. Wildhagen et al. (1985) have considered ternary film diffusion controlled ion exchange kinetics to determine the most appropriate effective diffusivity. Effective diffusivity expressions were developed using the Nernst-Planck equation and the static film model. A new concentration variable based on the coion was defined. Their evaluation was limited to single resin studies and only one coion.

A step towards a more general solution of the Nernst-Planck equations for film diffusion controlled ion exchange was taken by Kataoka et al. (1987). They studied the liquid-side ion exchange mass transfer with a ternary system of ions. Flux expressions were derived for the cases of equal and arbitrary ionic valences. The solutions were exact for equal valence cases while they were approximate for arbitrary valences. Perturbation methods were used to obtain an approximate solution. However, this approximation is complicated and cannot be expanded to the general multicomponent case.

The next and successful step towards a more general solution was taken by Franzreb et al. (1993). They considered liquid-phase mass transfer in ion exchange for the general case of any arbitrary number of counterions and coions. The Nernst-Planck equations were solved analytically for the momentary fluxes. The advantages of this model are that the solution is analytical and reduces to all exact solutions available in the

literature for special cases. The disadvantage is that it is only an approximation for the general case of arbitrary systems. However, the quality of the approximation was demonstrated by comparison with the general numerical solution. For most applications the errors can be neglected compared with those caused by the idealizing assumptions of the film model. Most of the known solutions in the literature combine Nernst-Planck equations with the condition of no net electric current and integrate the resulting equations to obtain an expression for ionic flux. Unlike these earlier models, a different way was chosen in this work to eliminate the unknown flux J_i. Instead of integration, in this work, the above equations were differentiated to obtain a homogeneous second order differential equation. This is the uniqueness of this work. However, this work was limited to solution of Nernst-Planck equations for an arbitrary number of ions and did not make any column effluent predcitions. The general flux expression developed by Franzreb is:

$$J_i = \frac{D_i}{\delta}\left((1-\frac{N_i}{P})(C_i^* - C_i^0) + N_i A_i (1+\frac{1}{P})(C_T^* - C_T^0)\right) \qquad (2\text{-}3)$$

This flux expression is used in this work to develop a general column model.

Ultrapure Water

The term 'ultrapure water' is usually understood to imply water with ionic impurity levels of less than one part per billion (ppb) with correspondingly low levels of particulate and microbial contaminants (Sadler, 1993). Very high purity water is used in many industries, but the major users are the power and semiconductor manufacturing industries, with the pharmaceutical industry also having a strong interest. Now ultrapure water is considered a quality chemical and not just water. Its production involves the

13

removal of various impurities. These include dissolved gases, ionic, microbial and organic impurities and also particulate and colloidal impurities (including silica). All of these are important although the various industries have their own requirements regarding acceptable levels.

The manufacture of ultrapure water calls for a high degree of sophisticated processing and system expertise. Equal sophistication is required in the distribution network to insure the ultrapure water is not contaminated on its way to final use. Ultrapure water is defined by its impurity content. In Table I ultrapure water (semiconductor grade) is compared with typical city water (Blume, 1987).

The most significant developments in ultrapure water production in recent years have probably been made using the various membrane techniques. Reverse osmosis and electrodialysis are increasingly being used in the early stages of purification, and ultrafiltration finds uses both in pretreatment and in the final stage of ultrapure water preparation. Effective methods of sterilizing ultrapure water systems have also been developed along with techniques of ensuring that the microbial levels in the product water remain acceptably low.

Power Industry: The power industry is primarily concerned with impurities that could cause, or assist, corrosion to occur within the steam/water circuit of boilers or which could form deposits on critical components. This requires the removal of common ionic impurities like sodium, chloride and sulfate. Silica and particulate impurities such as iron oxide are also of concern. The quality demanded by the modern steam generators depends largely upon their design. Nuclear power plants pay particular attention to water quality in the steam/water circuits in view of the very high repair costs should corrosion arise. Those with once-through steam generators (OTSGs) have a special concern over particulate levels in feed water. Boiling water reactors (BWRs) have a special need to reduce crud levels which are radioactive and increase the occupational radiation doses.

14

Table I

Ultrapure water vs. city water quality (Blume, 1987)

Impurity		Ultrapure Water	City Water
Total Organic Carbon ppb		20.0	4,000
Total Solids (residue) ppb		50.0	288,000
Silica (dissolved)	ppb	5.0	5,000
Sodium	ppb	0.05	37,000
Potassium	ppb	0.10	5,300
Zinc	ppb	0.02	4
Copper	ppb	0.02	2
Chloride	ppb	0.05	13,000
Bacteria	Cells per 100 ml	0.0	0.0
Resistivity	MΩ.cm	18.0	0.025
Particles	(> 0.2 micron) per L	10,000	1,000,000

<u>Semi-conductor Manufacturing Industry</u>: The semi-conductor manufacturing industry has overtaken the power industry in its overall quality requirements for ultrapure water. During the production of silicon chips, large quantities of very pure water are used to remove chemical residues from the surface of the wafers following their immersion in various etchant solutions. In so doing, the water must not deposit any contaminants on the surfaces being cleaned. Hence, extremely tight constraints are placed on the levels of impurities in ultrapure water. The water quality demands for the manufacture of electronic devices up to 16M are shown in Table II. Higher density chips, 64M, will be in production by 1995 and even higher density chips are planned.

There are two main techniques used to attain these high qualities. The first is reverse osmosis, which may require an extensive pretreatmant train to prevent the membranes in the unit from being fouled or damaged. The second technique involves the use of ion exchange resins contained in roughing mixed beds (using anion and cation resins) and polishing mixed beds (which contain, in addition to those resins used in the previous unit, an inert resin, the sole function of which is to prevent cross-contamination during regeneration) (McCartney, 1987).

Ion Exchange Kinetics in Ultrapure Water Systems

Ion exchange is a very important and essential process among the several separation and purification techniques used in the production of ultrapure water. It continues to be used both in 'roughing' as well as the final stages. The continuous production of ultrapure water on an industrial scale uses ion exchange mixed beds as a major method of reducing ionic impurities to the low parts per trillion (ppt) level. Under such demanding operating conditions, particularly the high flow rate and high volume requirements of condensate purification in the power generation industry, it is kinetics

16

Table II

Water Quality Requirements for 16M Devices (Sadler, 1993)

Degree of Integration		256K	1M	4M	16M
Dissolved Oxygen	ppb	<100	<100	<50	<10
Silica	ppb	<10	<10	<5	<1
Iron	ppb	<1	<0.1	<0.003	<0.003
Copper	ppb	<1	<0.1	<0.002	<0.002
Sodium	ppb	<1	<0.1	<0.1	<0.1
Chloride	ppb	<1	<0.1	<0.1	<0.1

rather than the equilibria of the exchange processes that becomes the main controlling factor. Harries (1991) studied the interactions between anion and cation exchange rates, particularly with respect to changes in the aqueous phase pH within a bed of resins.

It has been observed that anion exchange rates are slower at higher pH and have a greater pH dependence as the resins age and deteriorate kinetically in service. Likewise, cation exchange kinetics are also pH dependent, but in the opposite sense, cation exchange rates being faster in alkaline solutions than in neutral or acidic solutions. For a mixed bed, pH will depend on factors such as resin volume ratio, degree of mixing, bead sizes of both resins, the influent ion concentrations, rate of ionic loading, and anion and cation exchange kinetics. For a single bed of resin, the within-bed pH depends on the ionic composition and feed concentrations. For beds in series, the nature and efficiency of the preceding exchange stage are also important. Investigations into mixed beds with new exchange resins have produced, in some instances, unexpectedly high outlet conductivities when dosed with either the chlorides or sulfates of ammonium or sodium (Harries 1991). These observed conductivities have been attributed to poor cation exchange kinetics due to the elution of residual polymeric material from the anionic resin and subsequently fouling the cationic resin. It was noted that sodium exchange was affected more than ammonium exchange.

CHAPTER III

MIXED BED ION EXCHANGE COLUMN MODELING
FOR MULTICOMPONENT SYSTEMS

Abstract

A model for multicomponent mixed bed ion exchange is developed and tested for various system parameters. The model is capable of handling an arbitrary number of species with arbitrary valences. The model is used to predict column effluent concentrations for influent water containing three cations and five anions including three divalent species. The model is capable of handling variations in cation-to-anion resin ratio, flow rate, bed composition, particle size, and temperature.

Introduction

Binary and ternary ion exchange systems have been investigated by many researchers. However, the area of multicomponent systems have had limited study. As pointed out in the preceding chapter, there are many ion exchange equilibrium models that can predict column effluents for multicomponent systems. Helfferich (1967), Klein et al. (1967) and Tondeur (1970) have made a lot of contributions in this area. But in ion exchange systems handling huge volumes of water at very high flowrates, it is kinetics, rather than equilibrium, that plays an important role. In the worst case, the influent water

19

passes out of the column in 10 secs (Harries, 1987). Hence, such ion exchange units should be addressed using rate models rather than equilibrium models.

Haub and Foutch (1986 a, b) were the first to take a step in this direction. They were the first workers to model mixed bed ion exchange columns at very low concentrations taking ion exchange kinetics into consideration. Zecchini and Foutch (1990) extended this work to ternary univalent systems. Pondugula and Foutch (1994) further extended this ternary system to include one divalent species. However, their model could not handle the complete system of ions as required by Pennsylvania Power & Light. The column input water used by Pennsylvania Power & Light contained sodium, calcium, chloride, sulfate, bicarbonate and carbonate. Their model did not include bicarbonate and carbonate in the system because of model limitations.

The objective of this work is to develop a general model which will be able to predict column effluent for any number of species. This model included bicarbonate and carbonate in the system of ions to address completely the needs of Pennsylvania Power & Light Co.

Temperature Sensitive Parameters

There are a number of temperature dependent parameters in the model. Divekar et al. (1987) incorporated equations to account for these temperature effects. These equations have been used in this work in addition to those required for this work. These include diffusion coefficients, equilibrium constants and solution viscosity.

The diffusion coefficients at a particular temperature can be estimated using Nernst equation (1888) which is:

$$D^0_{AB} = (\frac{RT}{F^2})(\frac{\lambda^0_+ \lambda^0_-}{\lambda^0_+ + \lambda^0_-})(\frac{Z_+ + Z_-}{Z_+ Z_-})$$ (3-1)

$$D_i^0 = (\frac{RT}{F^2})\lambda_i^0 \qquad\qquad (3-2)$$

Temperature and equivalent conductance at infinite dilution are correlated by a least squares method. The temperature correlations for the dissociation constant of water, first and second dissociation constants of carbonate equilibrium and viscosity of water are presented in Table III along with those for diffusion coefficients.

Model Development

The model addresses a multicomponent system of ions in a film controlled homogeneous mixed bed ion exchange column. The ions involved in this study are Na^+, Ca^{2+}, Cl^-, SO_4^{2-}, CO_3^{2-} and HCO_3^-. The film diffusion fluxes are described using the Nernst-Planck model. The equilibrium between the different forms of carbonic species is taken in to account. Column effluent concentrations are predicted by solving the material balance equations numerically. The equations derived to describe the various conditions involved are presented here, with detailed derivations in appendices.

Assumptions

The number of simplified assumptions involved have been limited to as few as possible to develop a generalized multicomponent multivalent model. The major assumption is that the mixed bed ion exchange process is film diffusion controlled. In developing the carbonate equilibrium model, it is assumed that the dissolved CO_2 concentration is negligible compared to that of HCO_3^-/CO_3^{2-}. Other important assumptions are bulk-phase neutralization, binary selectivity coefficients can be used to

21

Table III
Temperature Dependent Parameters (Divekar et al., 1987)

Ionic Diffusion Coefficients (cm2/s)

Hydrogen
$$D_A = \left(\frac{RT}{F^2}\right)\left(221.71 + 5.529T - 0.0144T^2\right)$$

Sodium
$$D_B = \left(\frac{RT}{F^2}\right)\left(23.0 + 1.064T + 0.0033T^2\right)$$

Calcium
$$D_C = \left(\frac{RT}{2F^2}\right)\left(23.27 + 1.575T\right)$$

Hydroxide
$$D_A = \left(\frac{RT}{F^2}\right)\left(104.74 + 3.807T^2\right)$$

Chloride
$$D_B = \left(\frac{RT}{F^2}\right)\left(39.649 + 1.391T + 0.0033T^2\right)$$

Sulfate
$$D_C = \left(\frac{RT}{2F^2}\right)\left(35.76 + 2.079T\right)$$

Carbonate
$$D_D = \left(\frac{RT}{2F^2}\right)\left(36.0 + 1.44T\right)$$

Bicarbonate
$$D_E = \left(\frac{RT}{F^2}\right)\left(44.5\right)$$

Dissociation Constants

Water
$$pK_w = -6.0875 + 0.0176T + \frac{4470.99}{T}$$

* CO_2 1st. dissociation
$$pK_1 = \frac{17052}{T} + 215.21 LOG(T) - 0.12675T - 545.56$$

* CO_2 2nd. dissociation
$$pK_2 = \frac{2902.39}{T} + 0.02379T - 6.498$$

Solution Properties (cp)

Viscosity
$$\mu = 1.5471 + 0.0317T + 2.334E - 04T^2$$

* -- Loewenthal and Marias, vol. 1, 1982.

Table IV

Model Assumptions

1. Film diffusion control.

2. Pseudo steady state exchange (variations of concentration with space are much more important than with time).

3. The Nernst-Planck model incorporates all interactions between diffusing ionic species.

4. No coion flux across the particle surface.

5. No net coion flux within the film.

6. No net current flow.

7. Local equilibrium at solid-film interface.

8. Selectivity coefficients are constant and independent of temperature.

9. Binary selectivity coefficients can be used for multicomponent ion exchange.

10. Bulk phase neutralization.

11. Reactions are instantaneous when compared with the rate of exchange.

12. Uniform bulk and resin phase compositions.

13. Curvature of the film is negligible.

14. Activity coefficients are constant and unity.

15. Negligible axial dispersion.

16. Plug flow

17. Negligible particle diffusion resistance.

18. Isothermal, isobaric operation.

19. Dissolved CO_2 concentration is negligible compared to that of HCO_3^-/CO_3^{2-}.

describe the multicomponent exchange, and selectivity coefficients are temperature independent. Table IV lists the assumptions used in this model development.

Carbonate Equilibrium

Carbonic species dissolved in water exist in four different forms: dissolved CO_2, carbonic acid H_2CO_3, and the ions HCO_3^- and CO_3^{2-}. The sum of these concentrations in the solution is the total carbonic species concentration (TCC). The carbonic species together with hydrogen and hydroxyl ions of the water exist in a state of dynamic equilibrium described by the following reactions:

$$CO_2 + H_2O \longleftrightarrow H_2CO_3 \tag{3-3}$$

$$H_2CO_3 \xleftrightarrow{K_1} H^+ + HCO_3^- \tag{3-4}$$

$$HCO_3^- \xleftrightarrow{K_2} H^+ + CO_3^{2-} \tag{3-5}$$

$$H_2O \xleftrightarrow{K_w} H^+ + OH^- \tag{3-6}$$

K_1 and K_2 are called first and second dissociation constants of carbonate equilibrium, respectively. K_w is the dissociation constant for water. These three constants are temperature dependent and Table III gives the temperature correlations for these constants (Loewenthal and Marias, vol. 1, 1982). The temperature correlation for K_1 was determined for the range of 0°C to 38°C while that for K_2 was determined for 0° C to 50°C. The correlation for water dissociation constant is valid up to a temperature of 60°C. In this work, due to lack of data, the K values at higher temperatures than mentioned above were calculated assuming the above equations applied. Plots of pK_1, pK_2 and pK_w for temperatures in the range of 0°C to 90°C are shown in Figure 1. It can be observed that as temperature increases all the pK values decrease, i.e. the K values increase.
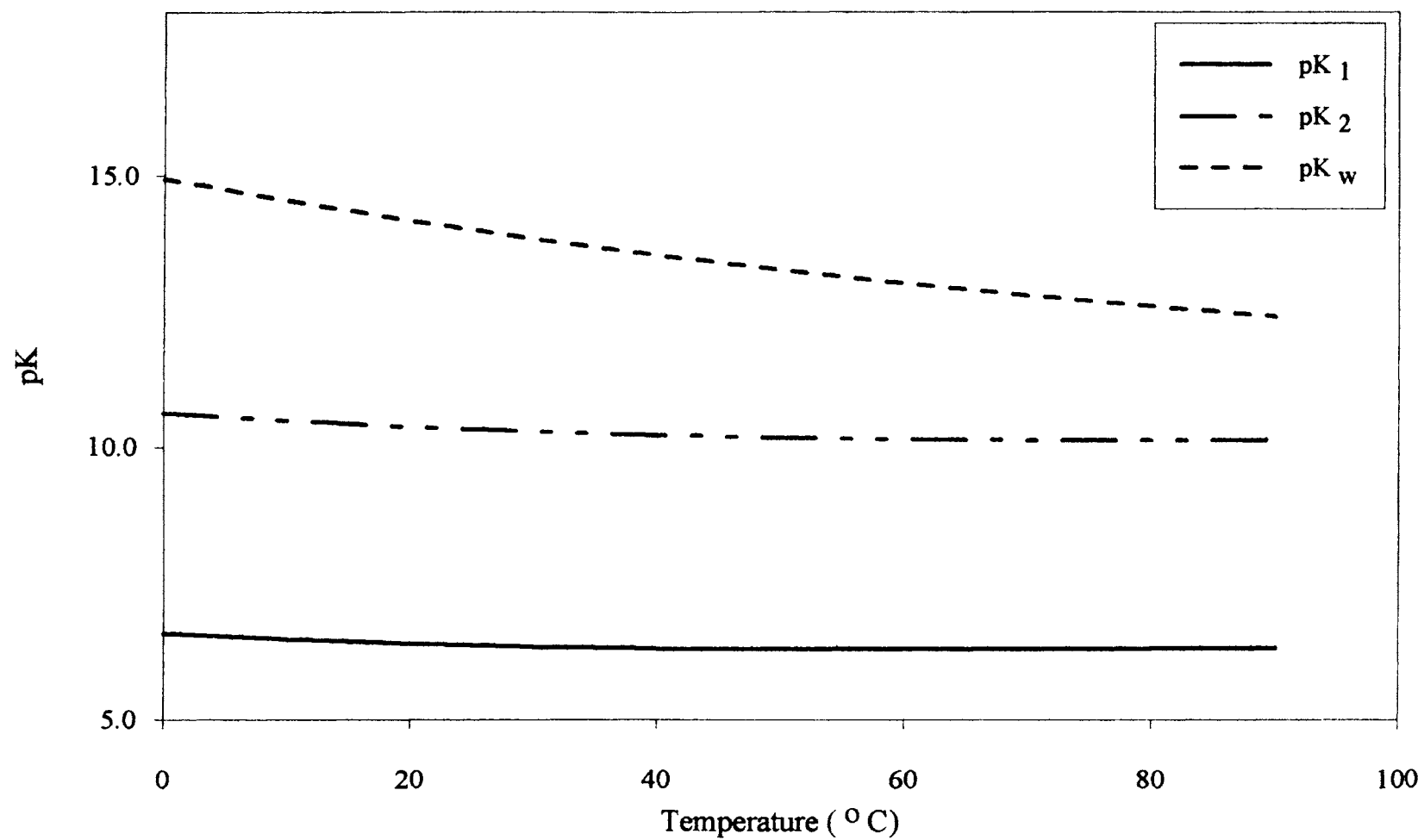
Figure 1. Temperature dependence of pK $_1$, pK $_2$ and pK $_w$

Equations relating the concentrations of each of the carbonic species with the hydrogen ion concentration are derived for equilibrium conditions in Appendix A. Using the known total carbonic species concentration and the electroneutrality condition, the concentrations of the individual species can be calculated using an iterative technique.

Interfacial Concentrations

Interfacial concentrations (solid-film interface) of the ions are determined using ion exchange equilibria. It is assumed that there is a local equilibrium at the solid-film interface. The selectivity coefficient expression for a general case, can be written using a mass action law, as follows:

$$K_A^B = \left(\frac{q_B}{C_B^*}\right)^{Z_A}\left(\frac{C_A^*}{q_A}\right)^{Z_B}$$ (3-7)

where q's are the concentrations in the resin phase while C^*'s are the surface concentrations. The above equation can be written in terms of equivalent fractions, total resin capacity and total interfacial concentration as follows:

$$K_A^B = \left(\frac{Y_B}{X_B^*}\right)^{Z_A}\left(\frac{X_A^*}{Y_A}\right)^{Z_B} Q^{(Z_A-Z_B)} C_T^{*(Z_B-Z_A)}$$ (3-8)

For 'n' counterions in the solution replacing ion A in the resin, we can write 'n' such expressions. However, given the resin loadings, resin capacity and total interfacial concentration, we will have n+1 unknown interfacial fractions. The extra equation

26

needed to completely specify the system is obtained from material balance at the solid-film interface.

$$\sum_{i=1}^{n} X_i^* = 1.0 \tag{3-9}$$

From Equation 3-9 it is evident that with an arbitrary valence case, the ion exchange equilibrium depends on the resin capacity and total interfacial concentration. This leads to an iterative solution to determine the interfacial concentrations. However, before we can determine these individual interfacial concentrations, we need to have an expression for the total interfacial concentration, C_T^*. This is discussed in the following section. The selectivity coefficient values of the ions considered in this system are given in Table V. The detailed equations for calculation of interfacial concentrations are presented in Appendix B.

Flux Expression

The task of developing analytic ionic flux expressions in the general case of arbitrary number of species with arbitrary valences is highly complicated. Zecchini and Foutch (1990) developed a model for ternary univalent system of ions. Pondugula and Foutch (1994) further extended this model to include a divalent species. Their model cannot be further extended to a generalized case of multicomponent system of ions because of mathematical complications. Zecchini (1990) discusses these complications in detail. Hence, in this general case, only an analytical approximation could be obtained. The flux expressions for the case of arbitrary number of counterions are derived in Appendix C. A method proposed by Franzreb et al. (1993) is used.

The Nernst-Planck equation, which is the basis of this work is as follows:

27

$$J_i = -D_i \left(\frac{\partial C_i}{\partial r} + \frac{C_i Z_i F}{RT} \frac{\partial \phi}{\partial r} \right) \qquad (3\text{-}10)$$

The method used eliminates the electric potential term in the Nernst-Planck equation using the no net coion flux in the film condition. With the introduction of total equivalent concentration, C_T, the electric potential term can be written as

Table V

Selectivity Coefficients

Ion	Value
K_H^{Na}	1.67
K_H^{Ca}	29.0
K_{OH}^{Cl}	16.5
$K_{OH}^{SO_4}$	53.4
$K_{OH}^{CO_3}$	37.5
$K_{OH}^{HCO_3}$	6.0

$$\frac{d\phi}{dr} = -\frac{RT}{Z_Y F C_p} \frac{dC_T}{dr} \qquad (3\text{-}11)$$

where Z_Y is a mean coion valence. Substitution of Equation 3-11 into Equation 3-10 along with the pseudo steady state assumption leads to the following:

$$J_i = -D_i \left(\frac{dC_i}{dr} + N_i \frac{C_i}{C_T} \frac{dC_T}{dr} \right) \qquad (3\text{-}12)$$

where N_i is the ratio of counterion to mean coion valence. After a series of mathematical manipulations the final form of the flux expression is as follows:

$$J_i = \frac{D_i}{\delta}\left[(1-\frac{N_i}{P})(C_i^* - C_i^0) + N_i A_i (1+\frac{1}{P})(C_T^* - C_T^0)\right] \qquad (3\text{-}13)$$

and the expression for total interfacial concentration, C_T^* is

$$C_T^* = \left(\frac{\sum_{i=1}^{n}(1+N_i)D_i X_i^0}{\sum_{i=1}^{n}(1+N_i)D_i X_i^*}\right)^{1/P+1} C_T^0 \qquad (3\text{-}14)$$

From Equations 3-14 and 3-8 it can be observed that the total interfacial concentration C_T^* and the individual interfacial equivalent fractions X_i^*'s are interdependent. Thus, an iterative solution had to be used to determine these quantities and subsequently the ionic fluxes. The solution strategy adopted in the computer code to determine the ionic fluxes is presented in Table VI.

Equation 3-13 is used to determine the overall effective diffusivity defined as:

$$D_e = \frac{\sum_{i=1}^{n}|J_i\delta|}{\sum_{i=1}^{n}|C_i^* - C_i^0|} \qquad (3\text{-}15)$$

The film thickness in Equation 3-13 is eliminated using the relation

$$\delta = D_e/K \qquad (3\text{-}16)$$

where K is a mass transfer coefficient proposed by Kataoka.

Table VI

Solution Strategy for Calculation of Ionic Fluxes

---

1.   Assume $C_T^* = C_T^0$.

2.   Calculate X_i^*'s using Equations 3-8 and 3-9.

3.   With the X_i^*'s obtained in step 2, calculate C_T^* using Equation 3-14.

4.   If the difference between new and old C_T^* exceeds the chosen tolerance, repeat steps 2 and 3.

5.   Calculate the ionic fluxes using Equation 3-13 and other necessary equations given in Appendix C.

Particle Rates: The rate of exchange is related to the flux of the species by:

$$\frac{d<C_i>}{dt} = -J_i a_s \tag{3-17}$$

The resin phase concentration $<C_i>$ can be represented as:

$$<C_i> = y_i Q \tag{3-18}$$

Now Equation 3-17 can be written as

$$\frac{dy_i}{dt} = \frac{-J_i a_s}{Q} \tag{3-19}$$

The rate of ion loadings into the resin can be determined using the above equation once the individual ionic fluxes are known.

Column Material Balances

The form of the material balance equations does not change from those used earlier. The final form of the non-dimensionalized material balance equations derived in Appendix D is

$$\frac{\partial x_i}{\partial \xi} + \frac{\partial y_i}{\partial \tau} = 0 \qquad (3\text{-}20)$$

The effluent concentrations from the column are determined from the solution of these equations. The method of characteristics is employed to solve the resultant system of equations. The resin and bulk phase fraction equations are then solved using fourth order Adams-Bashforth and fourth order Gears methods. These methods are briefly described in Appendix E.

CHAPTER IV

RESULTS AND DISCUSSION

The model presented in Chapter III was used to predict effluent concentration profiles for various cases, like different resin ratios, flow rates, temperatures and particle sizes. Also, the model was used to predict effluents from a MBIE column with resin bed heels. A base case was defined to which all other comparisons were made. The input water and bed conditions for the base case are

sodium:	4.78×10^{-8} eq/l (1.1 ppb)
calcium:	1.91×10^{-7} eq/l (3.8 ppb)
sulfate:	6.87×10^{-8} eq/l (3.3 ppb)
chloride:	4.58×10^{-8} eq/l (1.6 ppb)
carbonate/bicarbonate:	1.146×10^{-7} eq/l
initial resin composition:	1% (all ions)
cation-anion resin ratio:	1:1
flow rate:	42 gpm/ft^2
temperature:	60 °C
particle sizes:	0.08 cm (cation); 0.06 cm (anion)

Desulfation of cationic resins: Studies have proven that strongly acidic cationic resins release sulfur molecules into water (Fisher 1993, Fejes 1969, Marinsky and Potter 1953). This desulfation of cationic resins is strongly a function of temperature. Pondugula (1994) quantified the data provided by Fisher (1993). This mathematical expression, to

account for the desulfation of cationic resins, has been used in this model to predict the sulfate effluent concentrations. The rate constant for desulfation and the expression used in the computer code to calculate the desulfation are:

$$K = 7.5 \times 10^{-7} e^{(-10278.6/(T+273.16))}$$

$$DS = (7.5 \times 10^{-7} e^{(-10278.6/(T+273.16))} \times HT \times 3.14 D^2 \times Q_c)(vs \times d_{pa})$$
$$\times FCR / (NT \times 3600 \times FR \times KLC \times (1 - VD))$$

Effect of Resin Ratio

Column operation effluent concentration profiles are determined for three different cation to anion resin volume ratios:

Cation-Anion: 1.0/2.3 (30% cationic resin)

                  1.0/1.0 (50% cationic resin) **(base case)**

                  2.3/1.0 (70% cationic resin)

All other parameters are maintained at base case condition.

Figures on the following pages show that cation to anion resin ration can be used to adjust the time of breakthrough or to adjust the initial leakage. Higher FCR/FAR results in lower leakages of the cations and earlier breakthroughs of anions. On the other hand, lower FCR/FAR results in earlier breakthroughs for cations and delayed breakthroughs for anions.

As shown in Figure 2, the equilibrium leakages of sodium are not affected by change in the resin ratios. Sodium breakthrough occurs at about 500 days for the base case. When the column had only 30% cationic resin, sodium breakthrough occurs 300 days earlier and the breakthrough is delayed by 200 days for the case of 70% cationic
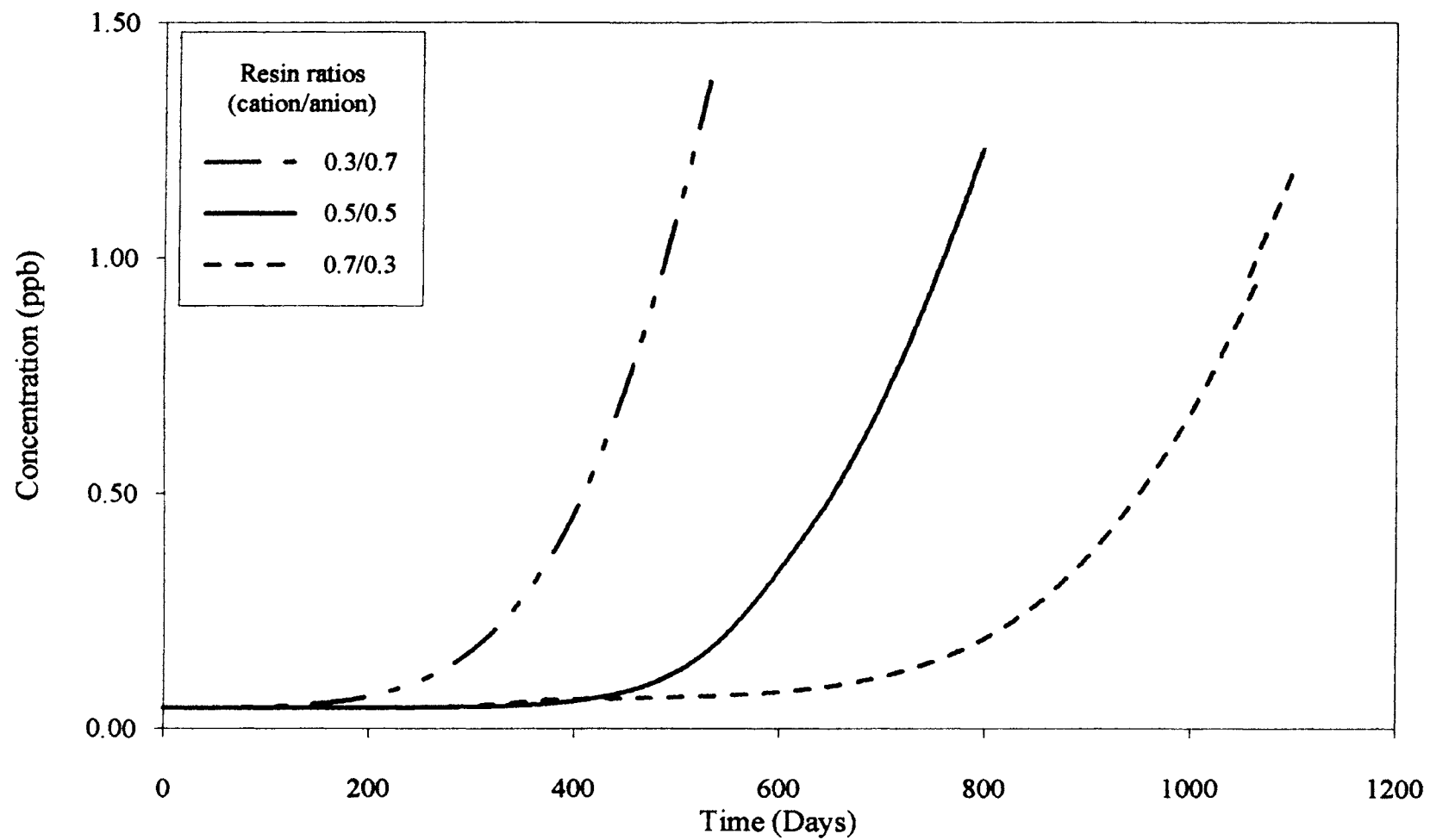
Figure 2. Effect of resin ratios on the effluent concentrations of sodium

resin ratio. This shows that the resin ratio parameter can be effectively used to alter the time of breakthrough for sodium. This is expected, as high cationic resin ratio brings about more number of exchange sites for cations resulting in a delayed breakthrough. Figure 3 shows the effluent concentrations of calcium for different resin ratios. Varying the resin ratio has effect on both the time of breakthrough as well as the initial leakage of calcium. A cationic resin ratio of 30% results in an early breakthrough by about 320 days while there is no breakthrough in the case of 70% cationic resin. For 30% cationic resin, initial leakage is about two orders of magnitude higher than that for base case. On the other hand they are lowered by two orders of magnitude for 70% cationic resin ratio case. This is probably due to the very high selectivity coefficient of calcium compared to that of sodium (29 for Ca; 1.5 for Na). This leads to more loading of calcium onto the resin. Thus when the cationic resin ratio is high, there is a decrease in calcium leakage and a delay in the breakthrough. The time of breakthrough of calcium can not be observed in Figure 3 because of the logarithmic scale chosen for the concentration axis. This scale is chosen to show the variation of initial leakage with varying resin ratios. A linear scale for the concentration axis would clearly show the breakthrough times of calcium for various cases. This applies to all calcium figures in this Chapter.

Figure 4 shows the chloride effluent profiles for varying resin ratios. As in the case of sodium, the resin ratios did not have any effect on the initial leakage of chloride. A cationic resin fraction of 70% results in a breakthrough 200 days earlier than the base case. In this case, a saturation is reached after about 920 days and the effluent concentration is equal to the inlet concentration. There is no breakthrough for the case of 30% cationic resin fraction. Figure 5 shows the sulfate effluent concentration profiles. As in the case of calcium, the resin ratio has a significant effect on the initial leakage of sulfate. A cationic resin fraction of 30% lowers the initial leakage by about 57% when compared to that of the base case. There is a 131% increase in the initial leakage of sulfate for the case of 70% cationic resin fraction. A breakthrough is observed for this

35

Figure 3. Effect of resin ratios on the effluent concentrations of calcium

Figure 4. Effect of resin ratios on the effluent concentrations of chloride
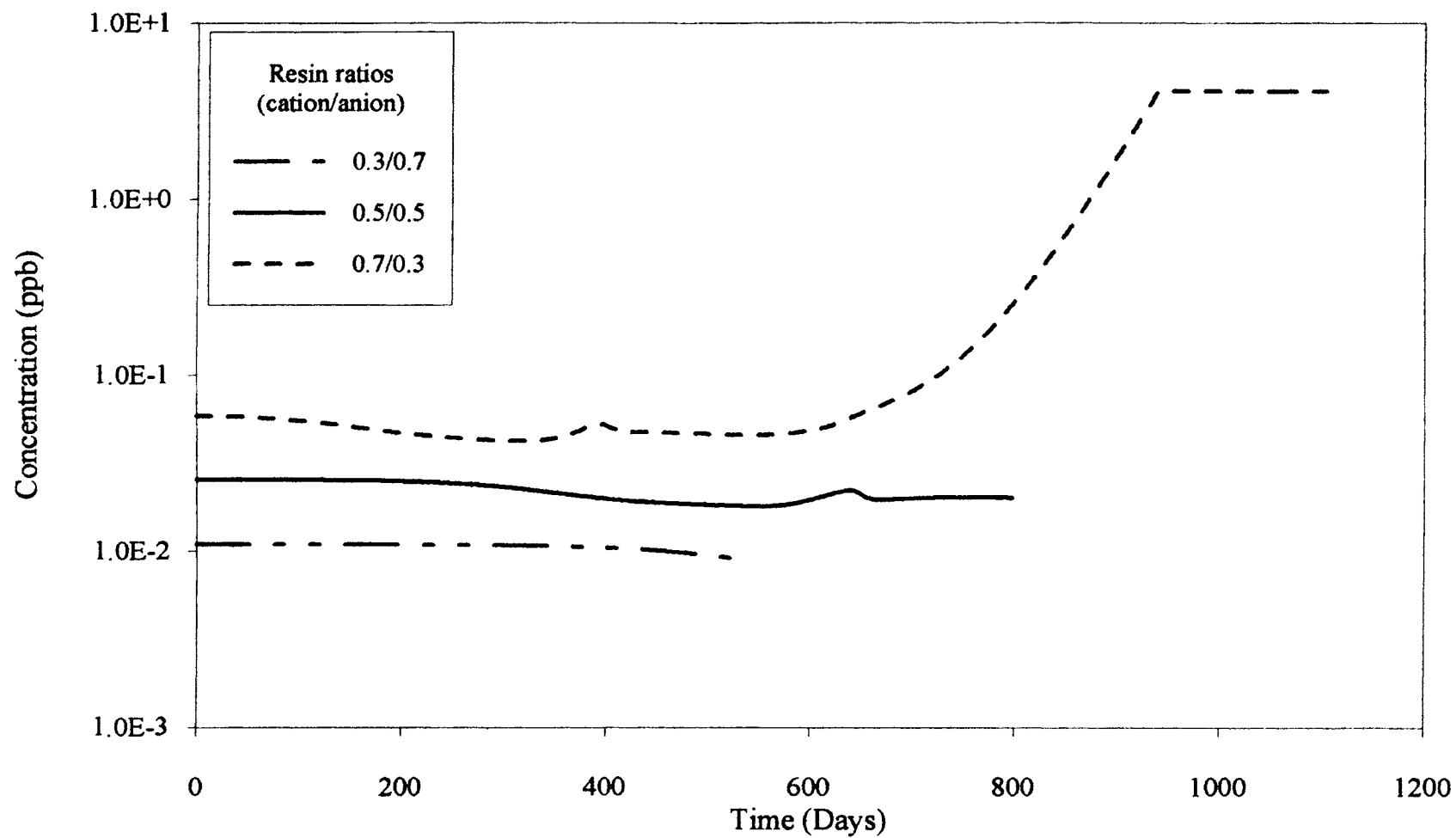
Figure 5. Effect of resin ratios on the effluent concentrations of sulfate

case after 600 days and as in the case of chloride, a saturation is reached after about 920 days after which there is no change in the effluent concentration of sulfate. There is no sulfate breakthrough in the other two cases.

It can be observed from Figure 4 that in the base case, after about 610 days, there is a change in the slope of the chloride curve. At this point the rate of increase of chloride effluent concentration is slightly reduced. This is probably due to the peak in the sulfate effluent profile which occurs at the same time. It can also be observed from the effluent profiles of carbonate and bicarbonate (Figures 6 and 7) that the effluent concentrations of these ions are nearly constant at this time. Thus, as more of sulfate comes out, there is more loading of chloride onto the resin in order to satisfy the material balance condition on the resin. These kind of interactions can be expected in a multicomponent system of ions like this. Unlike in a binary system, smooth breakthrough curves are not to be expected in a multicomponent system of ions. High anionic resin ratios lead to saturation of the resin resulting in the effluent concentration being equal to the feed concentration. However, in the case of sulfate, though the effluent concentration is constant after about 920 days, this is not equal to the feed concentration because of the constant desulfation of cationic resin. The significant change in the initial leakage of sulfate with varying resin ratios is due to the effect of cationic resin desulfation. A FCR/FAR of 0.7/0.3 leads to a 32% increase in the desulfation while a FCR/FAR of 0.3/0.7 reduces the same by about 39% when compared to that of base case. Thus we observe a decrease in the leakage of sulfate with lower anionic resin ratios and vice versa. Effect of cationic resin desulfation on sulfate exchange is described in detail in a further section. As in the case of calcium, the high selectivity coefficient of sulfate (54 for sulfate; 16 for chloride) is also a probable factor in significant change in the sulfate leakage with varying resin ratios.

Carbonate and bicarbonate showed similar effluent behavior as they are both guided by the equilibrium between the carbonate species and hydrogen and hydroxide ions (Figures 6, 7). For both ions, the resin ratio did not have any effect on the initial

39
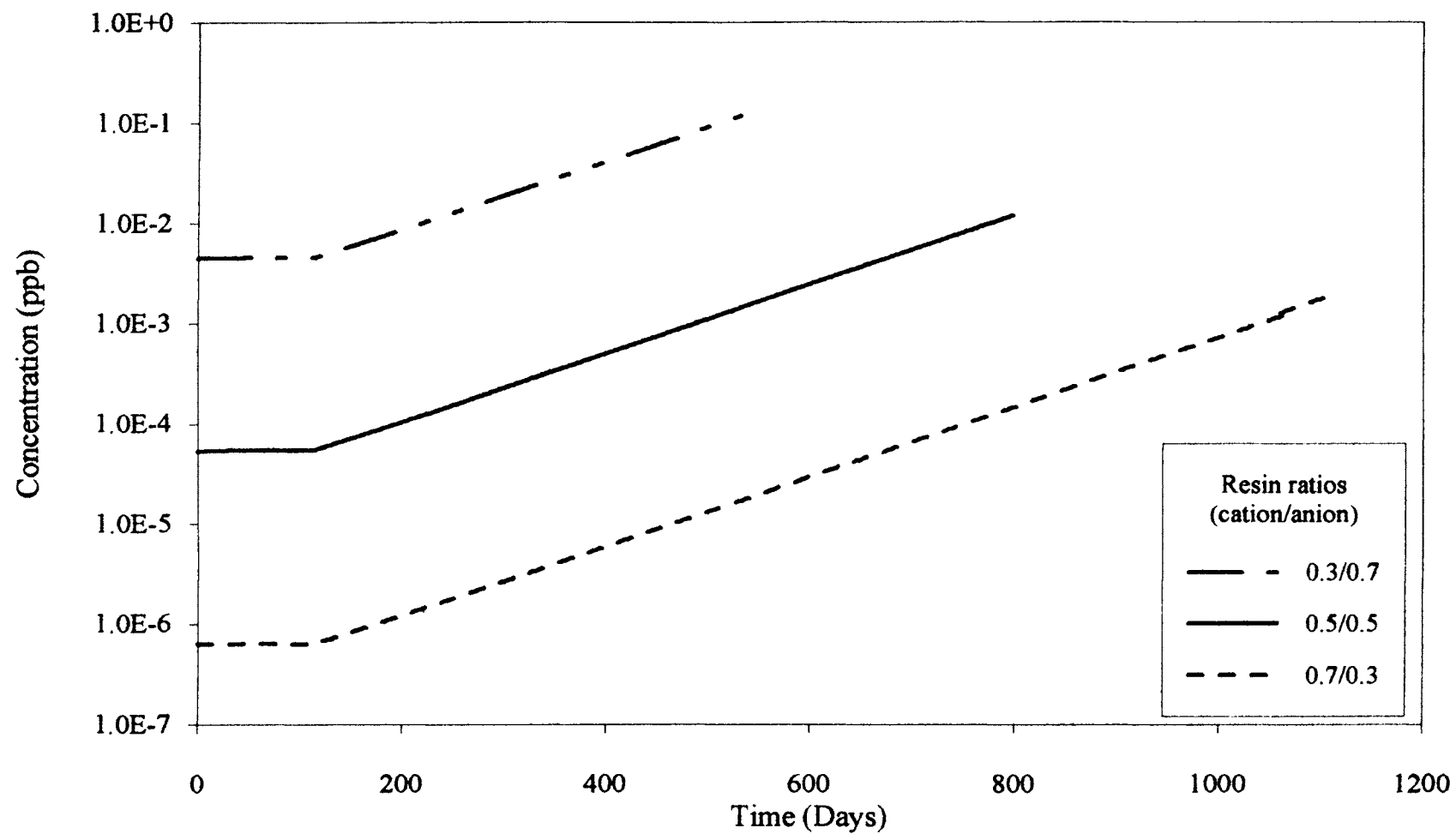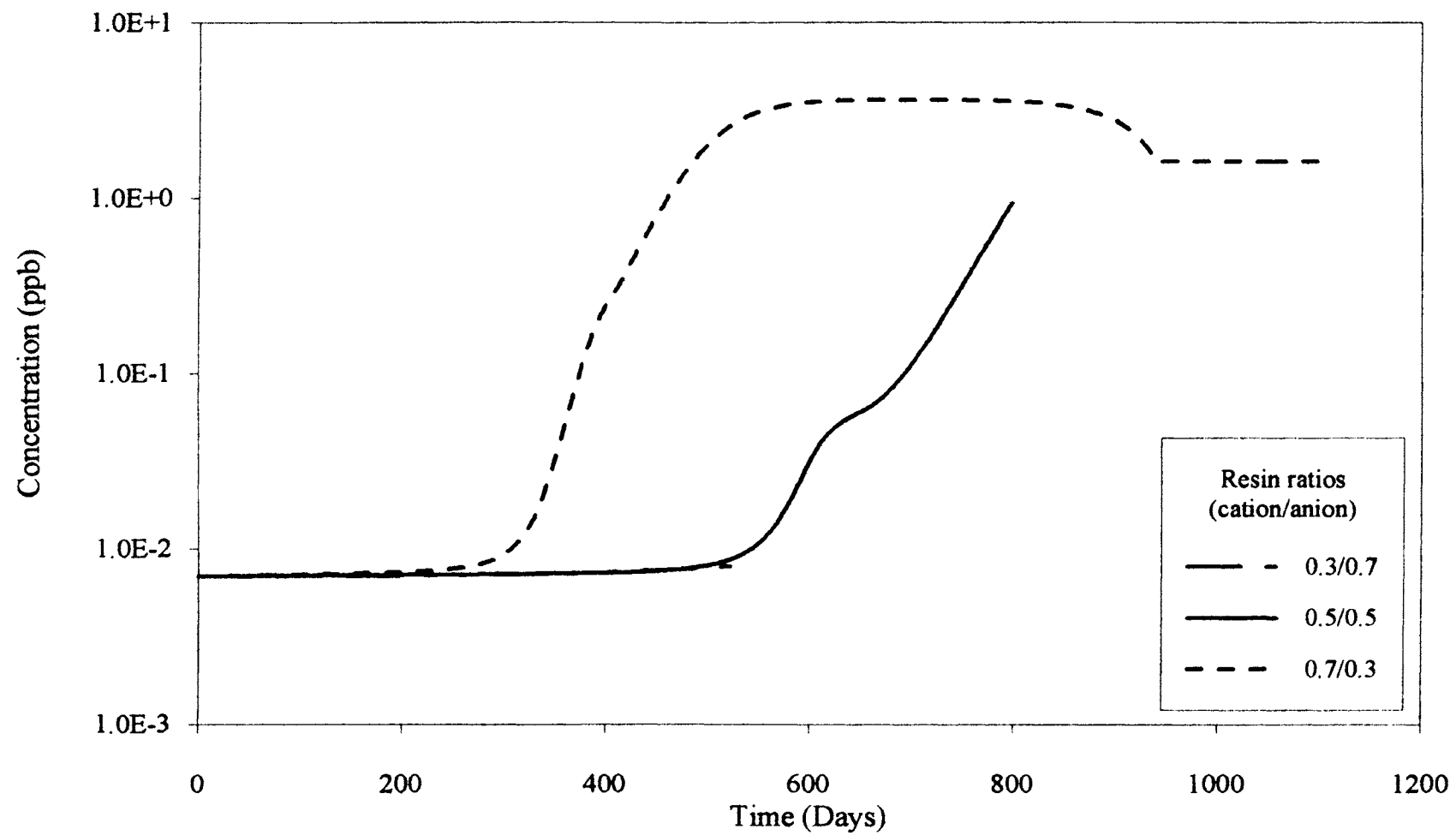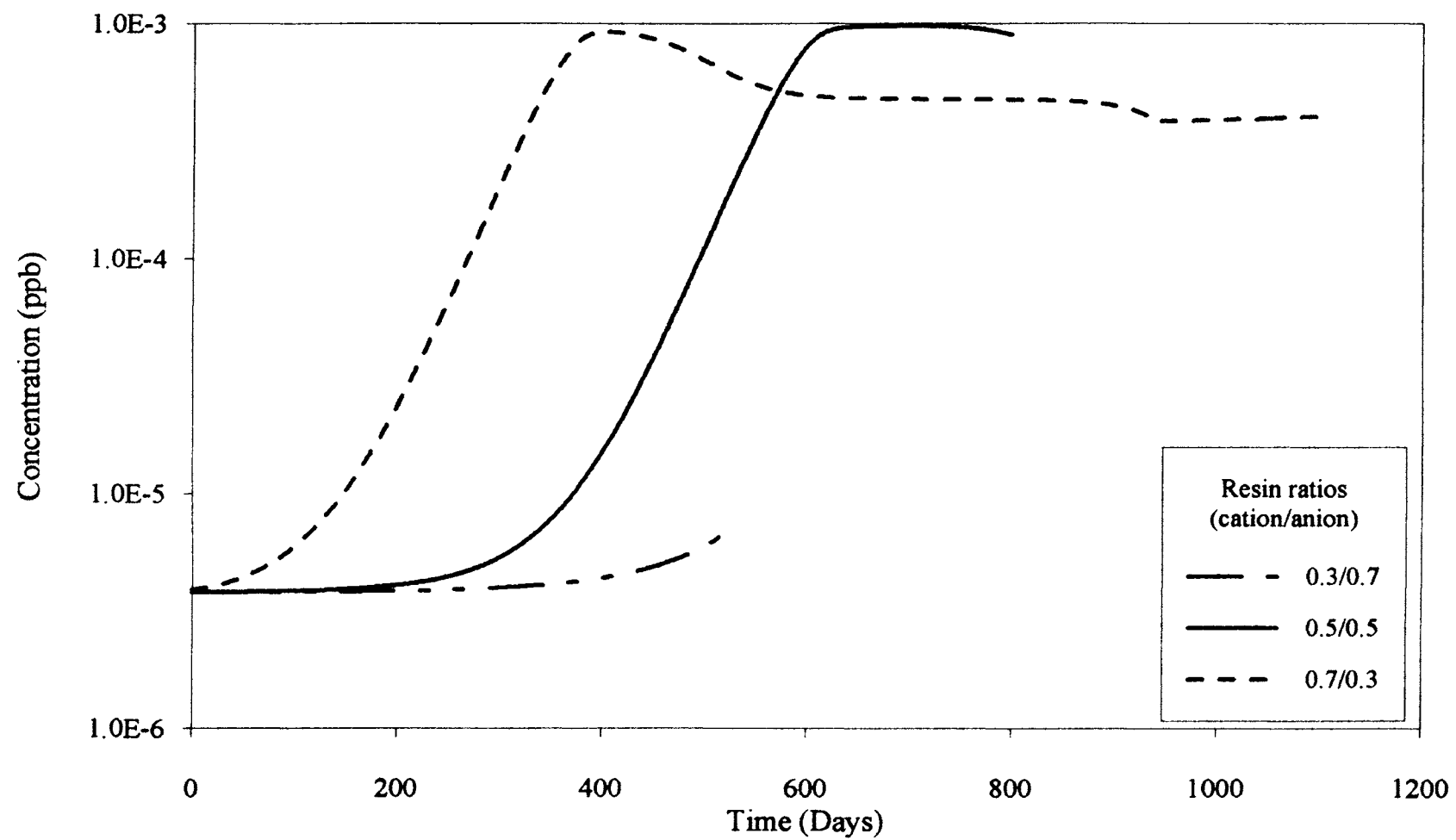
Figure 6. Effect of resin ratios on the effluent concentrations of carbonate
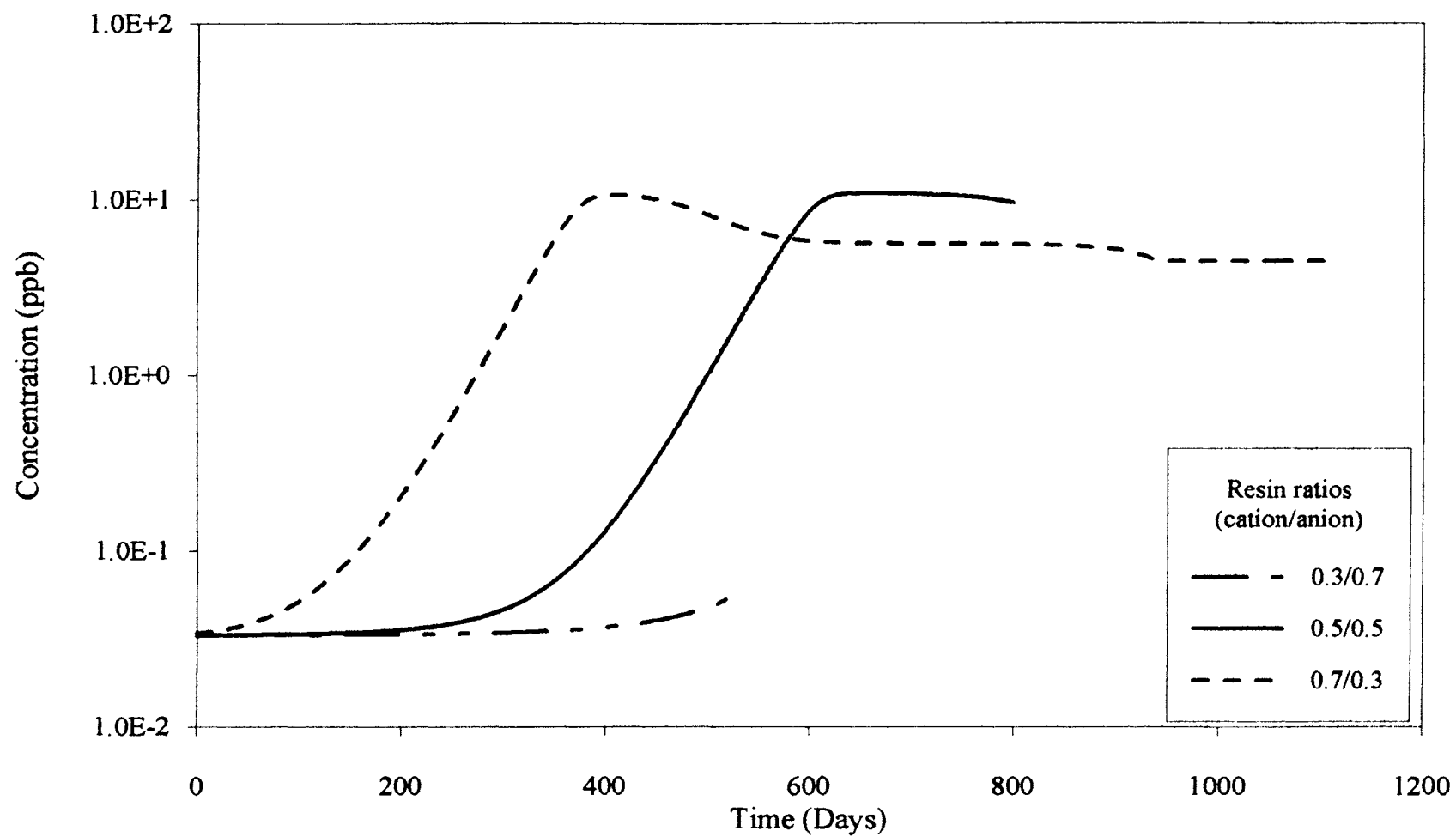
Figure 7. Effect of resin ratios on the effluent concentrations of bicarbonate

Table VII

Effect of resin ratios on ion effluents

Ion	FCR/FAR	Time of Breakthrough (Days)	Equilibrium Leakage (ppb)	% Change in Leakage
	0.7/0.3	700	0.043	0
Sodium	0.5/0.5	500	0.043	--
	0.3/0.7	200	0.043	0
	0.7/0.3	--	6.26×10^{-7}	-98
Calcium	0.5/0.5	600	5.30×10^{-5}	--
	0.3/0.7	280	4.42×10^{-3}	+99
	0.7/0.3	300	6.96×10^{-3}	0
Chloride	0.5/0.5	500	6.96×10^{-3}	--
	0.3/0.7	--	6.96×10^{-3}	0
	0.7/0.3	600	5.91×10^{-2}	131
Sulfate	0.5/0.5	--	2.55×10^{-2}	--
	0.3/0.7	--	1.09×10^{-2}	-57
	0.7/0.3	80	3.80×10^{-6}	0
Carbonate	0.5/0.5	220	3.80×10^{-6}	--
	0.3/0.7	--	3.80×10^{-6}	0
	0.7/0.3	80	3.30×10^{-2}	0
Bicarbonate	0.5/0.5	220	3.30×10^{-2}	--
	0.3/0.7	--	3.30×10^{-2}	0

leakage, while there is a significant change in the breakthrough time. Breakthrough occurs about 140 days earlier than the base case for a cationic resin fraction of 70%. Once again a saturation is reached after about 920 days. No significant breakthrough is observed in the case of 30% cationic resin fraction. This behavior of carbonate and bicarbonate is similar to that of chloride.

Effect of Flow Rate

Three different flow rates are selected in order to study the effect of flow rate on MBIE column performance. Flow rates of 42 gpm/ft^2, 50 gpm/ft^2, and 57 gpm/ft^2 are used. All other parameters are maintained at base case condition.

Figure 8 shows the effect of flow rate on sodium concentration profile. A sharper and earlier breakthrough occurs at high flow rates. Sodium breakthrough occurs about 120 days earlier than the base case (breakthrough after 500 days), for a flow rate of 50 gpm/ft^2. A flow rate of 57 gpm/ft^2 causes the breakthrough to occur about 200 days earlier than the base case. In all the three cases, the final effluent concentrations of sodium are approximately equal to 1.25 ppb. From the figure it can be concluded that flow rate has no effect on the initial leakage of sodium.

Figure 9 shows the concentration profiles of calcium for different flow rates. Unlike sodium, flow rate has significant effect on the initial leakage of calcium as well as the time of breakthrough. Higher flow rates result in higher initial leakages and earlier breakthrough. A flow rate of 50 gpm/ft^2 causes the initial leakage to increase by about 202% and by about 590% for a flow rate of 57 gpm/ft^2, when compared to that of base case of 42 gpm/ft^2. Calcium breaks about 150 days and 250 days earlier than the base case for flow rates 50 gpm/ft^2 and 57 gpm/ft^2, respectively. This is probably due to lesser contact time of the feed water with the resin leading to higher leakages at high flow rates. Figure 10 shows the chloride concentration profiles. The trends are very similar to that of

Figure 8. Effect of flow rate on the effluent concentrations of sodium

Figure 9. Effect of flow rate on the effluent concentrations of calcium
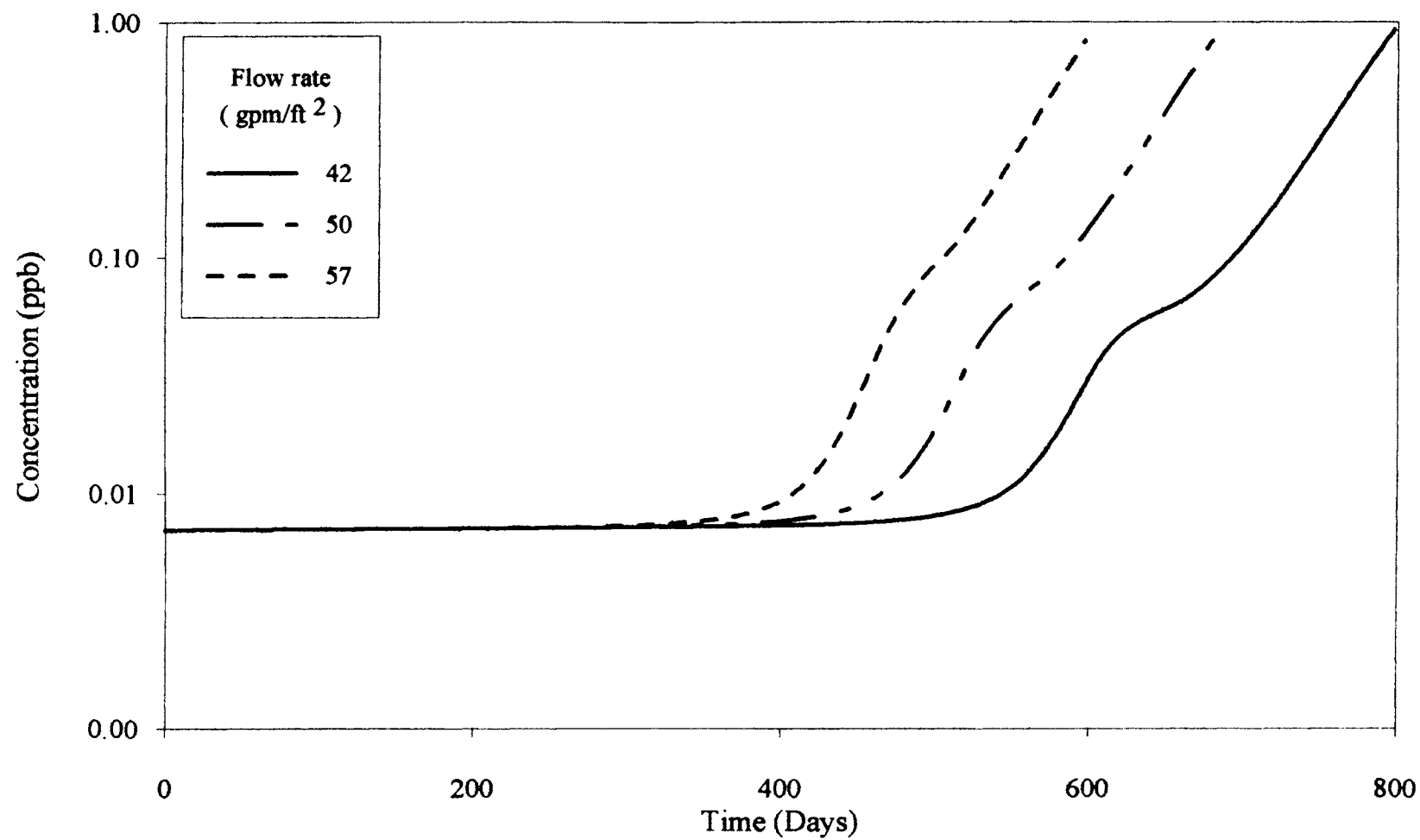
Figure 10. Effect of flow rate on the effluent concentrations of chloride

sodium with flow rate having no effect on the initial leakage of chloride and a significant effect on the time of breakthrough. The breakthrough occurs about 125 days earlier for a flow rate of 50 gpm/ft^2 and about 175 days earlier for a flow rate of 57 gpm/ft^2. Higher flow rates lead to early exhaustion of the bed, thereby resulting in sharper and earlier breakthrough.

Effect of flow rate on sulfate concentrations is shown in Figure 11. Flow rate has a significant effect on both initial leakage and time of breakthrough of sulfate. Unlike calcium, there is an opposite effect on the initial leakage of sulfate, with lower leakages at higher flow rates. As in the case of other ions, there is a similar effect of earlier breakthrough at higher flow rates. There is a 5% decrease in the initial leakage at a flow rate of 50 gpm/ft^2 and about 9.4% decrease at a flow rate of 57 gpm/ft^2. This can be attributed to the constant desulfation of cationic resin. This desulfation is inversely proportional to the flow rate, and is low at higher flow rates, thus resulting in lower leakages. A flow rate of 50 gpm/ft^2 results in a 7% decrease in desulfation while a flow rate of 57 gpm/ft^2 reduces the same by 13%. There is no sharp breakthrough for sulfate in these cases, but the sulfate peak shifted towards left on the time axis for higher flow rates. A slight change in the slope of the chloride effluent curves is observed in all three cases and simultaneously there are peaks in the sulfate effluent profile at the corresponding time for all three cases. This has already been explained in the earlier section.

Figures 12 and 13 show the carbonate and bicarbonate concentration profiles respectively for various flow rates. As in the case of chloride, flow rate had no effect on the initial leakage of these ions and breakthrough occurs earlier at higher flow rates. As explained earlier, carbonate and bicarbonate show similar trends as they are linked by equilibrium. Breakthrough occurs about 105 days earlier for a flow rate of 50 gpm/ft^2 and about 145 days earlier for a flow rate of 57 gpm/ft^2, for both carbonate and bicarbonate. For the base case, the effluent concentrations are constant after about 600

47
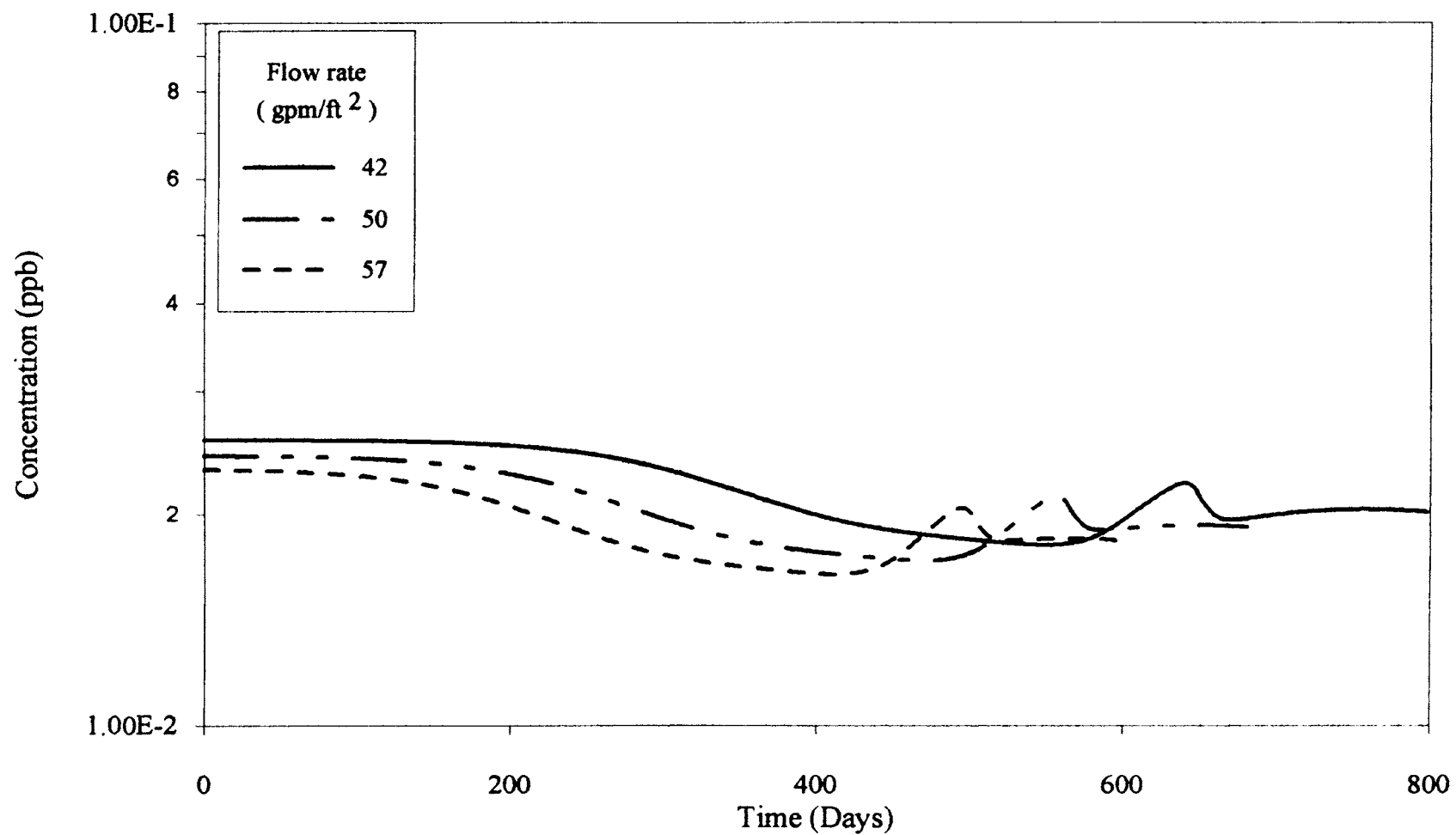
Figure 11. Effect of flow rate on the effluent concentrations of sulfate

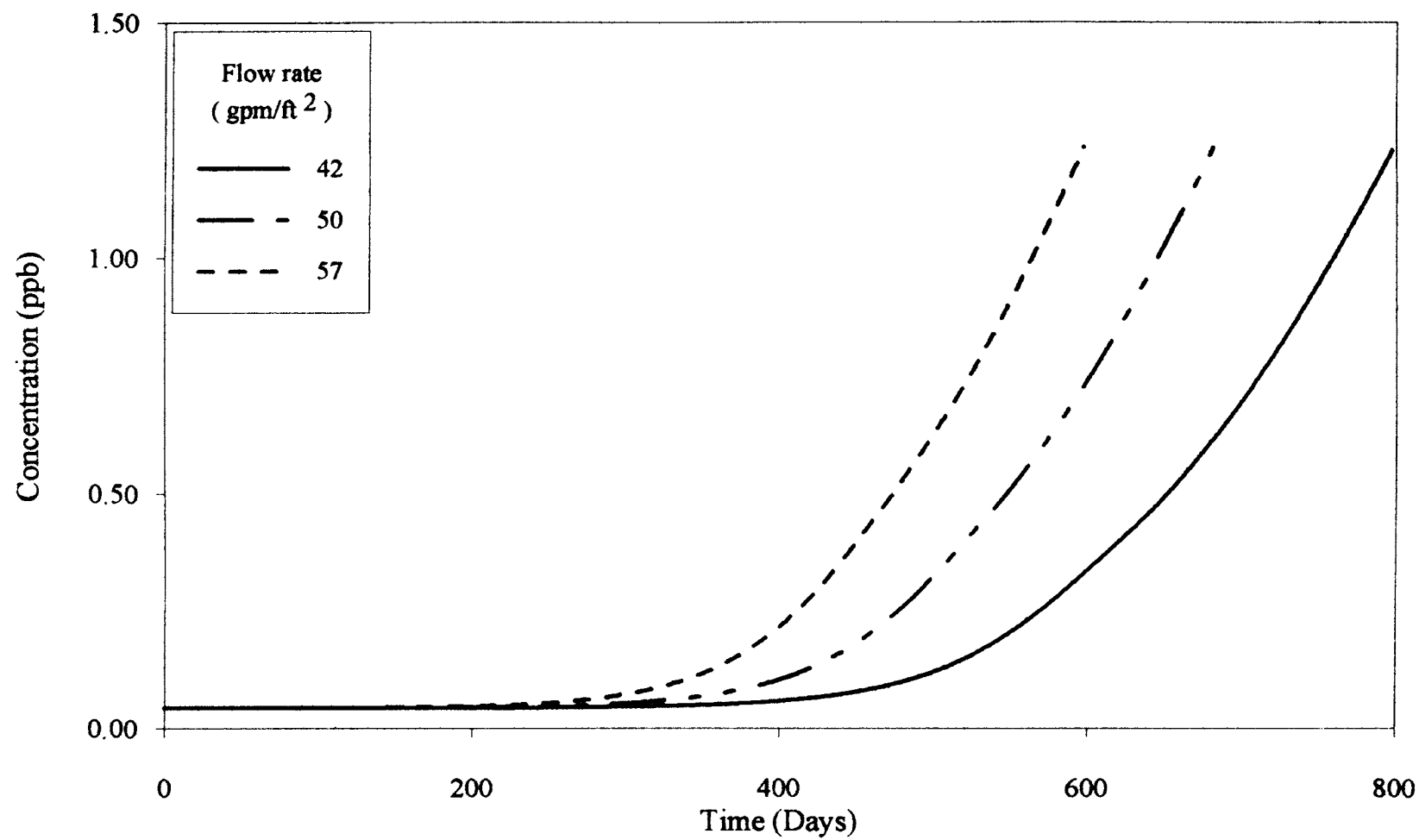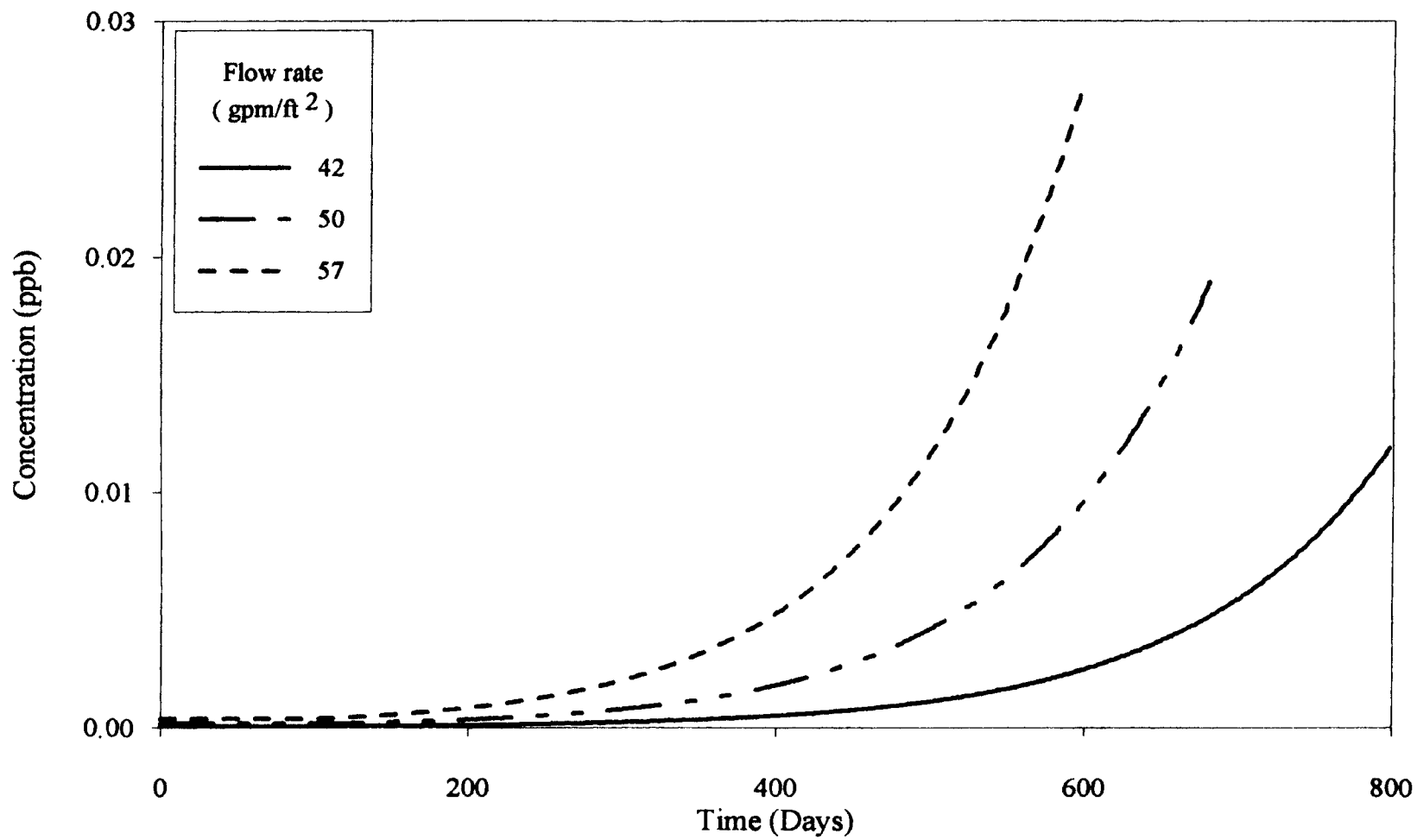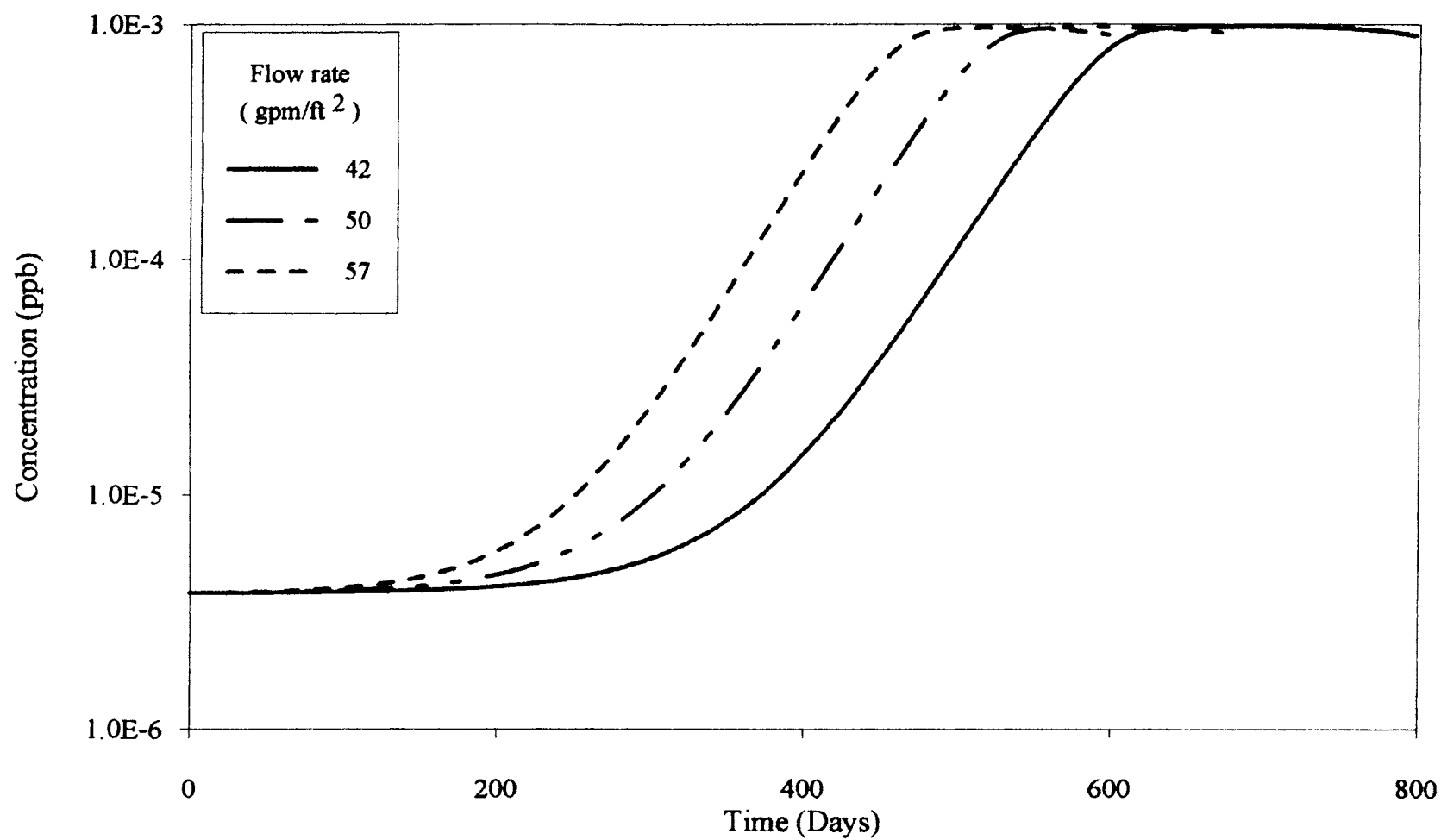Figure 12. Effect of flow rate on the effluent concentrations of carbonate
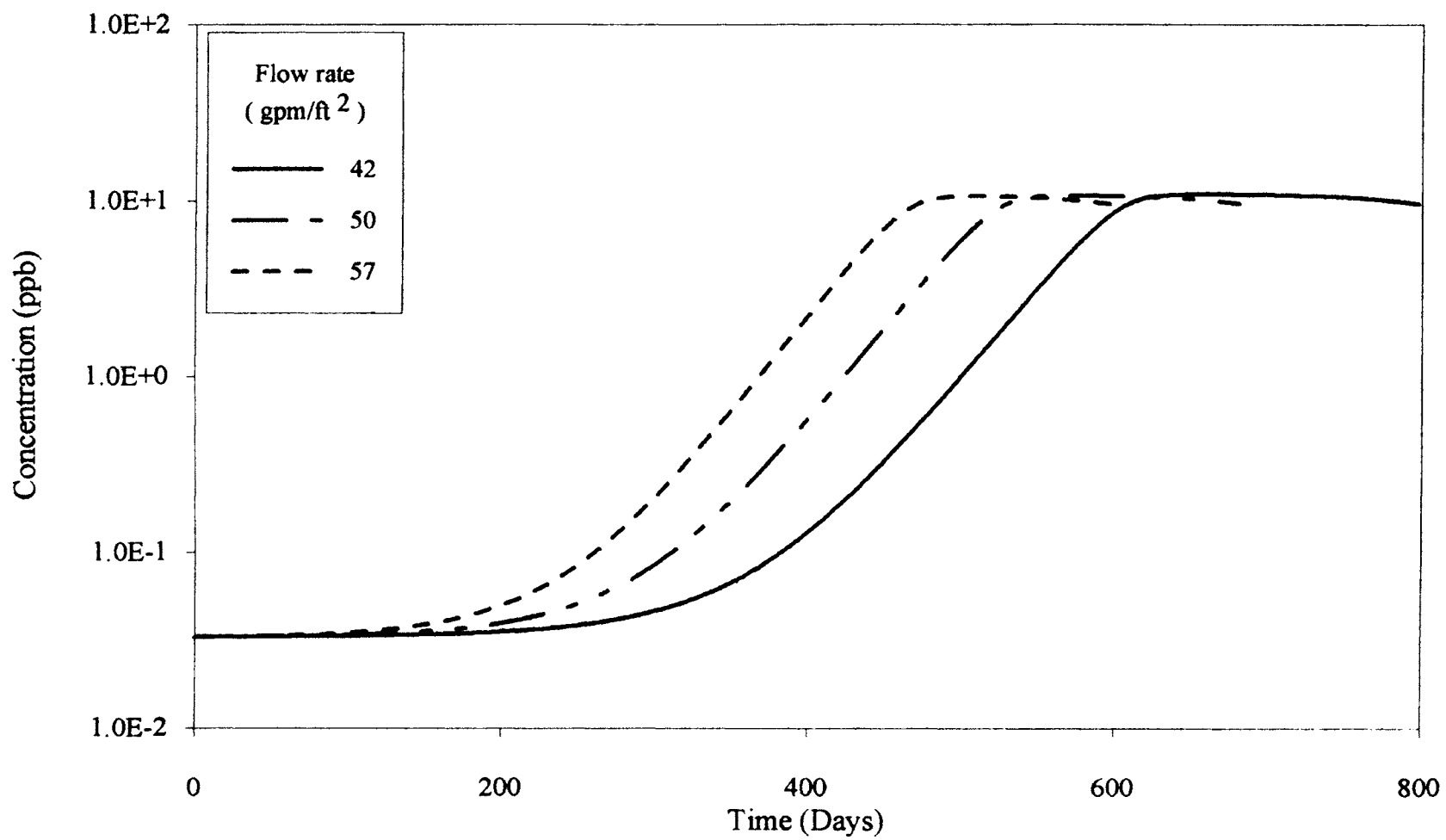
Figure 13. Effect of flow rate on the effluent concentrations of bicarbonate

Table VIII

Effect of flow rate on ion effluents

Ion	Flow Rate gpm/ft^2	Time of Breakthrough (Days)	Equilibrium Leakage (ppb)	% Change in Leakage
	42	500	4.35×10^{-2}	--
Sodium	50	380	4.35×10^{-2}	0
	57	300	4.35×10^{-2}	0
	42	600	5.30×10^{-5}	--
Calcium	50	450	1.60×10^{-4}	202
	57	350	3.68×10^{-4}	590
	42	575	6.96×10^{-3}	--
Chloride	50	450	6.96×10^{-3}	0
	57	400	6.96×10^{-3}	0
	42	--	2.55×10^{-2}	--
Sulfate	50	--	2.42×10^{-2}	-5
	57	--	2.31×10^{-2}	-9.4
	42	325	3.80×10^{-6}	--
Carbonate	50	220	3.80×10^{-6}	0
	57	180	3.80×10^{-6}	0
	42	325	3.30×10^{-2}	--
Bicarbonate	50	220	3.30×10^{-2}	0
	57	180	3.30×10^{-2}	0

days. The same occurs in the case of higher flow rates too, but earlier than that for base case. There is large difference in the magnitudes of carbonate and bicarbonate concentrations (carbonate: about 0.001 ppb; bicarbonate: about 11 ppb) because of the difference in their dissociation constants. The first dissociation constant K_1 is about 4.45×10^{-7} while the second dissociation constant K_2 is about 4.69×10^{-11}. Thus equilibrium favors the presence of bicarbonate over carbonate. Also, pH and the concentrations of other ions determine the equilibrium between carbonic species.

Effect of Temperature

The temperature dependent parameters in this model are listed in Table III, Chapter III. These are ionic diffusion coefficients, ionization constants for water and carbonic species, bulk solution viscosity and resin selectivity coefficients. However, Table III does not list any temperature correlations for selectivity coefficients because of lack of data in a multicomponent case. Foutch (1991) has discussed in detail the temperature effects on MBIE performance. Three different temperatures are selected by Pennsylvania Power & Light Co. for this study. These are 32.2°C, 48.9°C and 60°C (90° F, 120°F and 140°F respectively). All other parameters are maintained at the base case condition.

Figure 14 shows the effect of temperature on the effluent concentrations of sodium. High temperatures lead to steeper and earlier breakthrough. There is a small change in the initial leakage of sodium with temperature, leakage decreasing with decreasing temperature. Breakthrough is delayed by about 75 days at a temperature of 48.9°C and by about 110 days at a temperature of 32.2°C when compared to the base case. This may be due to the decrease in the diffusion coefficient of sodium with decrease in temperature. Also, ion exchange is an exothermic process with increasing temperature having an adverse effect on selectivity coefficient and equilibria. This leads
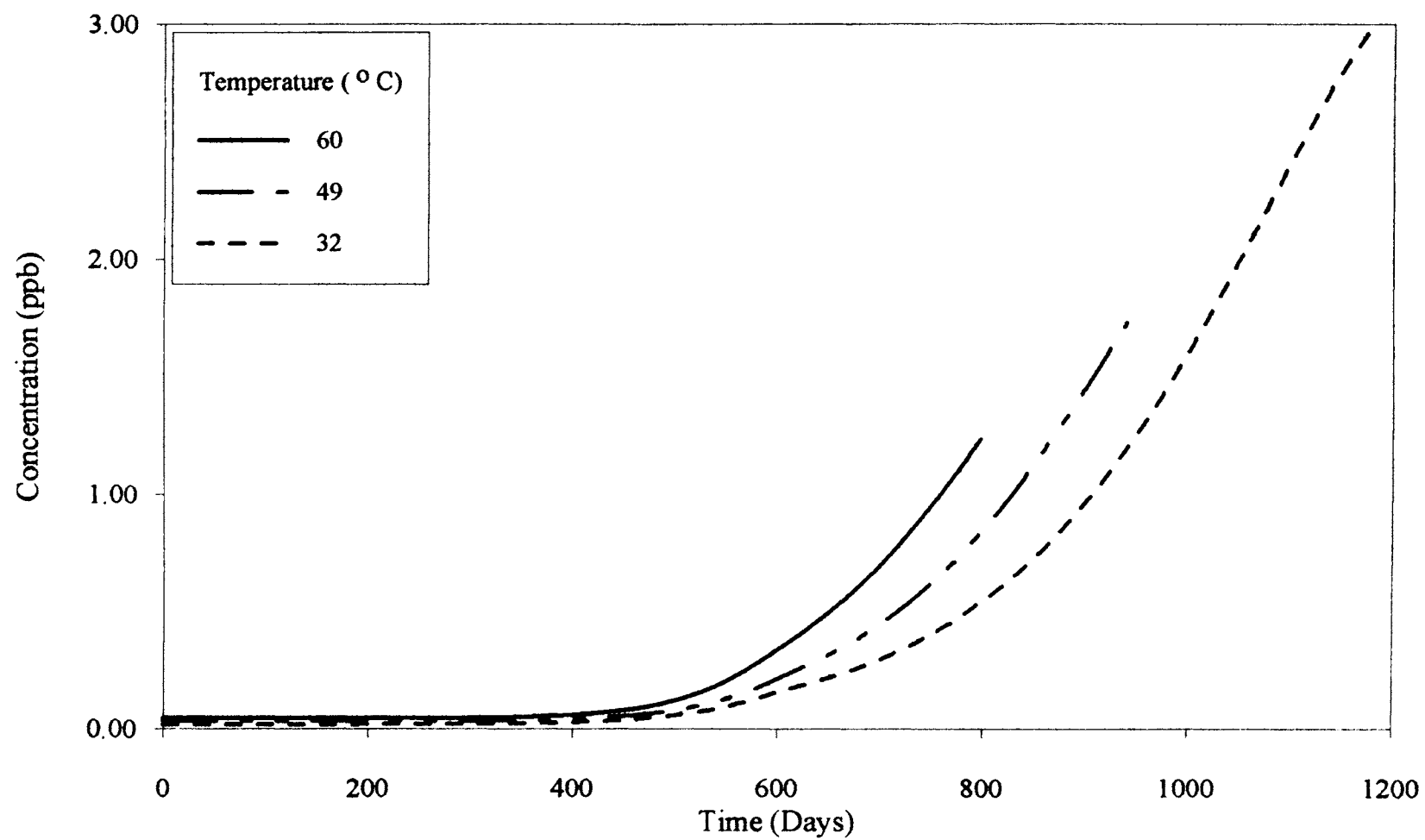
Figure 14. Effect of temperature on the effluent concentrations of sodium

to earlier breakthrough at higher temperatures. The final effluent concentrations of sodium vary significantly with temperature. High temperatures lead to early exhaustion of the bed and give lower effluent-to-feed concentration ratio. There is a 38% increase in final effluent-to-feed concentration ratio at a temperature of 48.9°C and about 130% increase at a temperature of 32.2°C.

The effect of temperature on calcium effluent concentrations is shown in Figure 15. As seen in the earlier effects, temperature has a significant effect on both the initial leakage and breakthrough of calcium. Initial leakage of calcium increases with a decrease in temperature. Initial leakage of about 1.97×10^{-4} ppb is observed at temperature of 48.9° C and about 1.44×10^{-3} ppb at 32.2°C when compared to that of 5.3×10^{-5} ppb at 60°C. This is probably due to a significant decrease in calcium diffusion coefficient at low temperatures leading to higher leakages. There is a 73% decrease in calcium diffusion coefficient when temperature is reduced from 60°C to 32.2°C. Decreasing temperatures result in delayed breakthrough. There is a breakthrough delay of about 100 days at a temperature of 48.9°C while the same is delayed by about 190 days at 32.2°C. As in the case of sodium, the final effluent to feed concentration is higher at lower temperatures.

Figure 16 shows chloride effluent concentrations for the three different temperatures. Chloride shows a similar trend as that of sodium. Lower temperatures increase the effluent to feed concentration ratio and there is a significant change in the initial leakage of chloride with change in temperature. But unlike sodium, temperature did not have any effect on breakthrough time of chloride. The final effluent concentration increases by about 3.0 ppb at a temperature of 48.9°C and by about 3.5 ppb at a temperature of 32.2°C when compared to 1.1 ppb at 60°C. The initial leakage decreases by about 28% and 57% for temperatures of 48.9°C and 32.2°C, respectively. A constant effluent concentration is observed after about 1000 days at a temperature of 32.2°C. In all three cases, a sharp change in the slope of the breakthrough is observed after about
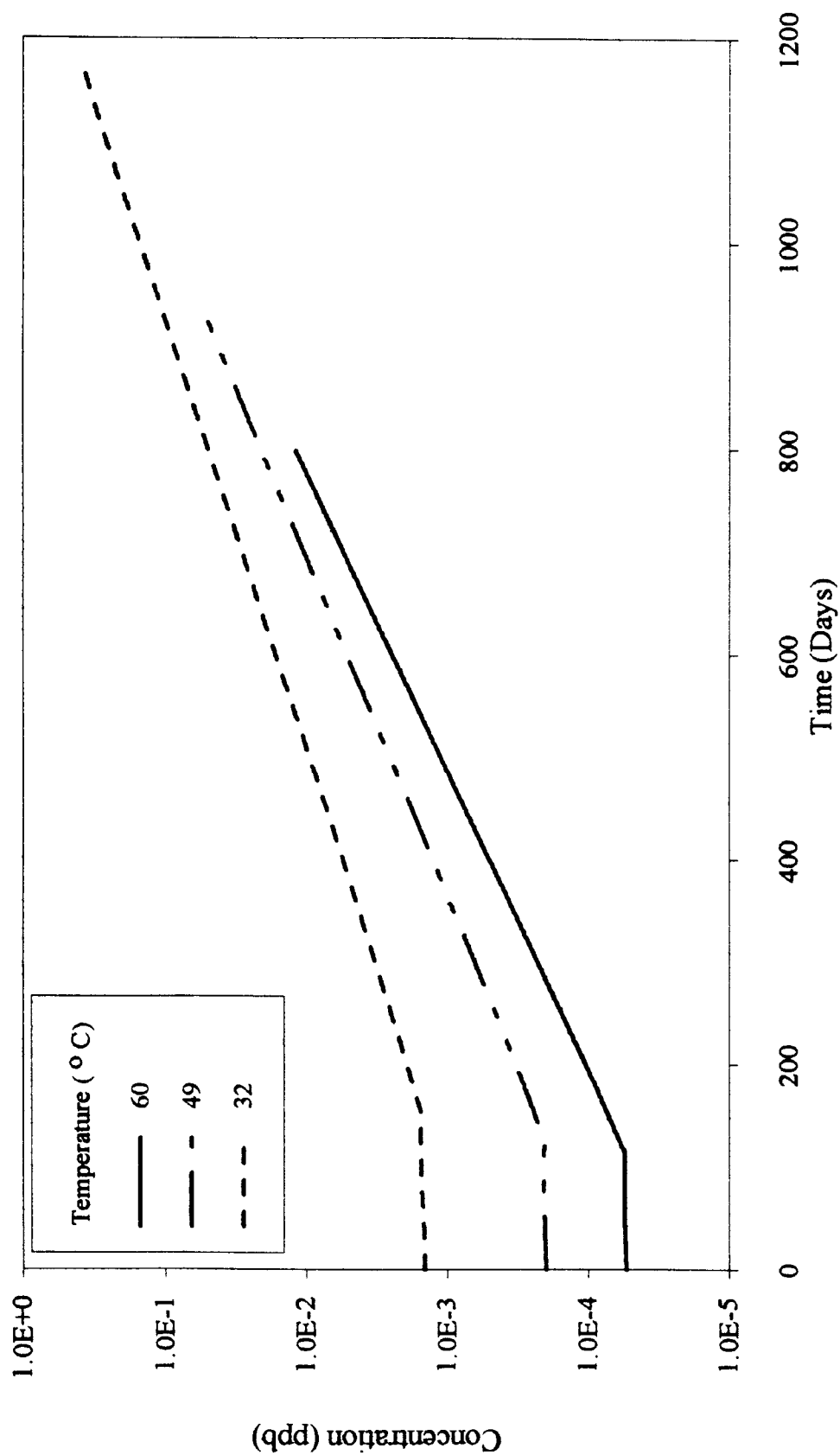
Figure 15. Effect of temperature on the effluent concentrations of calcium
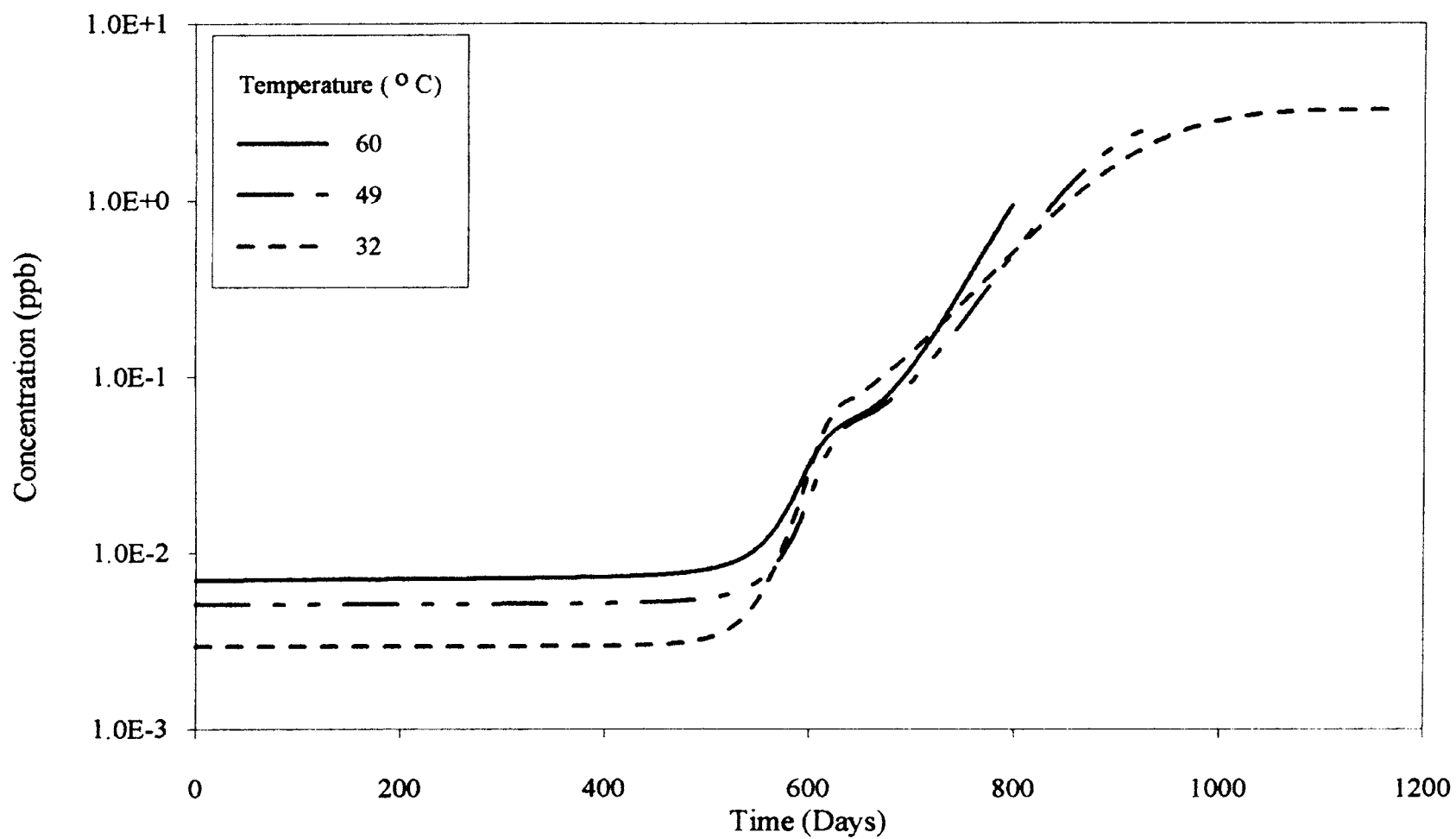
Figure 16. Effect of temperature on the effluent concentrations of chloride

600 days. This is due to a sudden peak in the sulfate effluent concentration profile resulting in more chloride loading onto the resin.

Figure 17 shows the sulfate effluent concentration profiles at different temperatures. As in the case of chloride, lower temperatures result in a decrease of the initial leakage of sulfate but on a larger scale. A 61% and 91% decrease in the initial leakage of sulfate is observed at temperatures of 48.9°C and 32.2°C, respectively. This is because of the cationic resin desulfation which is a strong function of temperature. There is a 87% decrease in the desulfation when temperature is reduced from 60°C 32.2°C. No significant breakthrough is observed at temperatures of 60°C and 48.9°C, while breakthrough occurs at about 1000 days at 32.2°C. In all three cases, a peak in the effluent profile is observed at about 600 days. As in the case of sodium and chloride, resin exhaustion is delayed by lowering temperature.

Effect of temperature on carbonate and bicarbonate effluent concentrations is shown in Figures 18 and 19. Once again, as in the case of chloride, temperature did not have a significant effect on the breakthrough time of these ions. However, it can be inferred from the curves that higher temperatures lead to earlier breakthrough. Breakthrough occurs at about 325 days for both the ions. Bicarbonate shows a greater decrease in the initial leakage with decrease in temperature, than carbonate. A temperature of 48.9°C leads to a 8.4% decrease in the initial leakage of carbonate and about 20% decrease in the case of bicarbonate. There is a 26% and 58% decrease in the initial leakage of carbonate and bicarbonate respectively at 32.2°C. This is because of stronger dependence of K_1 over K_2, on temperature. A change in temperature from 60°C to 32.2°C reduces K_1 by about 70% while, K_2 is reduced only by about 27%. Unlike chloride, temperature did not have much effect on the final effluent-to-feed concentration ratio. But it can be observed that lower temperatures lead to higher effluent-to-feed concentration ratio. For both carbonate and bicarbonate, an almost constant effluent concentration is observed after about 600 days in all three cases.
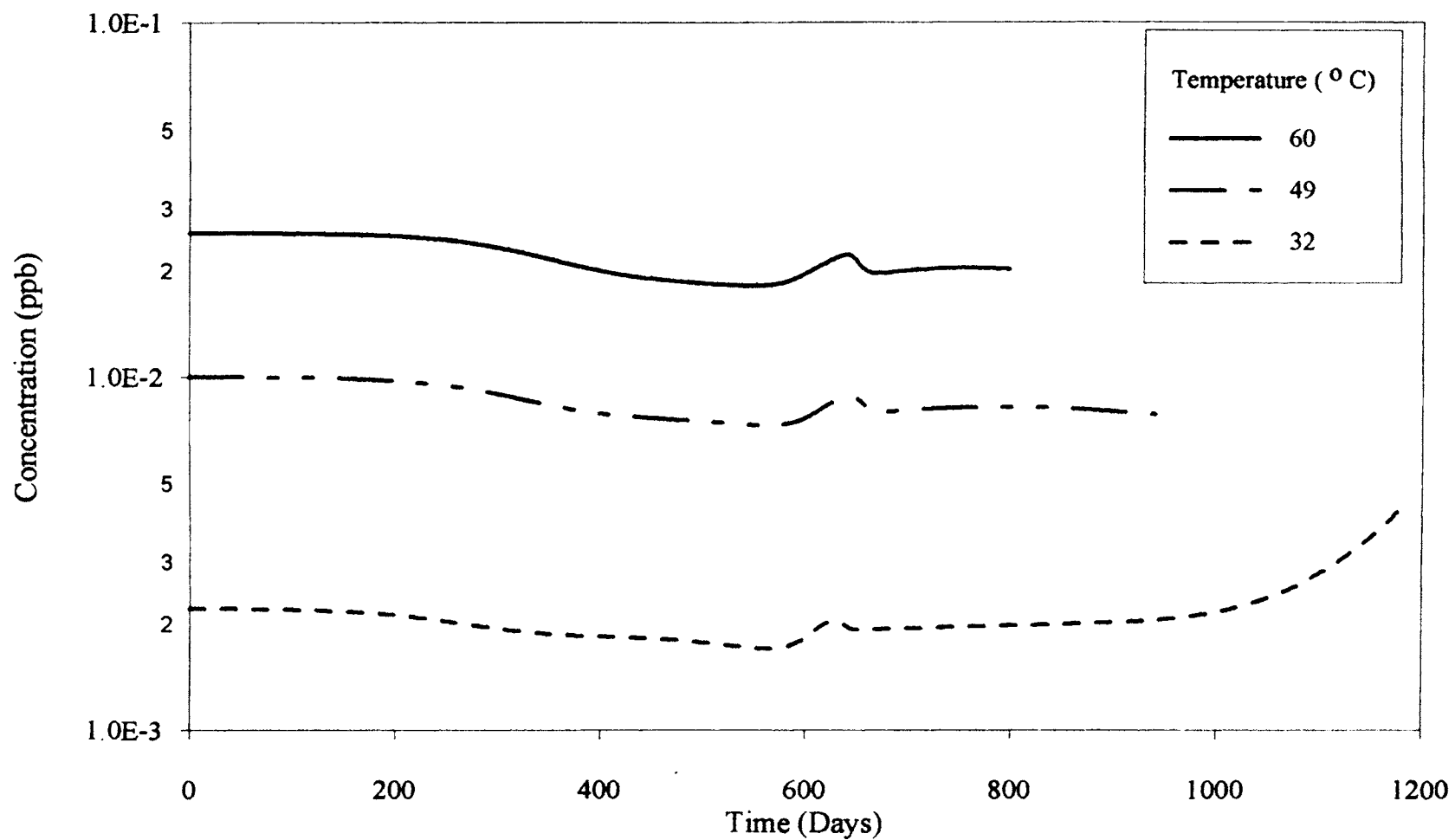
Figure 17. Effect of temperature on the effluent concentrations of sulfate
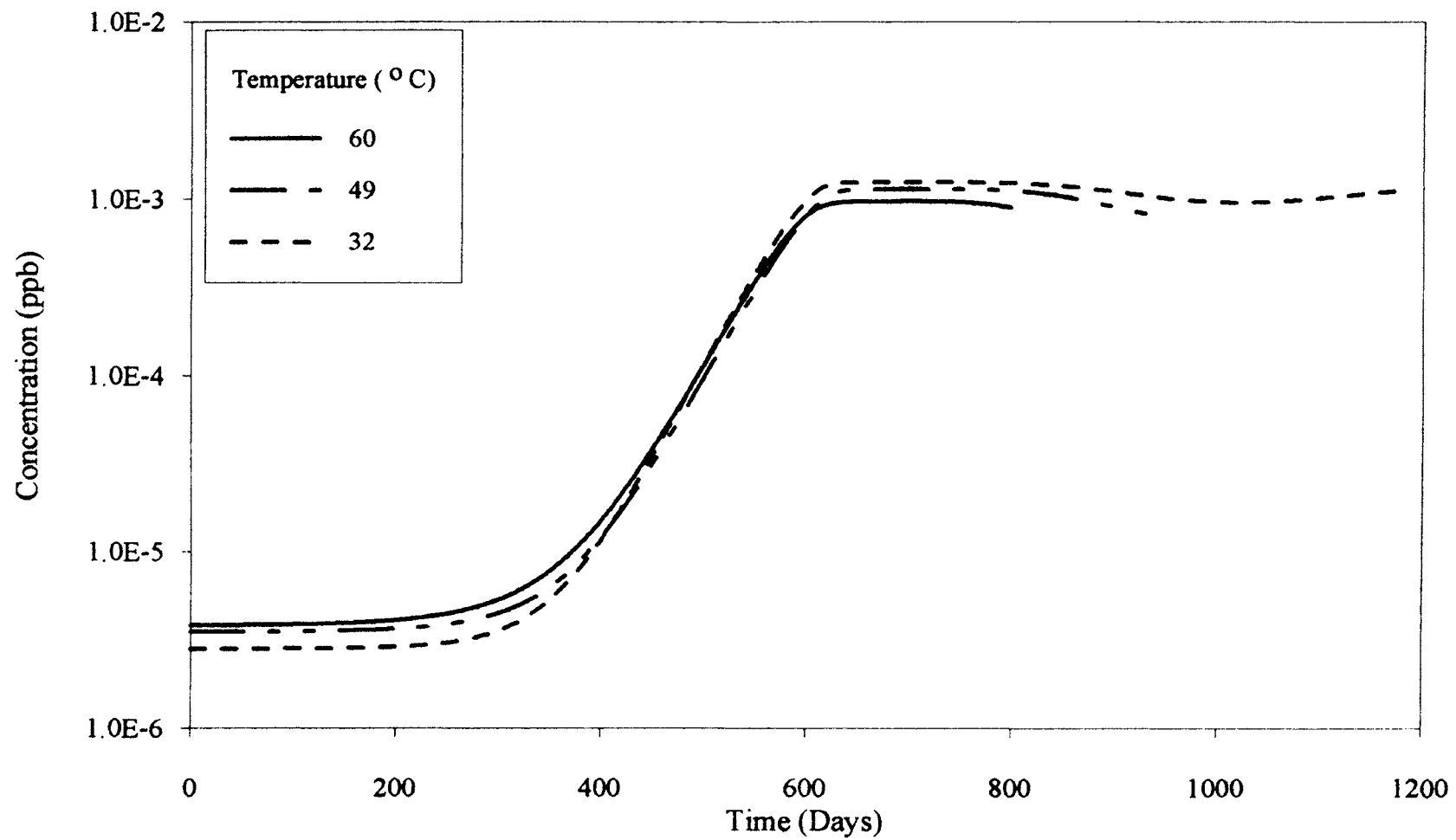
Figure 18. Effect of temperature on the effluent concentrations of carbonate
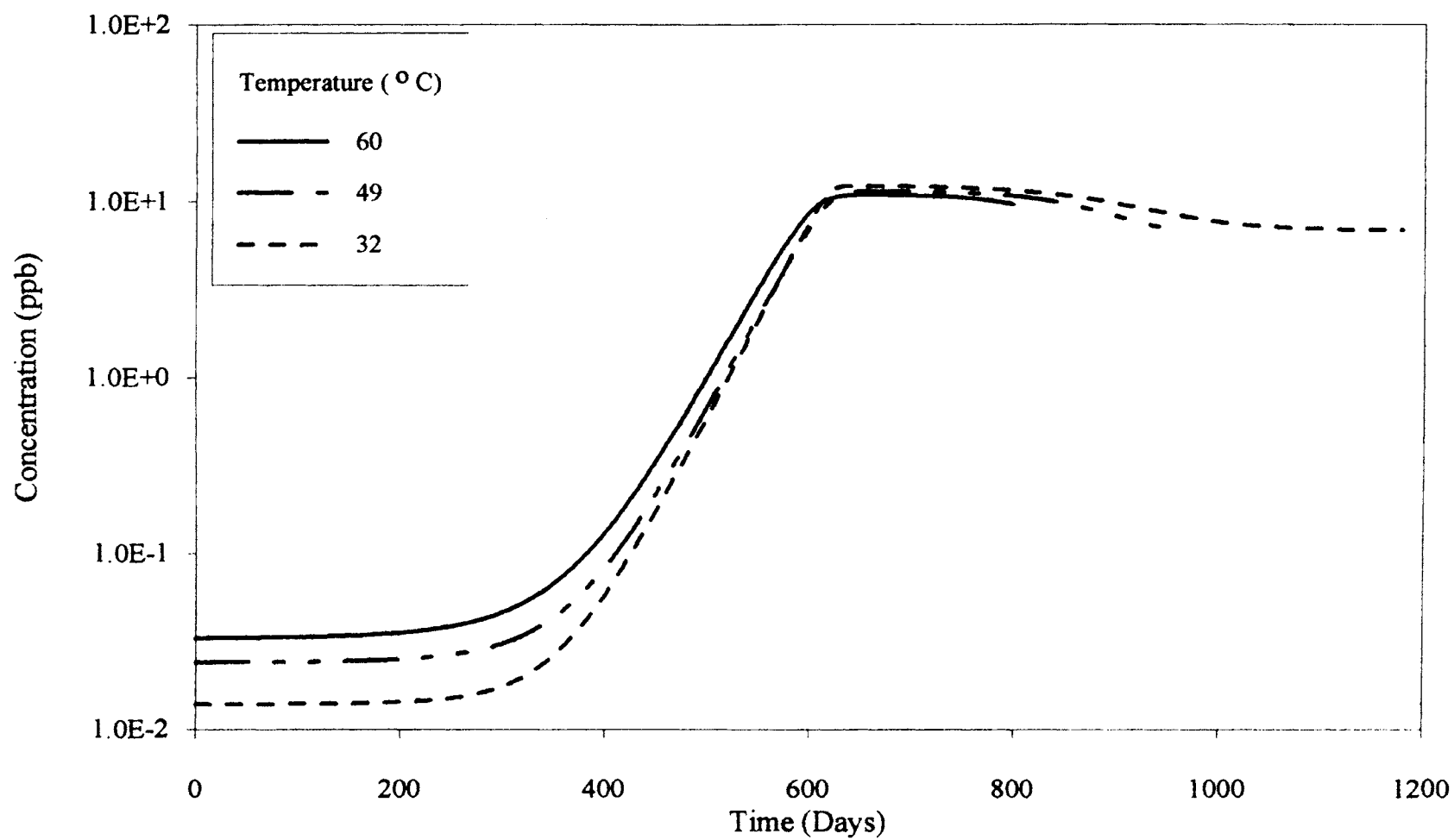
Figure 19. Effect of temperature on the effluent concentrations of bicarbonate

Table IX

Effect of temperature on ion effluents

Ion	Temperature (°C)	Time of Breakthrough (Days)	Equilibrium Leakage (ppb)	Final effluent Concentration (ppb)
Sodium	60	500	4.35×10^{-2}	1.23
	48.9	575	3.17×10^{-2}	1.73
	32.2	610	1.84×10^{-2}	2.98
Calcium	60	600	5.30×10^{-5}	1.18×10^{-2}
	48.9	700	1.97×10^{-4}	5.59×10^{-2}
	32.2	790	1.44×10^{-3}	3.96×10^{-1}
Chloride	60	510	6.96×10^{-3}	0.92
	48.9	510	5.00×10^{-3}	2.71
	32.2	510	2.94×10^{-3}	3.26
Sulfate	60	--	2.55×10^{-2}	2.01×10^{-2}
	48.9	--	1.00×10^{-2}	7.80×10^{-3}
	32.2	1000	2.20×10^{-3}	4.20×10^{-3}
Carbonate	60	325	3.80×10^{-6}	8.96×10^{-4}
	48.9	325	3.48×10^{-6}	8.05×10^{-4}
	32.2	325	2.80×10^{-6}	1.11×10^{-3}
Bicarbonate	60	325	3.30×10^{-2}	9.60
	48.9	325	2.40×10^{-2}	7.16
	32.2	325	1.39×10^{-2}	6.84

Effect of Resin Heels

In industrial MBIE columns, it is difficult to achieve a well mixed bed in service vessels. About 10% of the bed, primarily in the form of cationic resin (due to its weight), classifies at the bottom of the bed during the ultrasonic vessel cleaning up process. It was believed that these cation rich heels at the outlet contributed to high sulfate levels observed in reactor water (Foutch et al, 1994). Personnel at Pennsylvania Power & Light Co. have tried replacing the cationic heels with an anionic underlay. In this work, simulations were run with cationic and anionic heels to predict the effect of such heels on the effluent concentrations and to compare them with the ideal case of a homogeneous mixed bed (base case). The bottom 5 cm. of the bed is considered to be a 5:1 anionic resin rich layer for the anionic heel. The total resin capacity is assumed to be the same.

Figures 20 and 21 show the effluent concentration profiles for sodium and calcium respectively, for cationic and anionic heels. The initial leakage of sodium did not vary with the presence of heels while that of calcium increased for an anionic underlay and decreased for a cationic underlay. This is probably due to the very high selectivity coefficient of calcium leading to more loading in the case of a cationic heel and consequently lower initial leakage. An anionic underlay leads to a 33% increase in the initial leakage of calcium while a cationic heel reduces the same by about 45%. Presence of heels did not have any effect on the time of breakthrough of sodium or calcium. For both ions, an anionic heel results in a higher effluent to feed concentration ratio while a cationic heel lowers the same.

Chloride and sulfate effluent concentration profiles are shown in Figures 22 and 23 respectively. Initial leakage of chloride did not vary with the presence of heels while that of sulfate showed a lot of variation. Initial leakage of sulfate decreases by 69% with an anionic heel while it increases by about 127% with a cationic heel. It can also be observed from the figures that the effluent to feed concentration ratio is very low
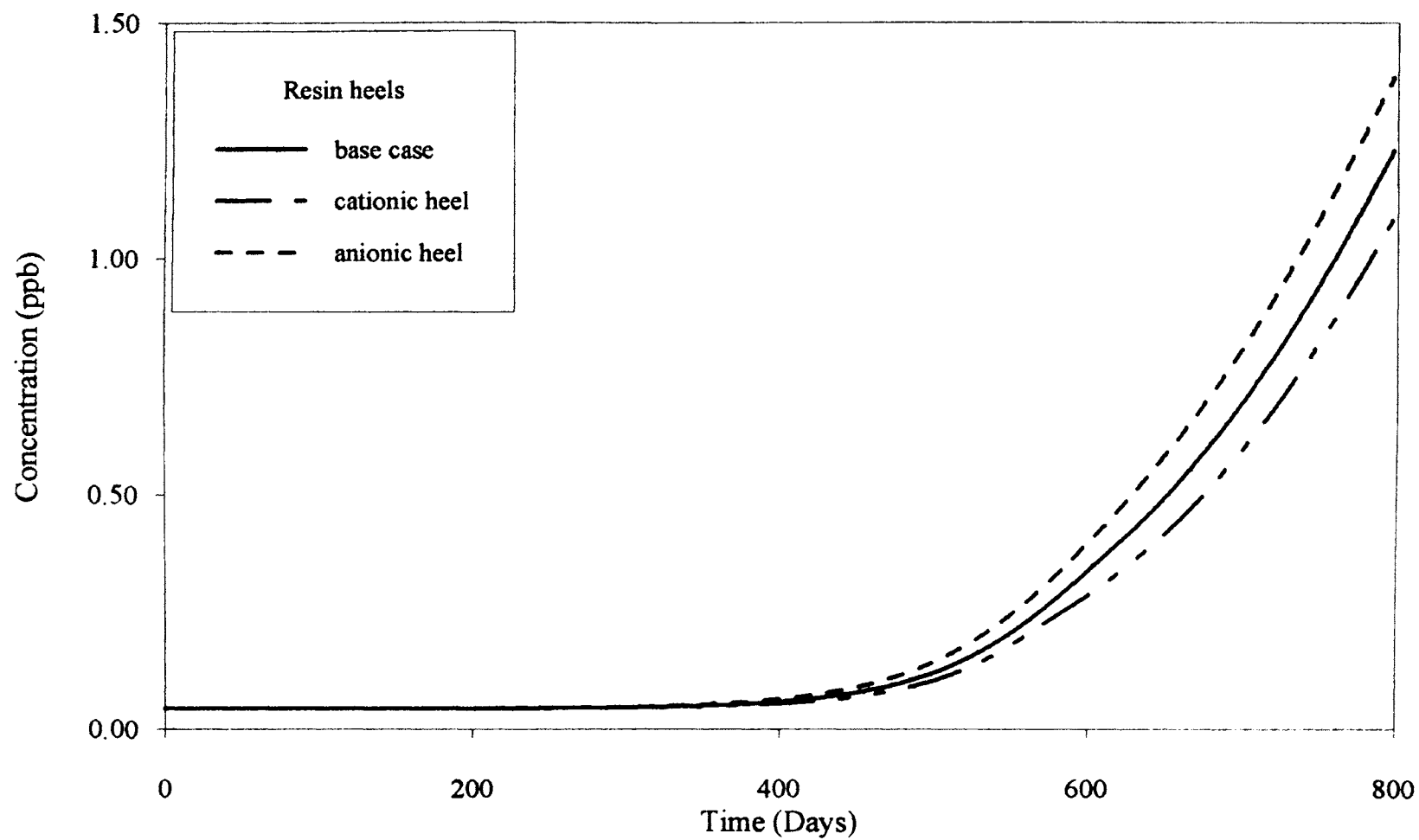
Figure 20. Effect of resin heels on the effluent concentrations of sodium
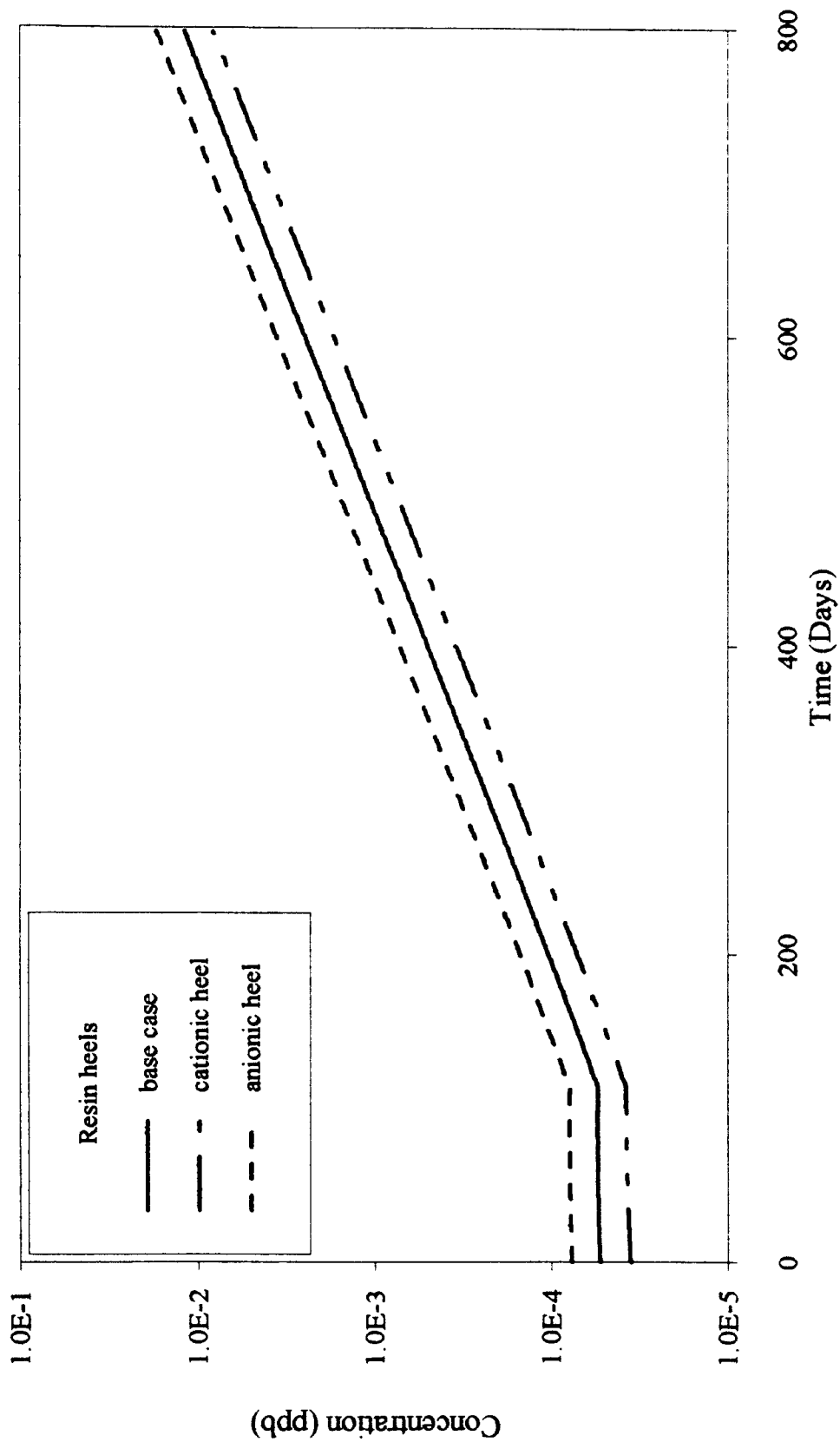
Figure 21. Effect of resin heels on the effluent concentrations of calcium
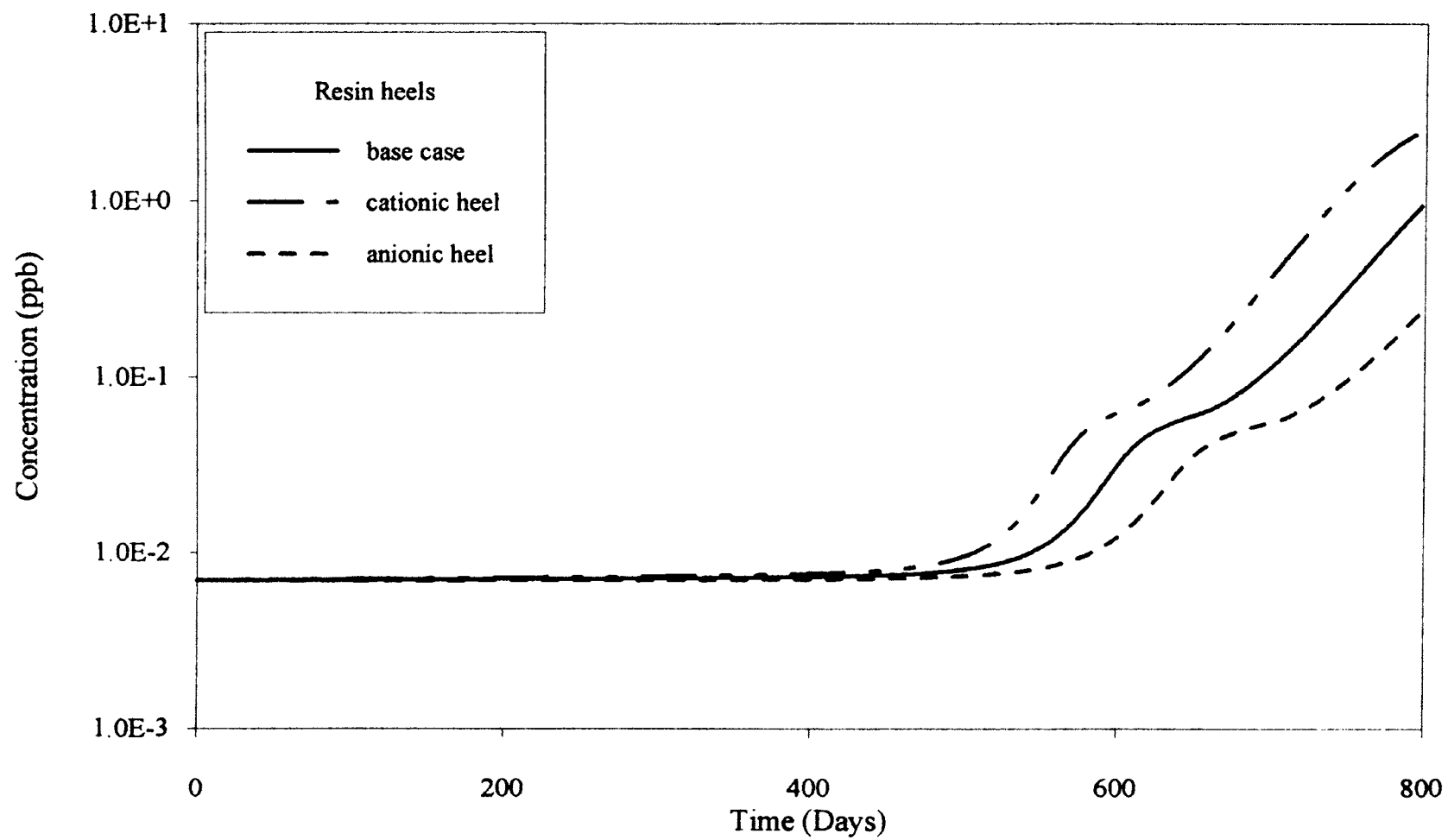
Figure 22. Effect of resin heels on the effluent concentrations of chloride
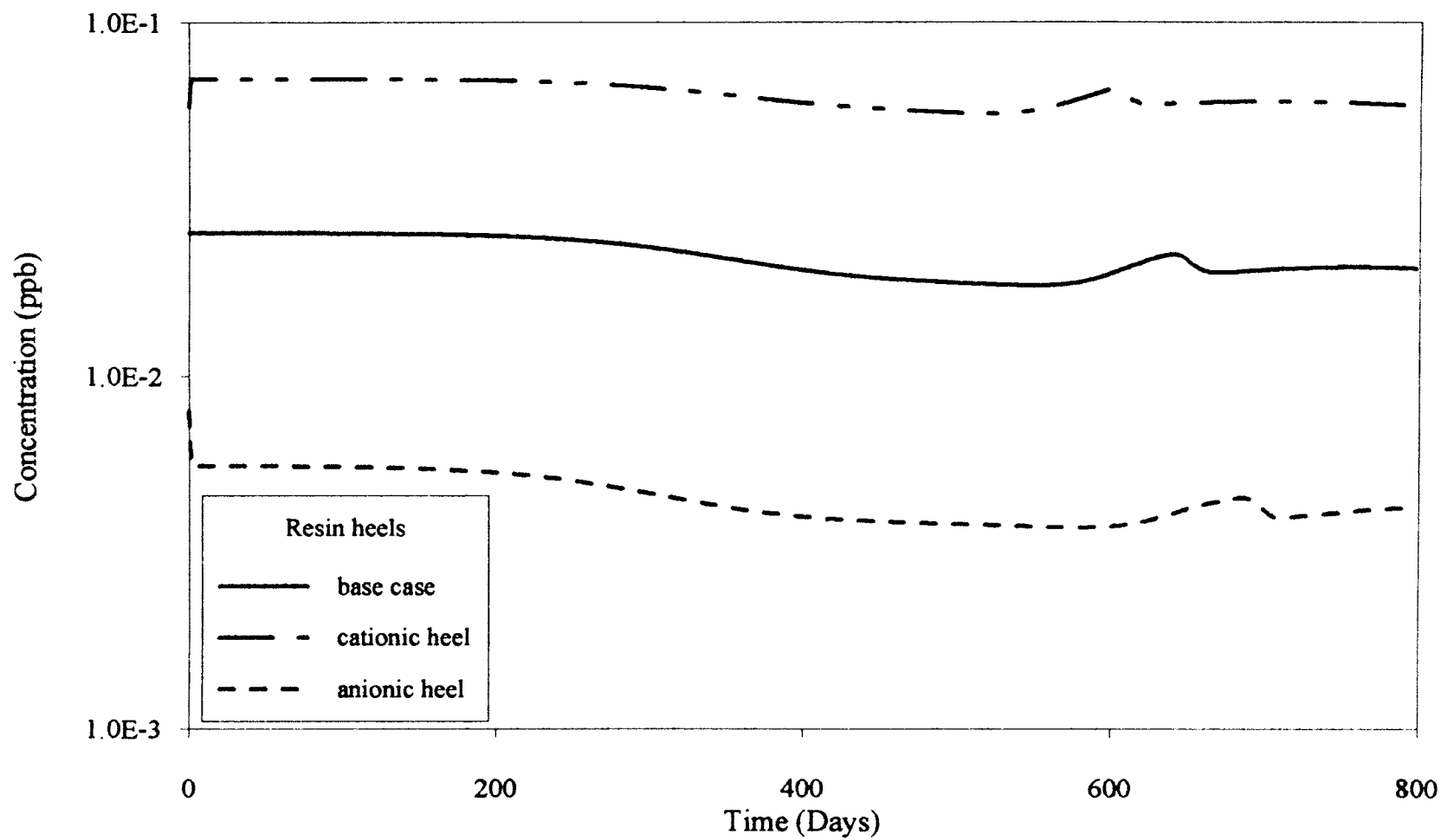
Figure 23. Effect of resin heels on the effluent concentrations of sulfate

(reduced by about 60%) in the presence of an anionic heel. There is a 68% increase in desulfation with a cationic heel while, the same reduces by about 67% in the presence of an anionic heel when compared to that of base case. This shows that an anionic heel is very effective in reducing the sulfate concentrations in the effluent water. This is because of the release of sulfate from cationic resin which accounts for most of the equilibrium leakage from the mixed bed. Chloride breakthrough is delayed by about 65 days with an anionic heel while a cationic heel lead to an earlier breakthrough by about 30 days when compared to the base case. There is no significant breakthrough of sulfate ion in all three cases.

Figures 24 and 25 show the effluent concentrations of carbonate and bicarbonate with and without resin heels. As in the case of chloride, the initial leakage is constant in all cases for both the ions. Breakthrough is slightly delayed in the presence of an anionic heel when compared to the base case (about 20 days for both ions). The effluent concentrations are approximately constant after 600 days in all three cases.

Effect of Particle Sizes

In this model, the mass transfer coefficient is calculated using Kataoka's correlation which can be approximately written as follows:

$$K_i \propto \left(d_p\right)^{-\frac{2}{3}}$$

Bead size enters the mass transfer coefficient through the particle Reynolds number. Two particle sizes are used in this study:

Cationic resin: 0.08 cm; Anionic resin: 0.06 cm

Cationic resin: 0.065 cm; Anionic resin: 0.055 cm
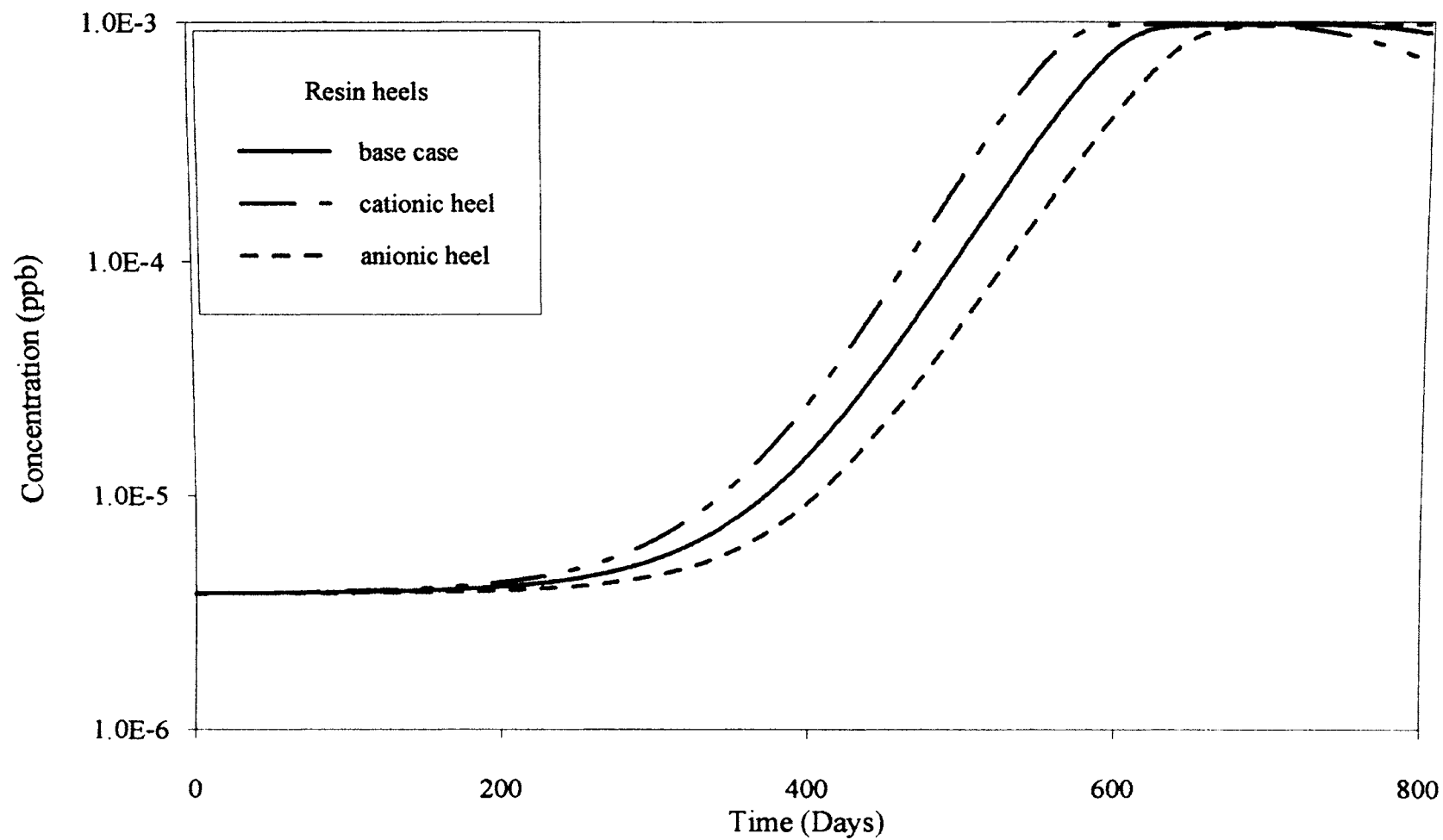
Figure 24. Effect of resin heels on the effluent concentrations of carbonate
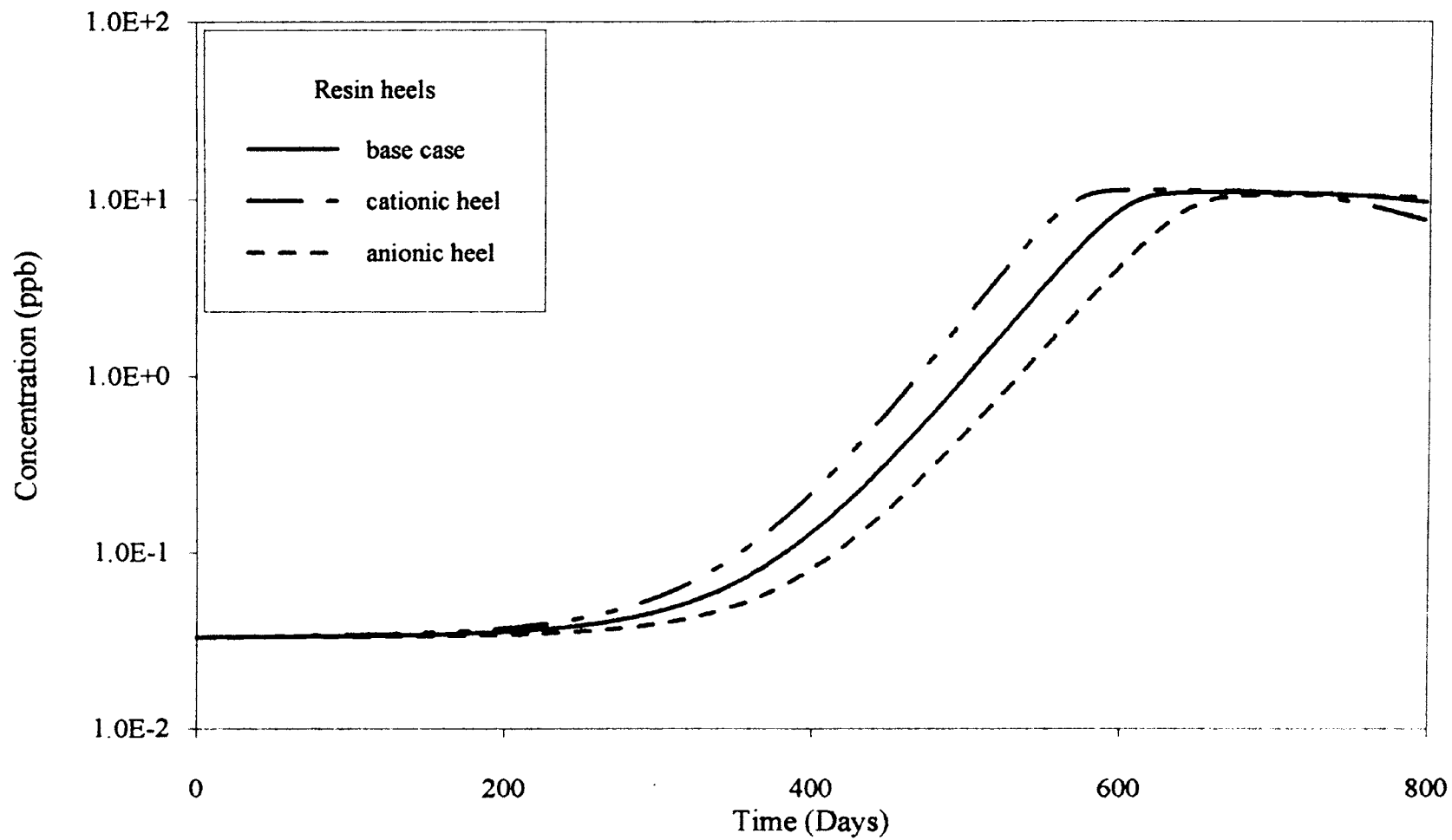
Figure 25. Effect of resin heels on the effluent concentrations of bicarbonate

Table X

Effect of resin heels on ion effluents

Ion	Resin Heel	Time of Breakthrough (Days)	Equilibrium Leakage (ppb)	% Change in Leakage
	Cationic heel	510	0.043	0
Sodium	Base case	500	0.043	--
	Anionic heel	495	0.043	0
	Cationic heel	610	3.53×10^{-5}	-33
Calcium	Base case	600	5.30×10^{-5}	--
	Anionic heel	580	7.68×10^{-5}	45
	Cationic heel	470	6.96×10^{-3}	0
Chloride	Base case	500	6.96×10^{-3}	--
	Anionic heel	565	6.96×10^{-3}	0
	Cationic heel	--	5.79×10^{-2}	127
Sulfate	base case	--	2.55×10^{-2}	--
	Anionic heel	--	7.98×10^{-3}	-69
	Cationic heel	210	3.80×10^{-6}	0
Carbonate	Base case	220	3.80×10^{-6}	--
	Anionic heel	240	3.80×10^{-6}	0
	Cationic heel	210	3.30×10^{-2}	0
Bicarbonate	Base case	220	3.30×10^{-2}	--
	Anionic heel	240	3.30×10^{-2}	0

70

All other parameters are maintained at the base case condition.

Figure 26 shows the effect of cationic bead size on sodium effluent concentrations. A particle size of 0.065 cm leads to about 40 days delay in sodium breakthrough. It can be seen that the initial leakage is not affected. This is because of a higher mass transfer coefficient and an increase in total resin surface area with a smaller particle size thereby resulting in a sharper reaction front. A sharper reaction front leads to a delayed breakthrough with only equilibrium leakage as the column effluent. Calcium effluent concentrations are shown in Figure 27. Unlike sodium, initial leakage of calcium varied a lot with particle size. There is a decrease in the initial leakage by about 99% and a breakthrough delay by about 80 days with decrease in particle size to 0.065 cm.

Chloride concentration profiles are shown in Figure 28. There is a very little effect of particle size on chloride effluent concentrations. The trend is very much similar to that of sodium. Figure 29 shows the effluent concentrations of sulfate for the two different particle sizes. As with calcium, initial leakage of sulfate also varies with particle size. There is a 14% decrease in the equilibrium leakage of sulfate when the anionic particle size is reduced to 0.055 cm from 0.06 cm. This is because of the desulfation of cationic resin which is directly proportional to the particle size. Actually, there is a 12% decrease in desulfation with the above mentioned change in particle size. There is no significant breakthrough of sulfate.

Carbonate and bicarbonate effluent concentration profiles are shown in Figures 30 and 31. Particle size did not have any effect on the initial leakage of either of these ions. The trend is similar to that of sodium and chloride with a slightly delayed breakthrough with smaller particle size. The breakthrough is delayed by about 20 days for both the ions with an anionic particle size of 0.055 cm. The effluent concentrations are constant after about 600 days and are the same in both the cases.
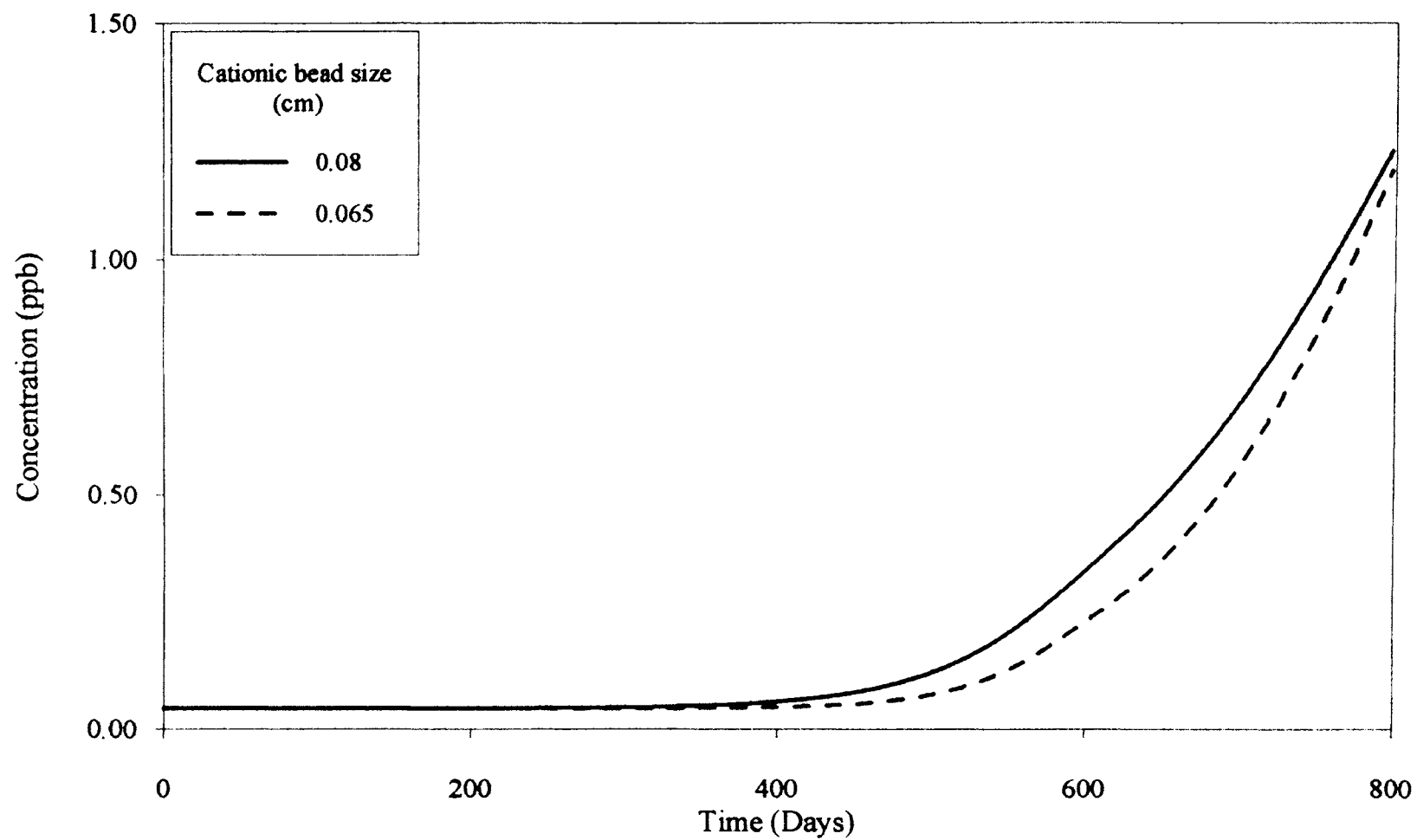
Figure 26. Effect of cationic bead size on the effluent concentrations of sodium
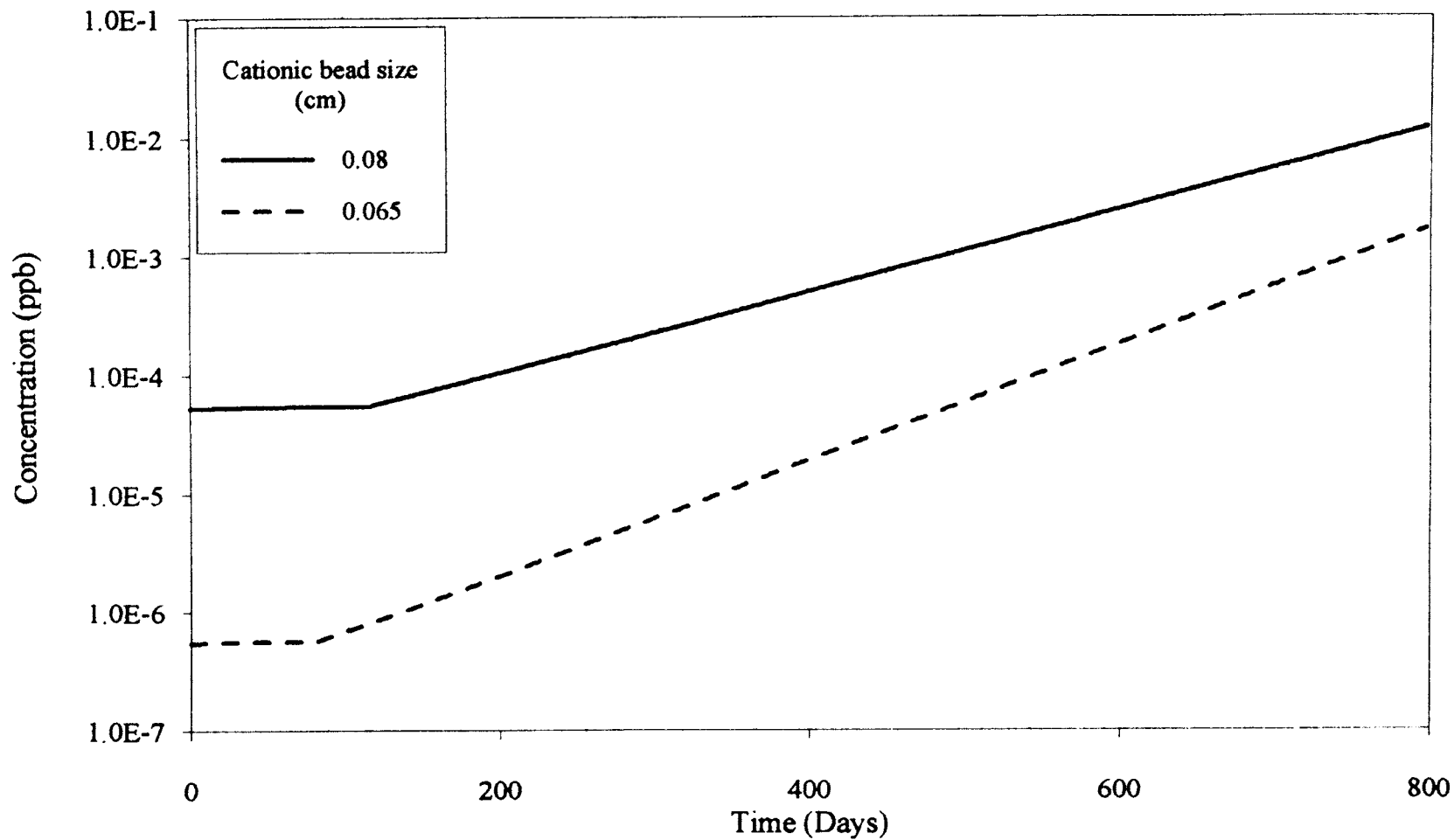
Figure 27. Effect of cationic bead size on the effluent concentrations of calcium
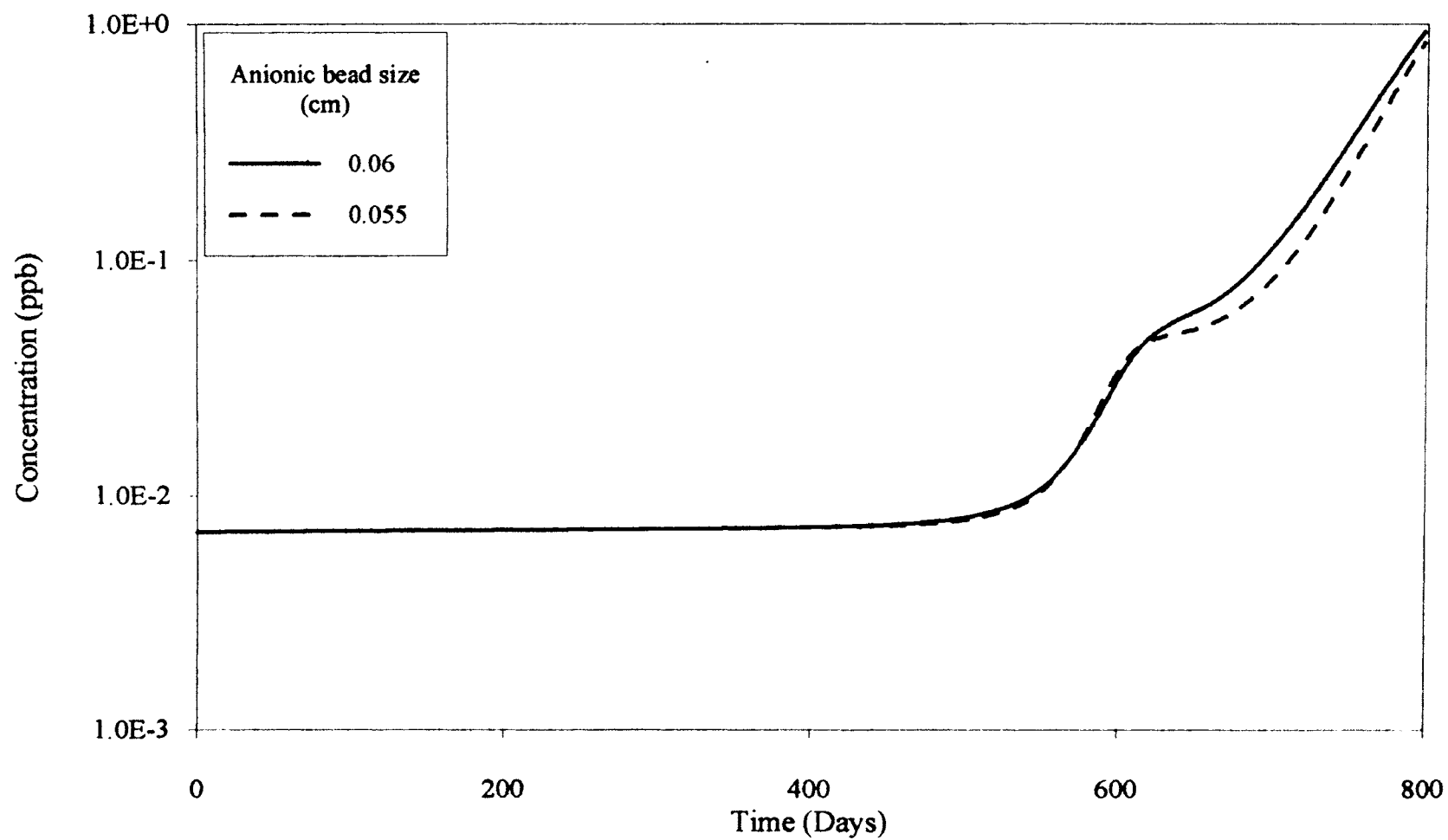
Figure 28. Effect of anionic bead size on the effluent concentrations of chloride
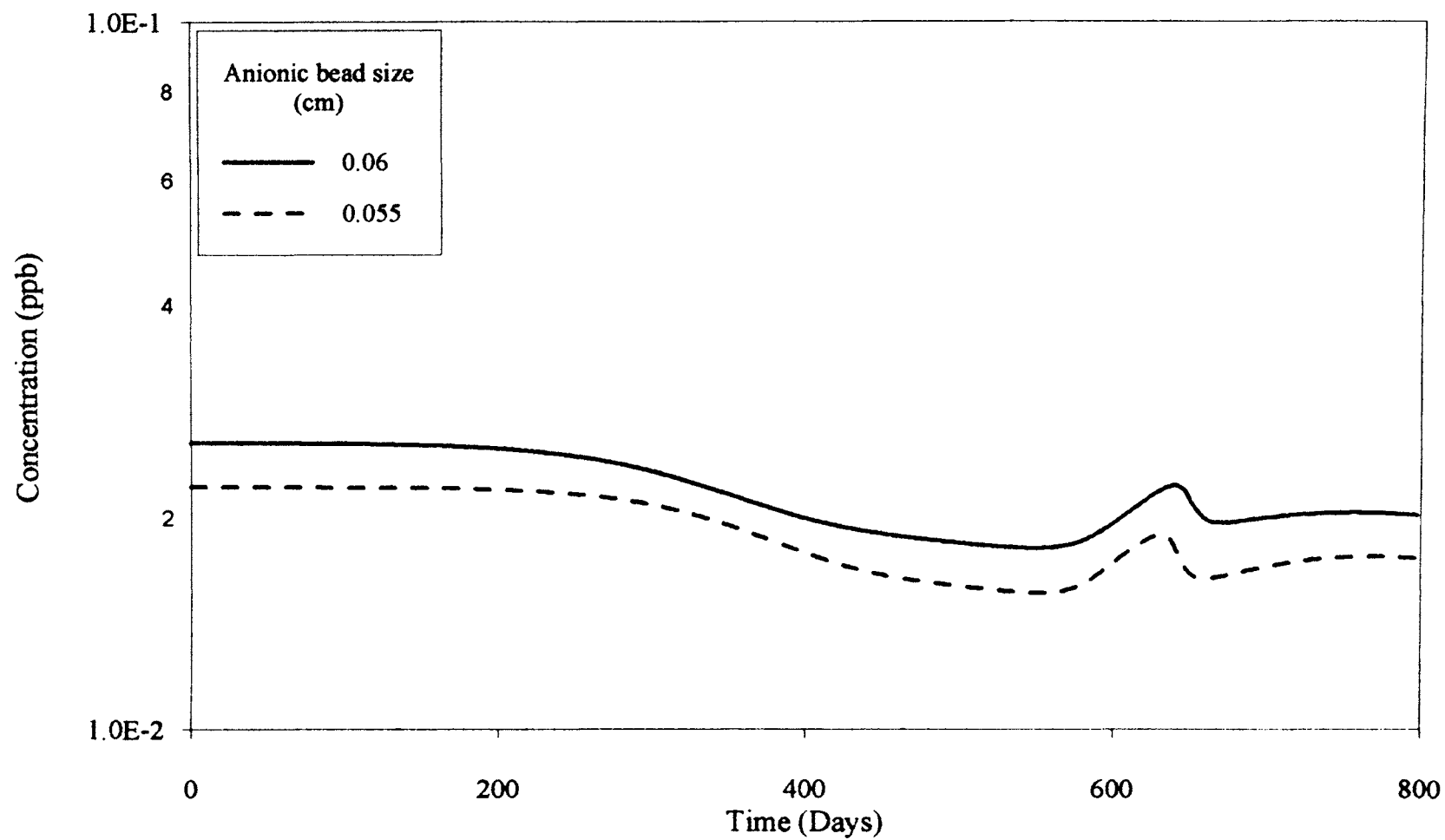
Figure 29. Effect of anionic bead size on the effluent concentrations of sulfate
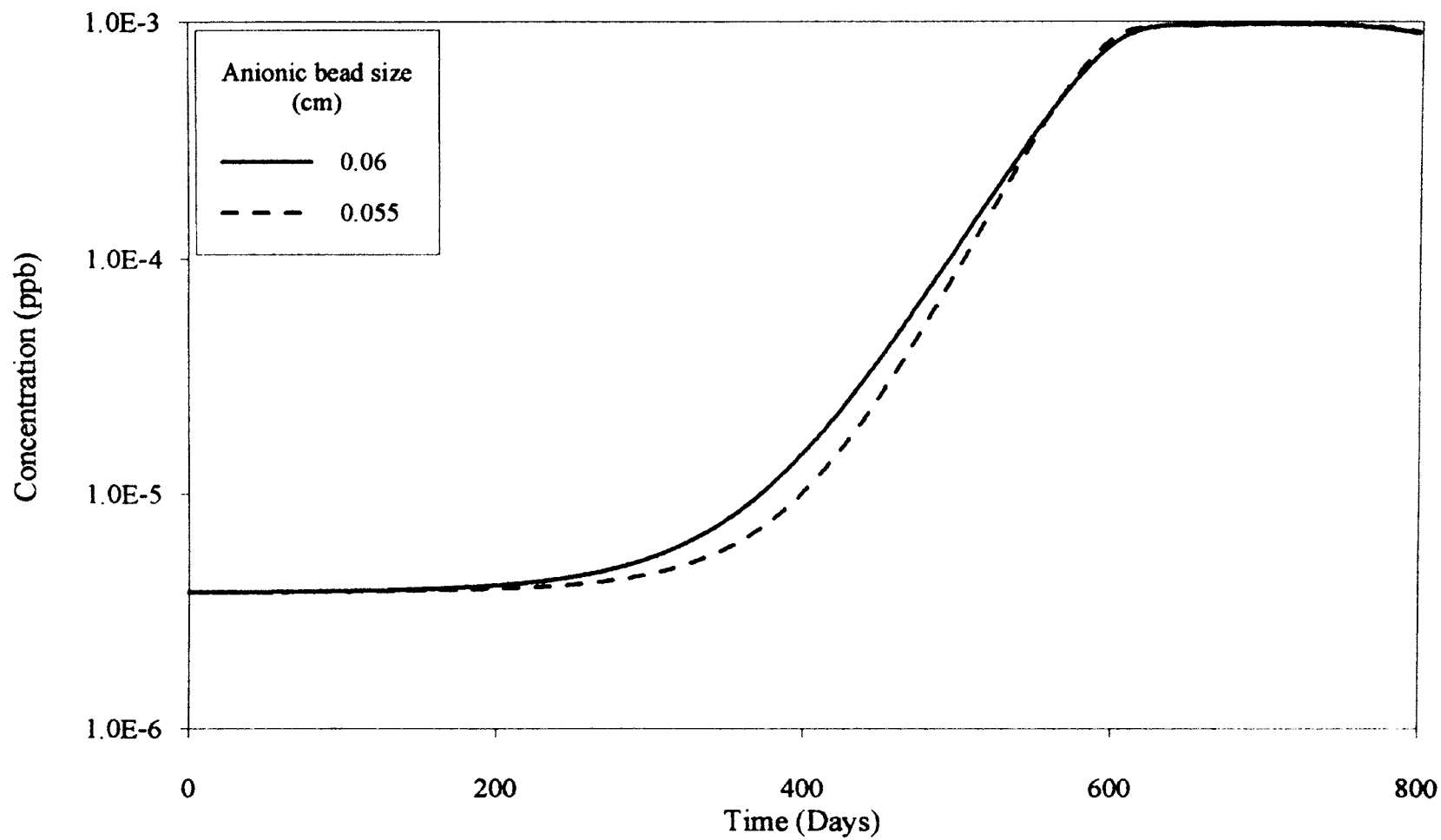
Figure 30. Effect of anionic bead size on the effluent concentrations of carbonate
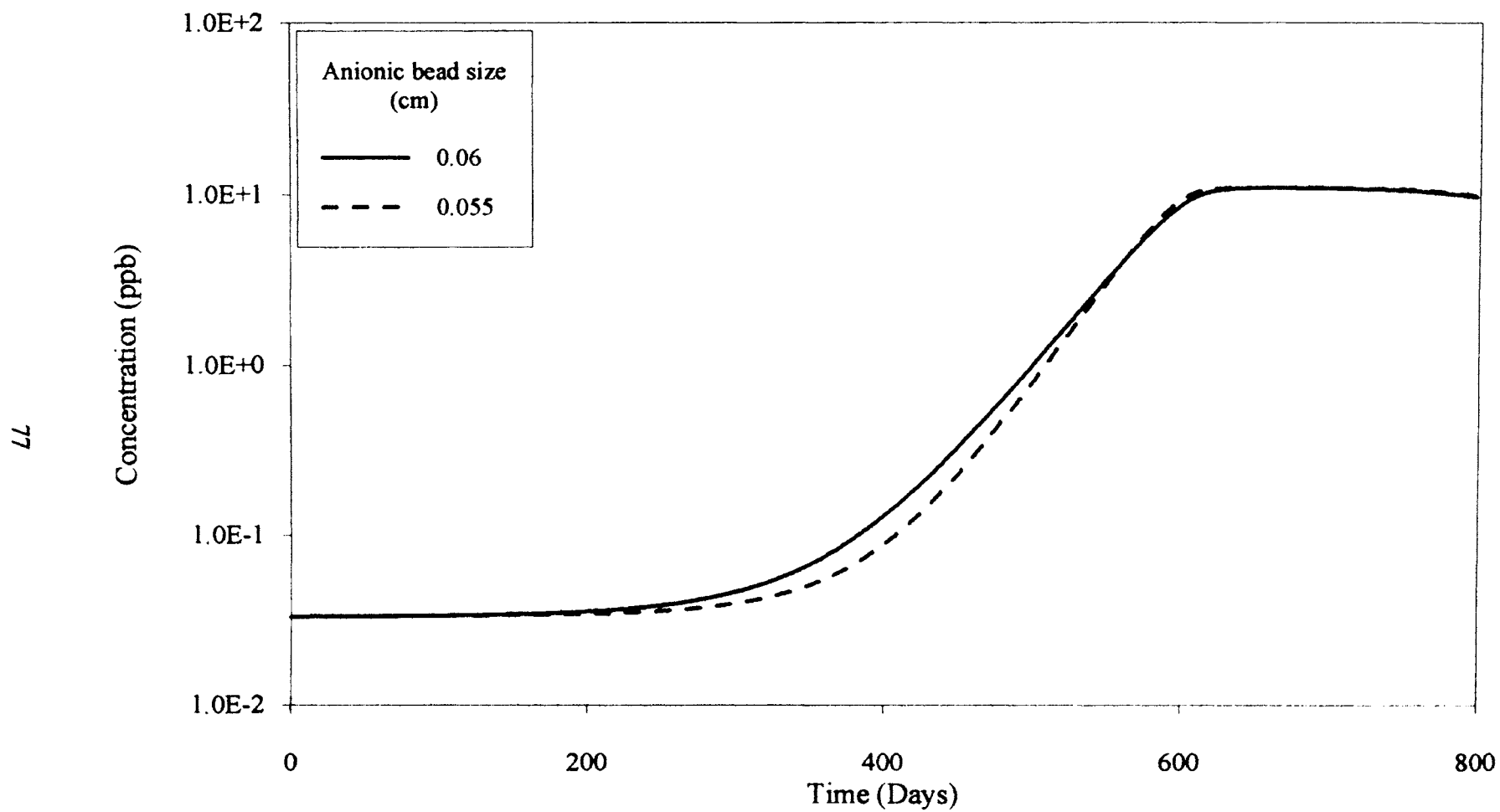
Figure 31. Effect of anionic bead size on the effluent concentrations of bicarbonate

Table XI

Effect of particle size on ion effluents

Ion	Particle Size Cat/Ani (cms)	Time of Breakthrough (Days)	Equilibrium Leakage (ppb)	% Change in Leakage
Sodium	0.08/0.06	500	0.043	--
	0.065/0.055	480	0.043	0
Calcium	0.08/0.06	600	5.30×10^{-5}	--
	0.065/0.055	680	5.41×10^{-7}	-99
Chloride	0.08/0.06	470	6.96×10^{-3}	--
	0.065/0.055	470	6.96×10^{-3}	0
Sulfate	0.08/0.06	--	2.55×10^{-2}	--
	0.065/0.055	--	2.20×10^{-2}	-14
Carbonate	0.08/0.06	300	3.80×10^{-6}	--
	0.065/0.055	320	3.80×10^{-6}	0
Bicarbonate	0.08/0.06	300	3.30×10^{-2}	0
	0.065/0.055	320	3.30×10^{-2}	--

Effect of Cationic Resin Desulfation

Water chemistry analyses at Pennsylvania Power & Light Co. indicated that strongly acidic cationic resins release sulfur containing molecules to the system, resulting in reactor-water sulfate concentrations in the range of 6 to 8 ppb (Foutch et al, 1994). This is called desulfation of cationic resins and was quantified in the form of a mathematical expression by Pondugula (1994). The same has been explained in detail earlier in this chapter. It was believed that the desulfation of cationic resins contributed to the high sulfate levels observed in the reactor-water. In this study, simulations were conducted with and without considering the desulfation effect of cationic resins to get a better understanding of the sulfate removal process.

Figures 32 and 33 show the chloride and sulfate effluent concentrations respectively, with and without considering the desulfation effect. As expected, desulfation of cationic resins did not have much effect on chloride effluent concentrations. The initial leakage of chloride is the same in both cases and breakthrough is slightly delayed (20 days) in the case of no desulfation. The final effluent to feed concentration ratio of chloride lowers by about 40% when desulfation is neglected. This is probably due to relatively less sulfate concentration for exchange, thereby allowing more chloride onto the resin. On the other hand, there is a huge difference in the sulfate effluent concentrations when the desulfation is not considered. The equilibrium leakage is about 2.0×10^{-2} ppb with desulfation term included while it is about 1.0×10^{-9} ppb without the desulfation. This shows that in MBIE columns operating with strongly acidic cationic resins, desulfation of cationic resins contributes most of the sulfate in the effluent water. These results from the model support the water chemistry analyses at Pennsylvania Power & Light Co.
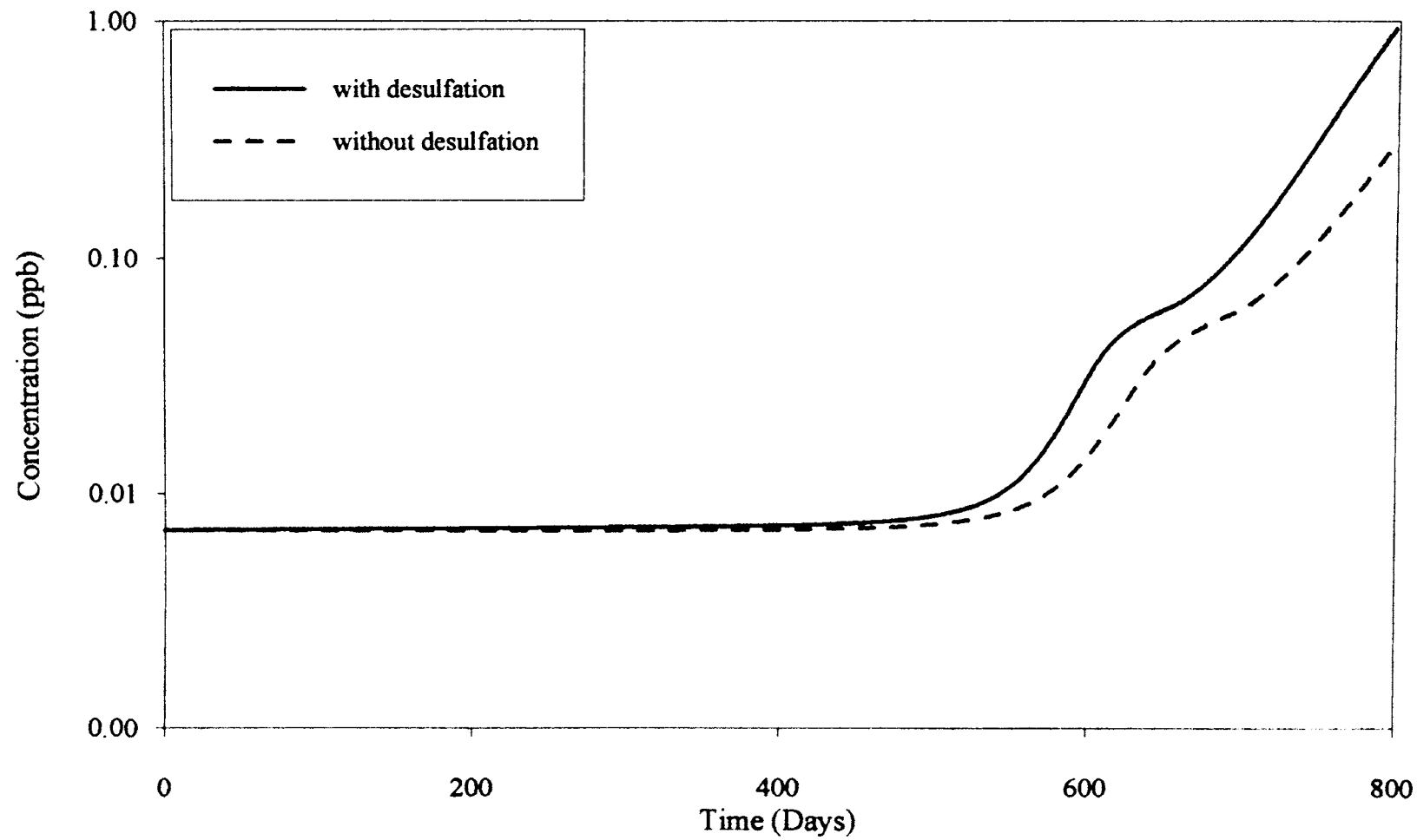
Figure 32. Comparison between the effluent concentrations of chloride with and without desulfation
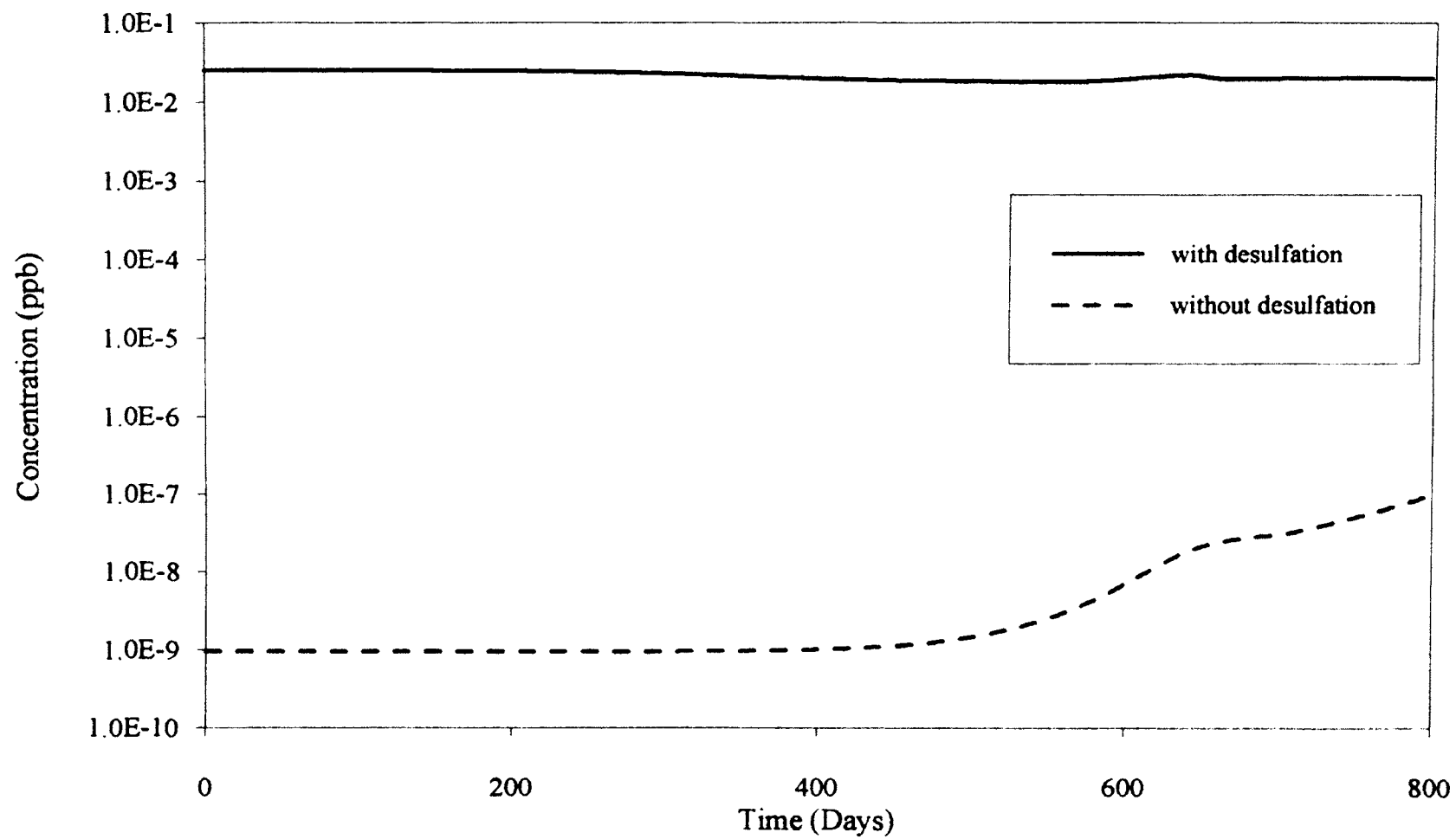
Figure 33. Comparison between the effluent concentrations of sulfate with and without desulfation

CHAPTER V

CONCLUSIONS AND RECOMMENDATIONS

The model developed in Chapter III is successfully used with column operating conditions of Pennsylvania Power & Light Co. to predict effluent concentrations. The model can predict mixed bed ion exchange column effluents for a wide variety of operating conditions. Simulations are conducted using the model to study the effect of various parameters like resin ratio, flowrate, temperature and particle size. The model is also used to predict the effect of cationic and anionic rich resin heels on the ion effluent concentrations. The system of ions studied included sodium and calcium among cations and chloride, sulfate, carbonate and bicarbonate among anions. An equilibrium subroutine for carbonic species is developed to account for the equilibrium between these species and determine the equilibrium concentrations of carbonate, bicarbonate, hydrogen and hydroxide ions.

The trends that are observed and the rates calculated in these low concentration ranges agree conceptually with what would be expected. However, the lack of any experimental data for Multicomponent systems in the ultra-low concentration ranges eliminates the possibility of evaluating the model's quantitative abilities. The model developed in this work is only an approximation for the multicomponent case. An exact model should be able to further improve the quality of predictions.

There is total lack of information on the temperature dependency of selectivity coefficients. This impairs the model's capability to predict temperature effects exactly. Moreover, the selectivity coefficients used in this work are actually for a binary system of

ions. Because of lack of multicomponent selectivity coefficients, binary data had to be used. There is also a lack of data on carbonate selectivity coefficient. Available temperature correlations for the dissociation constants of carbonic species are limited to a certain temperature range. The same correlations are used in this work for temperatures exceeding this range. Also, there is lack of data on temperature dependency of bicarbonate diffusivity coefficient.

The concentrations involved in this work are very low and close to the computer machine precision. This along with the limitations of numerical methods used, lead to errors and numerical instability in the code predictions. Very low time and distance increments need to be used to avoid instability. Also the computer code developed in this work is computationally very slow because of these low time and distance increments. There is a need to study the numerical methods that can be effectively used for the kind of differential equations involved in this work at these low numbers. This would also help optimize the code run-time.

The approximate model developed in this work represents the first step towards a general multicomponent MBIE model. There is a need for further model development as well as accurate experimental data for model evaluation.

BIBLIOGRAPHY

Bajpai, R. K. , Gupta, A. K. and Gopala Rao, M. (1974). Single particle studies of
binary and ternary cation exchange kinetics. AIChE J., 20 (5), 989-995.

Blume, R. (1987). Preparing ultrapure water. Chem. Eng. Prog. (Dec), 55-57.

Bokx, P. K. de and Boots,. H. M. J. (1989). The ion exchange equilibrium. J. Phys.
Chem., 93, 8243-8248.

Bokx, P. K. de and Boots, H. M. J. (1990). The compensating-mixture model for
multicomponent systems and its applications to ion exchange. J. Phys. Chem., 94,
6489-6495.

Calmon, C. (1986). Recent developments in water treatment by ion exchange. Reactive
polymers, 4, 131-146.

Copeland, J. P., Henderson, C. L. and Marchello, J. M. (1967). Influence of resin
selectivity on film diffusion controlled ion exchange. AIChE J., 13, 449-452.

Divekar, S. V., Foutch, G. L., and Haub, C. E. (1987). Mixed bed ion exchange at
concentrations approaching the dissociation of water. Temperature effects. Ind.
Eng. Chem. Res., 26(9), 1906-1909.

Dranoff, J. S. and Lapidus, L. (1958). Multicomponent ion exchange column
calculations. Ind. Eng. Chem., 50, 1648-1653.

Dranoff, J. S. and Lapidus, L. (1961). Ion exchange in ternary systems. Ind. Eng.
Chem., 53, 71-76.

Franzreb, M., Holl, W. H. and Sontheimer, H. (1993). Liquid-phase mass transfer in
multicomponent ion exchange I. Systems without chemical reactions in the film.
Reactive Polymers, 21, 117-133.

Garcia, R., Lopez, M., Rosal, R., Coca, J. and Sastre, H. (1992). Multicomponent ion exchange in fixed beds. Computation and modelization. Afinidad, 442, 375-378.

Harries, R. R. (1991). Ion exchange kinetics in ultrapure water systems. J. Chem. Tech. Biotechnol., 51, 437-447.

Haub, C. E. (1984). M.S. Thesis, Oklahoma State University, Stillwater, OK.

Haub, C. E. and Foutch, G. L. (1986a). Mixed-bed ion exchange at concentrations approaching the dissociation of water 1. Model development. Ind. Eng. Chem. Fund., 25, 373-381.

Haub, C. E. and Foutch, G. L. (1986a). Mixed-bed ion exchange at concentrations approaching the dissociation of water 2. Column model applications. Ind. Eng. Chem. Fund., 25, 381-385.

Helfferich, F. G. (1962). Ion Exchange. McGraw Hill Book Company, New York.

Helfferich, F. G. (1984). Conceptual view of column behavior in multicomponent adsorption or ion exchange systems. AIChE Symposium Series, 80, (233), 1-13.

Helfferich, F. G. (1990). Models and physical Reality in ion-exchange kinetics. Reactive Polymers, 13, 191-194.

Helfferich, F. G. (1967). Multicomponent ion exchange in fixed beds. Ind Eng. Chem. Fund., 6, (3), 362-364.

Horst, J., Wolfgang H. Holl and Siegfried H. Eberle. (1990). Application of the surface complex formation model to the exchange equilibria on the ion exchange resins. Reactive Polymers, 13, 209-231.

Hwang, Y. L., and Helfferich, F. G. (1987). Generalized model for multispecies ion exchange kinetics including fast reversible reactions. Reactive Polymers, 5, 237-253.

Kataoka, T., Yoshida, H. and uemura T. (1987). Liquid-side ion exchange mass transfer in a ternary system. AIChE J., 33, 202-210.

Klein, G., Tondeur, D., and Vermeulen, T. (1967). Multicomponent ion exchange in fixed beds. Ind. Eng. Chem. Fund., 6 (3), 339-352.

Klein, G., Nassiri, M. and Vislocky, J. M. (1984). Multicomponent fixed-bed sorption with variable initial and feed compositions. Computer prediction of local-equilibrium behavior. AIChE Symposium Series, 80, No. 233, 14-20.

Kunin, R. (1960). Elements of ion exchange. Reinhold publishing corporation, N.Y.

Lopez, M.,Rosal, R., Coca, J., Garcia, R. and Sastre, H. (1992). Modeling and experimental behavior of multicomponent anion exchange with amberlite IRA-410. Hungarian J. Ind. Chem., 20, 109-112.

Lucas, Antonio. De., Zarca, J., and Canizares, P. (1992). Ion exchange equilibria of Ca^{2+}, Mg^{2+}, K^{+}, Na^{+}, and H^{+} ions on Amberlite IR-120: Experimental Determination and Theoretical Prediction of the Ternary and Quaternary Equilibrium Data. Separation Science and Technology, 27 (6), 823-841.

McCartney, B. (1987). Ultrapure water for the silicon chip industry. The Chemical Engineer (Jan.), 24-26.

Noye, J. (1984). Computational techniques for differential equations. Elsevier Science Publishers B. V. Netherlands, North Holland Mathematics Studies, 83.

Omatete, O. O., Vermeulen, T. and Clazie, R. N. (1980a). Column dynamics of ternary ion exchange. Part I. Diffusion and mass transfer relations. Chem. Engineering J., 19, 229-240.

Omatete, O. O., Vermeulen, T. and Clazie, R. N. (1980b). Column dynamics of ternary ion exchange. Part II. Solution mass transfer controlling. Chem. Engineering J., 19, 241-250.

Pondugula, S. K. (1994). Mixed bed ion exchange modeling for divalent ions in a ternary system. M.S. thesis, Oklahoma State University, Stillwater, OK.

Sadler, M.A. (1993). Developments in the production and control of ultrapure water. Ion Exchange Processes: Advances and Applications, 15-28.

Schlogl, R. and Helfferich, F.G. (1957). comment on the significance of diffusion potentials in ion exchange. J. Chem. Phys., 26, 5-7.

Smith, R. P. and Woodburn, E. T. (1978). Prediction of multicomponent ion exchange equilibria for the ternary system SO_4^{2-} - NO_3^- - Cl from data of binary systems. AIChE J., 24 (4), 577-587.

Tan, H. K. S. and Spinner, I. H. (1994). Multicomponent ion exchange column dynamics. Canadian J. Chem. Eng., 72, 330-341.

Tondeur, D. (1970). Theory of ion exchange columns. The Chemical Engineering Journal, 1.

Triay, I.R. and Rundberg, R. S. (1989). Determination of selectivity coefficient distributions by deconvolution of ion exchange isotherms. J. Phys. Chem., 91, 5269-5274.

Wildhagen, G. R. S., Qassim, R. Y. and Rajagopal, K. (1985). Effective liquid-phase diffusivity in ion exchange. Ind.Eng. Chem. Fund., 24, 423-432.

Yoon, T. (1990). Ph.D. Dissertation, Oklahoma State University, Stillwater, OK.

Yoshida, H., and Kataoka, T.,(1987). Intraparticle ion exchange mass transfer in ternary system. Ind. Eng. Chem., 26, 1179-1184.

Zecchini, E. J. (1990). Solutions to selected problems in multi-component mixed bed ion exchange modeling. Ph.D. Thesis, Oklahoma State University.

Zecchini, E. J., and Foutch, G. L. (1991). Mixed bed ion-exchange modeling with amine form cation resins. Ind. Eng. Chem. Res., 30 (8), 1886.

APPENDIX A

CARBONATE EQUILIBRIUM EQUATIONS

Carbonic species dissolved in water exist in four different forms: dissolved CO_2, carbonic acid H_2CO_3, and the ions HCO_3^- and CO_3^{2-} (Loewenthal and Marias, 1982). The sum of these concentrations in the solution is the total carbonic species concentration (TCC). The carbonic species together with hydrogen and hydroxyl ions of the water exist in a state of dynamic equilibrium described by the following reactions:

$$CO_2 + H_2O \longleftrightarrow H_2CO_3 \qquad (A-1)$$

$$H_2CO_3 \xleftrightarrow{\ K_1\ } H^+ + HCO_3^- \qquad (A-2)$$

$$HCO_3^- \xleftrightarrow{\ K_2\ } H^+ + CO_3^{2-} \qquad (A-3)$$

$$H_2O \xleftrightarrow{\ K_w\ } H^+ + OH^- \qquad (A-4)$$
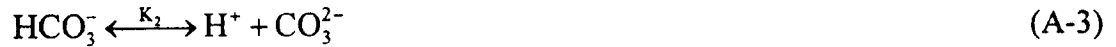
It is assumed that the concentration of dissolved CO_2 is negligible when compared to that of HCO_3^-/CO_3^{2-}. This will let us define

$$\left[H_2CO_3\right] + \left[CO_2\right] = \left[H_2CO_3^*\right] \qquad (A-5)$$

This way, we would be able to eliminate one unknown quantity. Now the dissociation constants can be written as:

$$K_1 = \frac{[H^+][HCO_3^-]}{[H_2CO_3^*]} \qquad (A\text{-}6)$$

$$K_2 = \frac{[H^+][CO_3^{2-}]}{[HCO_3^-]} \qquad (A\text{-}7)$$

$$K_w = [H^+][OH^-] \qquad (A\text{-}8)$$

The total carbonic species concentration in solution, C_{Tc}, is defined as:

$$C_{Tc} = [H_2CO_3^*] + [HCO_3^-] + [CO_3^{2-}] \qquad (A\text{-}9)$$

Once the total carbonic species concentration C_{Tc} of the input water is given, equations relating the concentrations of each of the individual ions with the hydrogen ion concentration can be derived for equilibrium conditions as follows:

Solving for the carbonate and carbonic acid species concentrations, we have

$$[H_2CO_3^*] = \frac{[H^+][HCO_3^-]}{K_1} \qquad (A\text{-}10)$$

$$[CO_3^{2-}] = \frac{K_2[HCO_3^-]}{[H^+]} \qquad (A\text{-}11)$$

Substituting equations A-10 and A-11 in equation A-9 would lead to

$$C_{Tc} = \frac{[H^+][HCO_3^-]}{K_1} + [HCO_3^-] + \frac{K_2[HCO_3^-]}{[H^+]} \qquad (A\text{-}12)$$

Now an expression for bicarbonate concentration can be written as:

$$\left[HCO_3^-\right] = \frac{C_{Tc}}{X} \qquad (A\text{-}13)$$

where X is

$$X = \frac{\left[H^+\right]}{K_1} + \frac{K_2}{\left[H^+\right]} + 1 \qquad (A\text{-}14)$$

The expressions for the concentrations of other ions can now be written as:

$$\left[H_2CO_3^*\right] = \frac{\left[H^+\right]C_{Tc}}{K_1X} \qquad (A\text{-}15)$$

$$\left[CO_3^{2-}\right] = \frac{K_2C_{Tc}}{\left[H^+\right]X} \qquad (A\text{-}16)$$

$$\left[OH^-\right] = \frac{K_w}{\left[H^+\right]} \qquad (A\text{-}17)$$

We have four equations (13, 15, 16, 17) and five unknown concentrations. The system can be completely specified by an additional equation which is the overall charge balance.

$$\left[Na^+\right] + \left[Ca^{2+}\right] + \left[H^+\right] = \left[Cl^-\right] + \left[SO_4^{2-}\right] + \left[OH^-\right] + \left[CO_3^{2-}\right] + \left[HCO_3^-\right] \qquad (A\text{-}18)$$

We should note that carbonic acid is a neutral species and is not involved in exchange. Substituting equations 13, 16 and 17 in equation 18 we get

$$V1 + \left[H^+\right] - \frac{K_W}{\left[H^+\right]} - \frac{C_{Tc}}{X}\left[1 + \frac{K_2}{\left[H^+\right]}\right] = 0 \qquad (A\text{-}19)$$

where $V1 = \left[Na^+\right] + \left[Ca^{2+}\right] - \left[Cl^-\right] - \left[SO_4^{2-}\right]$ \qquad (A-20)

Equation 19 has only one unknown, hydrogen ion concentration, which can be solved iteratively. Newton-Raphson method was used to solve this equation with an initial guess of 3.0E-07 meq/ml. The concentrations of other ions involved in the equilibrium can then be determined using the appropriate equations described above.

APPENDIX B

INTERFACIAL CONCENTRATIONS

Interfacial concentrations (solid-film interface) of the ions are determined using ion exchange equilibria. It is assumed that there is a local equilibrium at the solid-film interface. The selectivity coefficient expression for a general case, can be written using mass action law, as follows:

$$K_A^B = \left(\frac{q_B}{C_B^*}\right)^{Z_A}\left(\frac{C_A^*}{q_A}\right)^{Z_B} \tag{B-1}$$

where q is the resin phase concentration and C^* is the surface concentration:

$$q_i = Y_i Q \tag{B-2}$$

$$C_I^* = X_i^* C_T^* \tag{B-3}$$

The above equation can be written in terms of equivalent fractions, total resin capacity and total interfacial concentration as follows:

$$K_A^B = \left(\frac{Y_B}{X_B^*}\right)^{Z_A}\left(\frac{X_A^*}{Y_A}\right)^{Z_B} Q^{(Z_A-Z_B)} C_T^{*(Z_B-Z_A)} \tag{B-4}$$

The interfacial fractional concentration of ion B can be written from the above equation as:

$$X_B^* = Y_B \left(K_A^B\right)^{-1/z_A} \left(\frac{X_A^*}{Y_A}\right)^{z_B/z_A} \left(\frac{Q}{C_T^*}\right)^{1-z_B/z_A} \tag{B-5}$$

For ion A in the resin and ions B, C, D and E in the solution phase, the following exchange reactions can occur:

1. $A \leftrightarrow B$

2. $A \leftrightarrow C$

3. $A \leftrightarrow D$

4. $A \leftrightarrow E$

At this point it is assumed that these are the only exchange reactions possible and that there are no exchange reactions between the competing counterions B, C, D and E. Then we have

$$X_C^* = Y_C \left(K_A^C\right)^{-1/z_A} \left(\frac{X_A^*}{Y_A}\right)^{z_C/z_A} \left(\frac{Q}{C_T^*}\right)^{1-z_C/z_A} \tag{B-6}$$

$$X_D^* = Y_D \left(K_A^D\right)^{-1/z_A} \left(\frac{X_A^*}{Y_A}\right)^{z_D/z_A} \left(\frac{Q}{C_T^*}\right)^{1-z_D/z_A} \tag{B-7}$$

$$X_E^* = Y_E \left(K_A^E\right)^{-1/z_A} \left(\frac{X_A^*}{Y_A}\right)^{z_E/z_A} \left(\frac{Q}{C_T^*}\right)^{1-z_E/z_A} \tag{B-8}$$

It can be seen that we have four equations and five unknowns. The extra equation needed to completely specify the system is obtained from material balance at the solid-film interface.

$$\sum_{i=1}^{n} X_i^* = 1.0 \qquad \text{(B-9)}$$

Rewriting the interfacial fractional concentrations as

$$X_i^* = \lambda_i \left(X_A^*\right)^{\frac{Z_i}{Z_A}} \qquad \text{(B-10)}$$

where $\lambda_i = Y_i \left(K_A^i\right)^{-1/Z_A} \left(Y_A\right)^{-Z_i/Z_A} \left(\dfrac{Q}{C_T^*}\right)^{1-Z_i/Z_A}$ \qquad (B-11)

and substituting these in equation 9 for ions B, C, D and E would lead to

$$X_A^* + \lambda_B \left(X_A^*\right)^{\frac{Z_B}{Z_A}} + \lambda_C \left(X_A^*\right)^{\frac{Z_C}{Z_A}} + \lambda_D \left(X_A^*\right)^{\frac{Z_D}{Z_A}} + \lambda_E \left(X_A^*\right)^{\frac{Z_E}{Z_A}} = 1 \qquad \text{(B-12)}$$

This is a polynomial in X_A^* and could be solved using an iteration technique. Newton-Raphson method was used in this work. In the above equations, the total interfacial concentration, C_T^*, is still unknown. The expression for this is derived in Appendix C.

APPENDIX C

IONIC FLUX EXPRESSIONS

Flux expressions describing multicomponent ion exchange process are derived using Nernst-Planck model and basic principles of ion exchange. Haub and Foutch (1984) and Zecchini and Foutch (1990) successfully applied Nernst-Planck model to describe film diffusion controlled mixed bed ion exchange process. A similar approach will be followed to derive the necessary flux expressions.

The Nernst-Planck equation is used to describe the flux of a given species within the static film that is assumed around the resin bead. Neglecting the curvature of the film, this expression is:

$$J_i = -D_i \left(\frac{\partial C_i}{\partial r} + \frac{C_i Z_i F}{RT} \frac{\partial \phi}{\partial r} \right)$$

(C-1)

where ϕ is the electric potential and Z_i is the ion valence. Assuming pseudo steady state allows us to replace the partial derivatives by ordinary derivatives. The flux expressions derived in this model are based on bulk-phase neutralization.

The conditions that must be satisfied within the film surrounding the resin are:

$$\sum Z_i C_i = \sum Z_j C_j \qquad \text{(Electroneutrality)}$$

(C-2)

where 'i' stands for counterions and 'j' stands for coions.

95

$$Z_j J_j = 0 \qquad \text{(No coion flux)}$$

(C-3)

$$\sum Z_i J_i = \sum Z_j J_j \qquad \text{(No net current flow)} \qquad \text{(C-4)}$$

From equations C-3 and 4 we have

$$\sum Z_i J_i = 0 \qquad \text{(No net current flow)} \qquad \text{(C-5)}$$

The total equivalent ion concentration can be defined as:

$$C_T = \omega \sum_{i=1}^{n} Z_i C_i = \omega_j \sum_{j=1}^{m} Z_j C_j \qquad \text{(C-6)}$$

where 'n' is the number of counterions, 'm' is the number of coions and $\omega = +1$ for cations and -1 for anions.

Using the no coion flux condition (equation C-3), we have

$$\frac{d\phi}{dr} = -\frac{RT}{F} \frac{Z_j \frac{dC_j}{dr}}{Z_j^2 C_j} \qquad \text{(C-7)}$$

From the no coion flux condition we have that the sum of the coion fluxes in the film is also zero. Now the electric potential term in the Nernst-Planck equation can be eliminated in terms of the total equivalent concentration as:

96

$$\frac{d\phi}{dr} = -\frac{RT}{F} \frac{\sum\limits_{j=1}^{m} Z_j \frac{dC_j}{dr}}{\sum\limits_{j=1}^{m} Z_j^2 C_j} \tag{C-8}$$

Introducing a mean coion valence defined as

$$Z_Y = \frac{\sum\limits_{j=1}^{m} Z_j^2 C_j}{\sum\limits_{j=1}^{m} Z_j C_j} \tag{C-9}$$

and combining with the definition for total concentration (equation C-6), equation C-8 reduces to

$$\frac{d\phi}{dr} = \frac{-RT}{Z_Y F} \frac{1}{C_T} \frac{dC_T}{dr} \tag{C-10}$$

Now the Nernst-Planck expression for counterions can be written as:

$$J_i = -D_i \left(\frac{dC_i}{dr} - \frac{C_i Z_i}{C_T Z_Y} \frac{dC_T}{dr} \right) \tag{C-11}$$

Using the no net current flow condition (equation C-5) and equation C-11, we get

$$\sum\limits_{i=1}^{n} Z_i D_i \frac{dC_i}{dr} + \sum\limits_{i=1}^{n} Z_i D_i N_i \frac{C_i}{C_T} \frac{dC_T}{dr} = 0 \tag{C-12}$$

where $N_i = -\frac{Z_i}{Z_Y}$.

For monovalent system of ions or equal valence system of ions, the above equation could be easily integrated to obtain a relation between C_i and C_T. This is not

97

possible in the case of arbitrary valences. At this point the method proposed by Franzreb (1993) is used to proceed further. In this method, equation C-11 is differentiated to eliminate the unknown J_i. This leads to a homogeneous second order differential equation:

$$\frac{d^2C_i}{dr^2} + \frac{N_i}{C_T}\frac{dC_i}{dr}\frac{dC_T}{dr} + N_i\frac{C_i}{C_T}\left(\frac{d^2C_T}{dr^2} - \frac{1}{C_T}\left(\frac{dC_T}{dr}\right)^2\right) = 0 \qquad (C\text{-}13)$$

This method leads to an exact solution for the case of equal valences and only an approximation for the case of arbitrary valences. For counterions of equal valences, summation of equation 13 for all the ions leads to

$$\sum_{i=1}^{n}\frac{d^2C_i}{dr^2} + \frac{1}{C_T}\frac{dC_T}{dr}\sum_{i=1}^{n}N_i\frac{dC_i}{dr} + \frac{1}{C_T}\frac{d^2C_T}{dr^2}\sum_{i=1}^{n}N_iC_i - \frac{1}{C_T^2}\left(\frac{dC_T}{dr}\right)^2\sum_{i=1}^{n}N_iC_i = 0 \quad (C\text{-}14)$$

Substituting equation C-6 and its derivatives in the above leads to

$$\frac{d^2C_T}{dr^2} = 0 \qquad (C\text{-}15)$$

From the above equation it can be understood that for the case of counterions of equal valences, the profile of the total concentration in the film is linear. Zecchini and Foutch (1990) arrived at the same conclusion in their model for univalent ternary ions. The above equation combined with equation C-6 can be used to obtain relationships between the derivatives of C_i and C_T. Substitution of all these derivatives in equation in C-14 leads to

$$\frac{d^2C_i}{dC_T^2} + \frac{N_i}{C_T}\frac{dC_i}{dC_T} - \frac{N_iC_i}{C_T^2} = 0 \qquad (C\text{-}16)$$

This is the Euler's differential equation the solution of which is

$$Z_i C_i = A_i C_T + B_i C_T^{-P}$$

(C-17)

For the case of equal valences, we have $P = N_i$. Using the boundary conditions

$$r = 0, C_T = C_T^*$$
$$r = \delta, C_T = C_T^o$$

the values of the parameters A_i and B_i can be determined as follows:

$$A_i = \frac{1}{C_T^o}\left(Z_i C_i^o - B_i \left(C_T^o\right)^{-P}\right)$$

(C-18)

and

$$B_i = \omega \frac{X_i^* - X_i^o}{\left(C_T^*\right)^{-P-1} - \left(C_T^o\right)^{-P-1}}$$

(C-19)

Equation C-17 gives us a relation between the individual ion concentrations, C_i and the total equivalent concentration, C_T. Substituting for C_i and its derivative in the modified Nernst-Planck equation (C-11), we get the following flux expression:

$$J_i = -\frac{D_i}{Z_i}\frac{dC_T}{dr}\left[\left(A_i - PB_i C_T^{-P-1}\right) + N_i\left(A_i + B_i C_T^{-P-1}\right)\right]$$

(C-20)

For the case of arbitrary valences, equation C-17 is only an approximation. In this case however, N_i is not the same for all the counterions and hence, P cannot be equal to N_i. Combining the above equation with the condition of no net current flow (C-5) results in

99

$$\left(\sum_{i=1}^{n} D_i A_i + \sum_{i=1}^{n} N_i D_i A_i \right) + \left(\sum_{i=1}^{n} N_i D_i B_i - P \sum_{i=1}^{n} D_i B_i \right) C_T^{-P-1} = 0 \qquad \text{(C-21)}$$

The only way the above equation can hold true is when both the terms are equal to zero. That leads to

$$\sum_{i=1}^{n} (1 + N_i) D_i A_i = 0 \qquad \text{(C-22)}$$

Substitution of A_i (equation C-18) in to above and some mathematical manipulations gives the desired expression for total interfacial concentration, C_T^*:

$$C_T^* = \left(\frac{\sum\limits_{i=1}^{n} (1 + N_i) D_i X_i^o}{\sum\limits_{i=1}^{n} (1 + N_i) D_i X_i^*} \right)^{\!\!1/_{P+1}} C_T^o \qquad \text{(C-23)}$$

Equating the second parentheses term to zero and substitution of B_i would give us the expression for the exponent P as:

$$P = \frac{\sum\limits_{i=1}^{n} N_i D_i \left(X_i^* - X_i^o \right)}{\sum\limits_{i=1}^{n} D_i \left(X_i^* - X_i^o \right)} \qquad \text{(C-24)}$$

In an equal valance case, P is equal to N_i and in an arbitrary case, it would be in the neighborhood of N_i. The concentrations involved in this work are very low and lead to lot of numerical errors and instability. Because of numerical discrepancies, sometimes the value of P computed in the code is unusually high and leads to problems in further computations. Hence the expression for P (Equation C-24) is modified as follows:

$$P = \frac{\sum_{i=1}^{n} N_i D_i abs(X_i^* - X_i^o)}{\sum_{i=1}^{n} D_i abs(X_i^* - X_i^o)}$$

(C-24A)

Once again substitution of the above equations in to C-11 and integrating between the boundary conditions given earlier, We would get the final desired form of the ionic flux expression:

$$J_i = \frac{D_i}{\delta}\left((1-\frac{N_i}{P})(C_i^* - C_i^0) + N_i A_i (1+\frac{1}{P})(C_T^* - C_T^0)\right)$$

(C-25)

Particle Rates

The rate of exchange is related to the flux of the species by:

$$\frac{d<C_i>}{dt} = -J_i a_s$$

(C-26)

The resin phase concentration $<C_i>$ can be represented as:

$$<C_i> = y_i Q$$

(C-27)

Now equation 3-17 can be written as

$$\frac{dy_i}{dt} = \frac{-J_i a_s}{Q}$$

(C-28)

The rate of ion loadings in to the resin can be determined using the above equation once the individual ionic fluxes are known.

The effective diffusivity is defined as:

$$D_e = \frac{\sum_{i=1}^{n} |J_i \delta|}{\sum_{i=1}^{n} |C_i^* - C_i^0|}$$

(C-29)

The film thickness in equation C-25 is eliminated using the relation

$$\delta = D_e/K$$

(C-30)

where K is a mass transfer coefficient proposed by Kataoka:

$$K = 1.85 \frac{U_s}{\varepsilon} \left(\frac{\varepsilon}{1-\varepsilon} \right)^{\frac{1}{3}} Sc^{-\frac{2}{3}} Re^{-\frac{2}{3}}$$

(C-31)

where Schmidt number is defined using the effective diffusivity as

$$Sc = \frac{\mu}{\rho D_e}$$

(C-32)

Substituting equation C-30 in the flux expression C-25, we get

$$\frac{J_i}{K} = \frac{D_i}{D_e} \left((1 - \frac{N_i}{P})(C_i^* - C_i^0) + N_i A_i (1 + \frac{1}{P})(C_T^* - C_T^0) \right)$$

(C-33)

This J_i/K is computed for each of the ions in the subroutine and returned to the main program, in the computer code developed for this model.

102

APPENDIX D

COLUMN MATERIAL BALANCES

Material balance equations around the column are required for determining the effluent concentration profiles. These material balances will use previously determined rate expressions for individual species. The overall column material balance for species i is given as:

$$\frac{u_s}{\varepsilon}\frac{\partial C_i}{\partial Z} + \frac{\partial C_i}{\partial t} + \frac{(1-\varepsilon)}{\varepsilon}\frac{\partial q_i}{\partial t} = 0 \tag{D-1}$$

where :

u_s = superficial velocity, and ε = void fraction.

This expression can be simplified by using dimension-less variables in time and distance. The dimension-less expressions are expressed as:

$$\tau = \frac{K_i C_T^f}{d_p Q}(t - \frac{\varepsilon Z}{u_s}) \tag{D-2}$$

and,

$$\xi = \frac{K_i(1-\varepsilon)}{u_s}\frac{Z}{d_p} \tag{D-3}$$

K_i is the non-ionic mass transfer coefficient for species i, d_p is the particle diameter, Q is the resin capacity and C_T^f is the total cationic feed concentration. The above expressions are differentiated with respect to time and distance respectively to yield:

$$\frac{\partial \tau}{\partial t} = \frac{K_i C_T^f}{d_p Q}, \qquad \frac{\partial \tau}{\partial Z} = \frac{K_i C_T^f \varepsilon}{d_p Q u_s},$$

$$\frac{\partial \xi}{\partial t} = 0 \text{ and} \qquad \frac{\partial \xi}{\partial Z} = \frac{K_i C_f^T \varepsilon}{d_p Q u_s}$$

$$\frac{\partial \tau}{\partial t} = \frac{K_i C_T^f}{d_p Q}, \qquad \frac{\partial \tau}{\partial Z} = \frac{K_i C_T^f \varepsilon}{d_p Q u_s},$$

$$\frac{\partial \xi}{\partial t} = 0 \quad \text{and} \qquad \frac{\partial \xi}{\partial Z} = \frac{K_i C_f^T \varepsilon}{d_p Q u_s}$$

Now using the chain rule the original derivatives are expressed as:

$$\frac{\partial C_i}{\partial Z} = \frac{\partial C_i}{\partial \xi}(\frac{\partial \xi}{\partial Z}) + \frac{\partial C_i}{\partial \tau}(\frac{\partial \tau}{\partial Z}) = \frac{K_i(1-\varepsilon)}{u_s d_p}(\frac{\partial C_i}{\partial \xi}) - \frac{K_i C_T^f \varepsilon}{d_p u_s Q}(\frac{\partial C_i}{\partial \tau}) \qquad \text{(D-3)}$$

$$\frac{\partial q_i}{\partial t} = \frac{\partial q_i}{\partial \tau}(\frac{\partial \tau}{\partial t}) + \frac{\partial q_i}{\partial \xi}(\frac{\partial \xi}{\partial t}) = \frac{K_i C_T^f}{d_p Q}\frac{\partial q_i}{\partial \tau} + 0\frac{\partial q_i}{\partial \xi} \qquad \text{(D-4)}$$

Replacing these into the material balance yields:

$$\frac{\partial C_i}{\partial \xi} + \frac{C_T^f}{Q}\frac{\partial q_i}{\partial \tau} = 0 \qquad \text{(D-5)}$$

This expression is easier to handle. Introducing the fractions in liquid phase and resin phase as:

$$x_i = C_i/C_T^f, \text{ and } q_i = Qy_i$$

This substitution into the material balance equation yields:

$$\frac{\partial x_i}{\partial \xi_j} + \frac{\partial y_i}{\partial \tau} = 0 \qquad \text{(D-6)}$$

In the current code, chloride is selected as the reference species. Since all the material balance is to be solved using same steps in τ and ξ, expressions for the base species result as:

$$\tau = \tau_c = \frac{K_c C_T^f}{d_{pa} Q_a}(t - \frac{\varepsilon Z}{u_s})$$

(D-7)

and

$$\xi = \xi_c = \frac{K_c(1-\varepsilon)}{u_s d_{pa}} Z$$

(D-8)

The partial derivatives of all the species can be written in terms of the reference ion as follows: Cations:

$$\frac{\partial x_i}{\partial \xi_c} = \frac{\partial x_i}{\partial \xi_i}(\frac{\partial \xi_i}{\partial \xi_c}) = \frac{K_i}{K_c} \frac{d_{pa}}{d_{pc}} \frac{\partial x_i}{\partial \xi_i}$$

(D-9)

$$\frac{\partial y_i}{\partial \tau_c} = \frac{\partial y_i}{\partial \tau_i}(\frac{\partial \tau_i}{\partial \tau_c}) = \frac{K_i}{K_c} \frac{d_{pa}}{d_{pc}} \frac{Q_a}{Q_c} \frac{\partial y_i}{\partial \tau_i}$$

(D-10)

and anions:

$$\frac{\partial x_i}{\partial \xi_c} = \frac{\partial x_i}{\partial \xi_i}(\frac{\partial \xi_i}{\partial \xi_c}) = \frac{K_i}{K_c} \frac{\partial x_i}{\partial \xi_i}$$

(D-11)

$$\frac{\partial y_i}{\partial \tau_c} = \frac{\partial y_i}{\partial \tau_i}(\frac{\partial \tau_i}{\partial \tau_c}) = \frac{K_i}{K_c} \frac{\partial y_i}{\partial \tau_i}$$

(D-12)

Replacing these partial derivatives into the general material balance equation and introducing the cation and anion resin volume fractions (FCR, FAR) within the bed, we get

$$\frac{\partial x_i}{\partial \xi_c} + FCR \frac{\partial y_i}{\partial y_c} = 0 \qquad \text{(cations)}$$

(D-13)

105

$$\frac{\partial x_i}{\partial \xi_c} + FAR \frac{\partial y_i}{\partial y_c} = 0 \qquad \text{(anions)} \qquad \text{(D-14)}$$

Now the rate expressions developed earlier have to be modified to incorporate the dimensionless variables that have been introduced. This involves changing t to τ_c as the basis for each of the individual ions.

$$\frac{dy_i}{dt} = \frac{-J_i a_s}{Q} \qquad \text{(D-15)}$$

Changing from t to τ_i results:

$$\frac{dy_i}{d\tau} = \left(\frac{-J_i a_s}{Q} \right) \left(\frac{d_p Q}{K_i C_f} \right) \qquad \text{(D-16)}$$

Now changing from τ to τ_c basis and noting that $a_s d_p = 6$, we get

$$\frac{\partial y_i}{\partial \tau_c} = \left(-\frac{6 J_i}{K_i C_f} \right) \frac{K_i}{K_c} \frac{d_{pa}}{d_{pc}} \frac{Q_a}{Q_c} \qquad \text{(cations)} \qquad \text{(D-17)}$$

$$\frac{\partial y_i}{\partial \tau_c} = \left(-\frac{6 J_i}{K_i C_f} \right) \frac{K_i}{K_c} \qquad \text{(anions)} \qquad \text{(D-18)}$$

This is the final form of the non-dimensionalized rate equations that describe the exchange process. These are combined with the material balances to predict the column effluent concentrations.

APPENDIX E

NUMERICAL METHODS

The material balance equations outlined in Appendix D for all the exchanging species are a system of partial differential equations that need to be solved for predicting the effluent concentrations from the MBIE column. Constant time and distance steps are used to calculate the particle loading and bulk phase liquid concentrations down the column. As seen in Appendix D, rate equation in general form is represented as

$$\frac{\partial x}{\partial \xi} = -\frac{\partial y}{\partial \tau} = \text{Rate} = f(y) \qquad \text{(eq. D-1)}$$

These system of partial differential equations are solved as ordinary differential equations keeping one of the parameters as constant while the other is evaluated. This involves the application of any numerical method using initial value problems.

The application of numerical methods for this model is classified into two categories based upon its function:

1) Predicting liquid phase concentrations using the distance parameter along the column.

2) Predicting particle loading using the time parameter.

The model is solved for effluent concentrations using backward differentiation formulas for stiff initial value problems. Backward Euler method of first order (also called Adams-Moulton method) is used for predicting particle loading.

Backward differentiation formulas are the most common method of solution for stiff systems. They are linear multi step methods of the form

$$\sum_{j=0}^{k} \alpha_j y_{n+j} = h \beta_k f_{n+k}$$

where

$$\alpha_k = 1, \alpha_0 \neq 0 \text{ and } \beta_k \neq 0$$

Their order, is equal to step number k, and for orders of one to six they are stiffly stable. The first order method is the backward Euler method, and it, together with the second and third order methods, is absolutely stable in the right half plane not particularly far from the origin. The higher-order methods do not suffer this problem, but instead are not absolutely stable in a region of the left half-plane near the imaginary axis. Coefficients for backward differentiation formulas are presented in Table E-I.

The backward differentiation formulas are implemented in the same variable order variable-step manner as the Adam's formulas. A pth order predictor of the form

$$y^0_{n+k} = h \beta^*_k f_{n+k-1} - \sum_{j=0}^{k-1} \alpha^*_j y_{n+j}$$

is used to provide the initial estimates for the corrector method described above. The model cannot use this method for the following reasons.

1) The predictor-corrector loop involves iterative procedure and this changes the interfacial concentration, which is controlled by kinetics of ion-exchange.

2) An iterative procedure on the interfacial concentration involves the already imposed Newton Raphson iterative method for finding interfacial concentration and this method may not converge at all.

Hence as a first estimate, Euler method of first order is used in combination with the backward differentiation predictor in the model to predict the liquid phase concentrations as a function of the bed depth (and consequently effluent concentrations).

Table E-I

Coefficients of backward differentiation formulas (Noye, J., 1984).

Order	β_k	α_0	α_1	α_2	α_3	α_4	α_5	α_6
1	1	-1	1					
2	2/3	1/3	-4/3	1				
3	6/11	-2/11	9/11	-18/11	1			
4	12/25	3/25	-16/25	36/25	-48/25	1		
5	60/137	-12/137	75/137	-200/137	300/137	-300/137	1	
6	60/147	10/147	-72/147	225/147	-400/147	450/147	-360/147	1

APPENDIX F

COMPUTER CODE

```
*************************************************************************
*                                                                       *
*        MULTIVALENT MULTICOMPONENT  ION EXCHANGE CODE                   *
*                                                                       *
*        THIS PROGRAM IS USED FOR PREDICTING THE EFFLUENT                *
*        CONCENTRATIONS FROM A MIXED BED ION EXCHANGE                    *
*        COLUMNFOR A MULTICOMPONENT SYSTEM OF IONS.                      *
*                                                                       *
*        DEVELOPED BY RAMESH BULUSU & DR. GARY FOUTCH                    *
*                                                                       *
*        P - PREFIX FOR CATIONS;  S - PREFIX FOR ANIONS                  *
*                                                                       *
*        PARTICIPATING IONS:                                            *
*        CATIONS                        ANIONS                          *
*        PA: HYDROGEN                    SA: HYDROXIDE                   *
*        PB: SODIUM                      SB: CHLORIDE                    *
*        PC: CALCIUM                     SC: SULFATE                     *
*                                        SD: CARBONATE                  *
*                                        SE: BICARBONATE                *
*************************************************************************
*
      IMPLICIT INTEGER (I-N), REAL*8 (A-H,O-Z)
        REAL*8 KLPB,KLPC,KLPD,KLPE,KLSB,KLSC,KLSD,KLSE,
       1 YPB(4,5000),YPC(4,5000),
       1 YSB(4,5000),YSC(4,5000),YSD(4,5000),YSE(4,5000),
       1 XPB(4,5000),XPC(4,5000),
       1 XSB(4,5000),XSC(4,5000),XSD(4,5000),XSE(4,5000),
       1 RTPB(4,5000),RTPC(4,5000),
       1 RTSB(4,5000),RTSC(4,5000),RTSD(4,5000),RTSE(4,5000)
        REAL*8 MPB,MPC,MSB,MSC,MSD,MSE,K1,K2
*       _____
*       CORRELATIONS-KATAOKA & CARBERRY
*       _____
       F1(R,S) = 1.15*VS/(VD*(S**(2./3.))*(R**0.5))
       F2(R,S) = 1.85*VS*((VD/(1.-VD))**(1./3.))/
       1 (VD*(S**(2./3.))*(R**(2./3.)))
*       _____
*       READING THE DATA
*       _____
        OPEN(UNIT=9,FILE='CAR1.D',STATUS = 'UNKNOWN')
        READ(9,*)KPBK, KPPR, TIME
        READ(9,*)YPBO,YPCO
        READ(9,*)YSBO,YSCO,YSDO,YSEO
        READ(9,*)PDC, PDA, VD
```

```fortran
      READ(9,*)FR, DIA, CHT
      READ(9,*)TAU, XI, FCR, TMP
      READ(9,*)DEN, QC, QA, FAR
      READ(9,*)PKAB,PKAC
      READ(9,*)SKAB,SKAC,SKAD,SKAE
      READ(9,*)CPBF,CPCF
      READ(9,*)CSBF,CSCF,CTF
      READ(9,*)ZPA,ZPB,ZPC
      READ(9,*)ZSA,ZSB,ZSC,ZSD,ZSE
      READ(9,*)MPB,MPC,MSB,MSC,MSD,MSE
*--------------------------------------------------------------
      WRITE (6,10)
      WRITE (6,11)
      WRITE (6,12) YPBO,YSBO
      WRITE (6,13) PDC,VD
      WRITE (6,14) QC,QA
*--------------------------------------------------------------
*
*     CALCULATIONS OF DIFFUSION COEFFICIENTS AND NON IONIC MASS
*     TRANSFER COEFFICIENTS
*
      CP = 1.43123+TMP*(0.000127065*TMP-0.0241537)
      TMPK=TMP+273.15
      ALOGKW = 4470.99/(TMPK)-6.0875+0.01706*(TMPK)
      DISS = 10**(-ALOGKW)
      ALOGK1 = (17052./TMPK)+(215.21*LOG10(TMPK))-(0.12675*TMPK)-545.56
      ALOGK2 = (2902.39/TMPK)+0.02379*TMPK-6.498
      K1 = 10**(-ALOGK1)
      K2= 10**(-ALOGK2)
      CALL EQB(DISS,K1,K2,CPA,CPBF,CPCF,CSA,CSBF,CSCF,CSDF,
     CSEF,CTF,CAC)
      CFCAT = CPBF + CPCF + CPA
      CFANI = CSBF + CSCF + CSDF+CSEF+CSA
      IF(ABS(CFCAT-CFANI).LE.(CFCAT/10000))GO TO 446
      IF(CFCAT.GT.CFANI) THEN
      WRITE(*,444)
444   FORMAT('TOTAL CATIONS IS GREATER THAN TOTAL ANIONS.')
      GO TO 448
      ELSE
      WRITE(*,447)
447   FORMAT(' TOTAL ANIONS IS GREATER THAN TOTAL CATIONS.')
      ENDIF
448   WRITE(*,445)CSA,CPA
445   FORMAT(' CSA = ',E12.5,'CPA =',E12.5)
446   CONTINUE
```

```fortran
      IF(CFCAT.GE.CFANI) THEN
CF = CFCAT
ELSE
CF = CFANI
ENDIF
WRITE (6,15) CF,FR,DIA,CHT

      RTF = (8.931D-10)*(TMP+273.16)
DPA = RTF*(221.7134+5.52964*TMP-0.014445*TMP*TMP)
DPB = RTF*(23.00498+1.06416*TMP+0.0033196*TMP*TMP)
DPC = RTF*(1.575*TMP+23.27)/2.

DSA = RTF*(104.74113+3.807544*TMP)
DSB = RTF*(39.6493+1.39176*TMP+0.0033196*TMP*TMP)
DSC = RTF*(2.079*TMP+35.76)/2.
DSD = RTF*(1.44*TMP+36.)/2.
DSE = RTF*44.5

AREA = 3.1415927*(DIA**2)/4.
   VS = FR/AREA
   REP = PDC*100.*VS*DEN/((1.-VD)*CP)        !REYNOLD'S NUMBER
   RES = PDA*100.*VS*DEN/((1.-VD)*CP)
   SPB = (CP/100.)/DEN/DPB
   SPC = (CP/100.)/DEN/DPC
   SSB = (CP/100.)/DEN/DSB
   SSC = (CP/100.)/DEN/DSC
   SSD = (CP/100.)/DEN/DSD
   SSE = (CP/100.)/DEN/DSE
         IF (REP.LT.20.) THEN
               KLPB= F2(REP,SPB)
               KLPC= F2(REP,SPC)
         ELSE
               KLPB= F1(REP,SPB)
               KLPC= F1(REP,SPC)

         ENDIF
      IF (RES.LT.20.) THEN
               KLSB= F2(RES,SSB)
               KLSC= F2(RES,SSC)
               KLSD= F2(RES,SSD)
               KLSE= F2(RES,SSE)
         ELSE
               KLSB= F1(RES,SSB)
               KLSC= F1(RES,SSC)
               KLSD= F1(RES,SSD)
```

```
            KLSE= F1(RES,SSE)
*

        ENDIF
*


* CALCULATE TOTAL NUMBER OF STEPS IN DISTANCE (NT) DOWN
  COLUMN: SLICES
*
        CHTD = KLSB*(1.-VD)*CHT/(VS*PDA)    !DISTANCE DIMENSIONLESS
        NT = CHTD/XI
*
* PRINT CALCULATED PARAMETERS
*
    WRITE (6,16) DPB,DSC,DPA
    WRITE (6,17) CP,DEN,TMP
    WRITE (6,18)
    WRITE (6,19)
    WRITE (6,20)
    WRITE (6,21) TAU,XI,NT
    WRITE (6,22) REP,KLPB
    WRITE (6,88) KLPC,DPC
    WRITE(6,89) KLSD,DSD
    WRITE (6,*)'SULFATE COEFFICIENT  : ',KLSC
    WRITE (6,23) VS
*
* SET INITIAL RESIN LOADING THROUGHOUT THE ENTIRE COLUMN
*
    MT = NT + 1
    DO 100 M=1,MT
    YPB(1,M)=YPBO
    YPC(1,M)=YPCO
*
    YSB(1,M)=YSBO
    YSC(1,M)=YSCO
    YSD(1,M)=YSDO
    YSE(1,M)=YSEO
 100 CONTINUE
*
* CALCULATE DIMENSIONLESS PROGRAM TIME LIMIT
*   BASED ON INLET CONDITIONS (AT Z=0)
*
    TMAXC = QC*3.142*(DIA/2.)**2.*CHT*FCR/(FR*CF*60.)
    TMAXA = QA*3.142*(DIA/2.)**2.*CHT*FAR/(FR*CF*60.)
    IF(TMAXC.GE.TMAXA) THEN
        TMAX = TMAXC
```

114

```fortran
      ELSE
          TMAX = TMAXA
      ENDIF
        TAUMAX = KLSB*CF*(TMAX*60.)/(PDA*QA)
        DMAX=TMAX/1440.
      WRITE(6,*)
      WRITE(6,*)
      WRITE(6,222)
      WRITE(6,223)DMAX
      WRITE(6,224)
  222 FORMAT('PROGRAM RUN TIME IS BASED ON TOTAL RESIN CAPACITY')
  223 FORMAT('AND FLOW CONDITIONS. THE PROGRAM WILL RUN
     FOR',F12.1)
  224 FORMAT(' DAYS OF COLUMN OPERATION FOR THE CURRENT
     CONDITIONS.')
*      _____
*  PRINT BREAKTHROUGH CURVE HEADINGS
*      _____
      IF (KPBK.NE.1) GO TO 50
      WRITE (6,24)
      WRITE (6,25)
      WRITE (6,26)
      WRITE (6,27)
      WRITE (6,*)
   50 CONTINUE
*      _____
*  PRINT CONCENTRATION PROFILE HEADINGS
*      _____
          T = 0.
       TAUPR = KLSB*CF*(TIME*60.)/(PDA*QA)
       IF (KPPR.NE.1) GO TO 60
       WRITE (6,30)
       WRITE (6,31) TIME
       WRITE (6,32)
       WRITE (6,33)
       WRITE (6,34)
   60 CONTINUE
*      _____
*  INITIALIZE VALUES PRIOR TO ITERATIVE LOOPS
*      _____
          J = 1
          JK = 1
        TAUTOT = 0.
         JFLAG = 0
          KK = 1
```

```
          KPRINT = 100
*
_____
* DESULFATION TERM (FISHER'S DATA)
*
_____

      S1 = (1.44485E+7*EXP(-10278.6/(TMP+273.16))*CHTD
     1      *3.1415927*(DIA**2.)*2.1)*(VS*PDA)*FCR
     1      /(NT*3600.*4.0*FR*KLSB*(1.-VD))

      DD = S1/CF
*

*
_____
* CALCULATE THE CONSTANT NONDIMENSIONALIZING TERMS
*
_____

      CONP = -6.*PDA/(KLSB*PDC*CF)
      CONS = -6./KLSB/CF
      CONY = QA/QC
*

*
_____
*  TIME STEP LOOP WITHIN WHICH ALL COLUMN CALCULATIONS ARE
*  IMPLEMENTED  TIME IS INCREMENTED AND OUTLET CONCENTRATION
CHECKED
*
_____
  1   CONTINUE
      IF (TAUTOT.GT.TAUMAX) GOTO 138
          IF (J.EQ.4) THEN
              JD = 1
          ELSE
              JD = J + 1
          ENDIF
*
_____
*  SET INLET LIQUID PHASE FRACTIONAL CONCENTRATIONS FOR EACH
*  SPECIES IN THE MATRIX
*
_____
          CSAO = CSA
          CPAO = CPA
*
      XPB(J,1) = CPBF/CF
      XPC(J,1) = CPCF/CF

      XSB(J,1) = CSBF/CF
      XSC(J,1) = CSCF/CF
      XSD(J,1) = CSDF/CF
      XSE(J,1) = CSEF/CF
*
```

116

```
*  _____
* LOOP TO INCREMENT DISTANCE (BED LENGTH) AT A FIXED TIME
*  _____
      DO 400 K=1,NT
         CPBO = XPB(J,K)*CF
         CPCO = XPC(J,K)*CF
*
         CSBO = XSB(J,K)*CF
         CSCO = XSC(J,K)*CF
         CSDO = XSD(J,K)*CF
         CSEO = XSE(J,K)*CF
*
*  _____
* CALL ROUTINES TO CALCULATE THE INTERFACIAL CONCENTRATIONS
*  AND IONIC FLUXES
*  _____

         IF((YPB(J,K)+YPC(J,K)).LT.0.999)THEN
         CALL MULT(YPB(J,K),YPC(J,K),PKAB,
     1 PKAC,XPB(J,K),XPC(J,K),DPA,DPB,DPC,
     1 QC,ZPA,ZPB,ZPC,ZSA,ZSB,ZSC,ZSD,ZSE,
     1 CPAO,CPBO,CPCO,
     1 CSAO,CSBO,CSCO,CSDO,CSEO,CF,RPB,RPC,DRP)
*
         ELSE
*
         RPB=0.0
         RPC=0.0
*
         ENDIF
*
         IF((YSB(J,K)+YSC(J,K)+YSD(J,K)+YSE(J,K)).LT.0.999)THEN
         CALL MULT1(YSB(J,K),YSC(J,K),YSD(J,K),YSE(J,K),SKAB,
     1 SKAC,SKAD,SKAE,XSB(J,K),XSC(J,K),XSD(J,K),XSE(J,K),DSA,DSB,DSC,
     1 DSD,DSE,QA,ZSA,ZSB,ZSC,ZSD,ZSE,ZPA,ZPB,ZPC,
     1 CSAO,CSBO,CSCO,CSDO,CSEO,
     1 CPAO,CPBO,CPCO,CF,RSB,RSC,RSD,RSE,DRS)
*
         ELSE
*
         RSB=0.0
         RSC=0.0
         RSD=0.0
         RSE=0.0
*
```

117

```
          ENDIF
*

      IF (K .EQ. 1) THEN
*

      SCP = (CP/100.)/DEN/DRP
      SCS = (CP/100.)/DEN/DRS
      AKP = F2(REP,SCP)
      AKS = F2(RES,SCS)
*

          WRITE(*,*)AKP,AKS
*

    RTPB(J,1) = (RPB*AKP*CONP)
    RTPC(J,1) = RPC*AKP*CONP
  *

    RTSB(J,1) = RSB*AKS*CONS
    RTSC(J,1) = RSC*AKS*CONS
    RTSD(J,1) = RSD*AKS*CONS
    RTSE(J,1) = RSE*AKS*CONS
*

    YPB(JD,1) = YPB(J,1)+TAU*RTPB(J,1)*CONY
    YPC(JD,1) = YPC(J,1)+TAU*RTPC(J,1)*CONY
*

    YSB(JD,1) = YSB(J,1)+TAU*RTSB(J,1)
    YSC(JD,1) = YSC(J,1)+TAU*RTSC(J,1)
    YSD(JD,1) = YSD(J,1)+TAU*RTSD(J,1)
    YSE(JD,1) = YSE(J,1)+TAU*RTSE(J,1)
*

    ENDIF
*
*_____
* IMPLEMENT IMPLICIT PORTION OF THE GEARS BACKWARD DIFFERENCE
METHOD
* FROM THE PREVIOUS FUNCTION VALUES.  FOR THE FIRST THREE STEPS
* USE EULERS FIRST ORDER METHOD
*_____
    IF (K.LE.3) THEN
*

    XPB(J,K+1) = XPB(J,K)-(XI*FCR*RTPB(J,K))
    XPC(J,K+1) = XPC(J,K)-(XI*FCR*RTPC(J,K))
*

    XSB(J,K+1) = XSB(J,K)-(XI*FAR*RTSB(J,K))
    XSC(J,K+1) = XSC(J,K)-(XI*FAR*RTSC(J,K))+DD
    XSD(J,K+1) = XSD(J,K)-(XI*FAR*RTSD(J,K))
    XSE(J,K+1) = XSE(J,K)-(XI*FAR*RTSE(J,K))
*
```

118

```
      ELSE
*

         COEPB=3.*XPB(J,K-3)/25. -16.*XPB(J,K-2)/25. +
     1   36.*XPB(J,K-1)/25. -48.*XPB(J,K)/25.
         XPB(J,K+1) =-XI*12.*FCR*RTPB(J,K)/25.-COEPB
*

         COEPC=3.*XPC(J,K-3)/25. -16.*XPC(J,K-2)/25. +
     1   36.*XPC(J,K-1)/25. -48.*XPC(J,K)/25.
         XPC(J,K+1) =-XI*12.*FCR*RTPC(J,K)/25.-COEPC
*

         COESB=3.*XSB(J,K-3)/25. -16.*XSB(J,K-2)/25. +
     1   36.*XSB(J,K-1)/25. -48.*XSB(J,K)/25.
         XSB(J,K+1) =-XI*12.*FAR*RTSB(J,K)/25.-COESB
*

         COESC=3.*XSC(J,K-3)/25. -16.*XSC(J,K-2)/25. +
     1   36.*XSC(J,K-1)/25. -48.*XSC(J,K)/25.
         XSC(J,K+1) =-XI*12.*FAR*RTSC(J,K)/25.-COESC+DD
*

         COESD=3.*XSD(J,K-3)/25. -16.*XSD(J,K-2)/25. +
     1   36.*XSD(J,K-1)/25. -48.*XSD(J,K)/25.
         XSD(J,K+1) =-XI*12.*FAR*RTSD(J,K)/25.-COESD
*

         COESE=3.*XSE(J,K-3)/25. -16.*XSE(J,K-2)/25. +
     1   36.*XSE(J,K-1)/25. -48.*XSE(J,K)/25.
         XSE(J,K+1) =-XI*12.*FAR*RTSE(J,K)/25.-COESE
*
*

      ENDIF
*
_____
* DETERMINE CONCENTRATIONS FOR THE  DISTANCE STEP AND
RECALCULATE
* BULK PHASE EQUILIBRIA
*
_____
*

      CPBO = XPB(J,K+1)*CF
      CPCO = XPC(J,K+1)*CF
*

      CSBO = XSB(J,K+1)*CF
      CSCO = XSC(J,K+1)*CF
      CSDO = XSD(J,K+1)*CF
      CSEO = XSE(J,K+1)*CF
*

      CTC = CAC+CSDO+CSEO
*

      CALL EQB(DISS,K1,K2,CPAO,CPBO,CPCO,CSAO,CSBO,CSCO,
```

119

```
      1 CSDO,CSEO,CTC,CAC)
*
*_____
* DETERMINE RATES AT CONSTANT XI FOR SOLUTIONS OF  THE TAU
* MATERIAL BALANCE
*
*_____

      IF((YPB(J,K+1)+YPC(J,K+1)).LT.0.999))THEN
*
      CALL MULT(YPB(J,K+1),YPC(J,K+1),PKAB,
     1 PKAC,XPB(J,K+1),XPC(J,K+1),DPA,
     1 DPB,DPC,QC,ZPA,ZPB,ZPC,ZSA,ZSB,ZSC,ZSD,ZSE,
     1 CPAO,CPBO,CPCO,
     1 CSAO,CSBO,CSCO,CSDO,CSEO,CF,RPB,RPC,DRP)
*
        SCP = (CP/100.)/DEN/DRP
        AKP = F2(REP,SCP)
*
        ELSE
*
        RPB=0.0
        RPC=0.0
*
        ENDIF
*
      IF((YSB(J,K+1)+YSC(J,K+1)+YSD(J,K+1)+YSE(J,K+1)).LT.0.999)THEN
*
      CALL MULT1(YSB(J,K+1),YSC(J,K+1),YSD(J,K+1),YSE(J,K+1),SKAB,
     1 SKAC,SKAD,SKAE,XSB(J,K+1),XSC(J,K+1),XSD(J,K+1),XSE(J,K+1),DSA,
     1 DSB,DSC,DSD,DSE,QA,ZSA,ZSB,ZSC,ZSD,ZSE,ZPA,ZPB,ZPC,
     1 CSAO,CSBO,CSCO,CSDO,CSEO,
     1 CPAO,CPBO,CPCO,CF,RSB,RSC,RSD,RSE,DRS)
*
        SCS = (CP/100.)/DEN/DRS
        AKS = F2(RES,SCS)
*
        ELSE
*
        RSB=0.0
        RSC=0.0
        RSD=0.0
        RSE=0.0
*
        ENDIF
*
      RTPB(J,K+1) = (RPB*AKP*CONP)
```

120

```
      RTPC(J,K+1) = RPC*AKP*CONP
*

      RTSB(J,K+1) = RSB*AKS*CONS
      RTSC(J,K+1) = RSC*AKS*CONS
      RTSD(J,K+1) = RSD*AKS*CONS
      RTSE(J,K+1) = RSE*AKS*CONS
*

*  _____
* INTEGRATE Y USING ADAMS BASHFORTH (CALCULATE NEXT PARTICLE
LOADING)
*  _____
*

      YPB(JD, K+1) = YPB(J,K+1)+TAU*RTPB(J,K+1)*CONY
      YPC(JD,K+1) = YPC(J,K+1)+TAU*RTPC(J,K+1)*CONY
*

      YSB(JD,K+1) = YSB(J,K+1)+TAU*RTSB(J,K+1)
      YSC(JD,K+1) = YSC(J,K+1)+TAU*RTSC(J,K+1)
      YSD(JD,K+1) = YSD(J,K+1)+TAU*RTSD(J,K+1)
      YSE(JD,K+1) = YSE(J,K+1)+TAU*RTSE(J,K+1)
*

400 CONTINUE
*  _____
*  PRINT BREAKTHROUGH CURVES
*  _____
      IF (KPBK.NE.1) GO TO 450
         PPB = CPBO/1.E-6*MPB
         PPC = CPCO/1.E-6*MPC
*

         PSB = CSBO/1.E-6*MSB
         PSC = CSCO/1.E-6*MSC
         PSD = CSDO/1.E-6*MSD
         PSE = CSEO/1.E-6*MSE
         TAUTIM = TAUTOT*PDA*QA/(KLSB*CF*60.)/1440.
            PH = 14.+LOG10(CSAO)
          IF (KPRINT.NE.100) GOTO 450
   77   WRITE(6,139) TAUTIM,PPB,PPC,PSB,PSC,PSD,PSE,PH
  139   FORMAT(F6.1,6(2X,E9.4),2X,F4.2)
*  _____
* STORE EVERY TENTH ITERATION TO THE PRINT FILE
*  _____
       KPRINT = 0
450  CONTINUE
      KPRINT = KPRINT+1
      JK = J
      IF (J.EQ.4) THEN
```

121

```
              J = 1
              ELSE
              J = J+1
              ENDIF
*   _____
*   END OF LOOP  RETURN TO BEGINNING AND STEP IN TIME
*   _____
        IF (JFLAG.EQ.1) STOP
        TAUTOT = TAUTOT + TAU
        GOTO 1
*   _____
*      PRINT OUT FORMATS
*   _____
    10 FORMAT (' MIXED BED SYSTEM PARAMETERS:')
    11 FORMAT (' ')
    12 FORMAT (' RESIN REGENERATION',2X,': YPB =',F5.3,
      1 ' YSC = ',F5.3)
    13 FORMAT (' RESIN PROPERTIES',4X,': PDC =',F6.4,5X,'VD =',F6.4)
    14 FORMAT (' RESIN CONSTANTS',5X,': QC =',F6.4,5X,'QA =',F6.4)
    15 FORMAT (' COLUMN PARAMETERS',3X,': CF =',E10.4,' FR =',E10.5,3X,
      1      'DIA =',F6.2,2X,'CHT =',F5.1)
    16 FORMAT (' IONIC CONSTANTS',5X,': DPB =',E10.4,'DSC =',E10.4,
      1      2X,'DH =',E10.4)
    17 FORMAT (' FLUID PROP.',8X,' : CP =',F7.5,4X,' DEN =',F6.3,
      1      4X,' TEMP =',F6.1)
    18 FORMAT (' ')
    19 FORMAT (' CALCULATED PARAMETERS :')
    20 FORMAT (' ')
    21 FORMAT (' INTEGRATION INCREMENTS   : TAU =',F7.5,5X,'XI =',F7.5,
      1      5X,'NT =',I6)
    22 FORMAT (' TRANSFER COEFFICIENTS    : REP=',E10.4,' KLPB =',E10.4)
    88 FORMAT (' ',25X,' KLPC = ',E10.4,2X, 'DPC=',E10.4)
    89 FORMAT (' ',25X,' KLSD = ',E10.4,2X, 'DSD=',E10.4)
    23 FORMAT (' SUPERFICIAL VELOCITY    : VS =',F7.3)
    24 FORMAT (' ')
    25 FORMAT (' BREAKTHROUGH CURVE RESULTS:')
    26 FORMAT (' ')
    27 FORMAT (1X,' TIME',3X,'CAT B',3X,'CAT C',3X,'ANI B',
      1      3X,'ANI C',3X,3X,'ANI D'
      1      ,3X,'ANI E',3X,'PH')
    29 FORMAT (' ',4(4X,E8.3),5X,F4.2)
    30 FORMAT (' ')
    31 FORMAT (' CONCENTRATION PROFILES AFTER ',F5.0,' MINUTES')
    32 FORMAT (' ')
    33 FORMAT (' ',5X,'Z',7X,'XNC',7X,'YNC',
```

122

```
  1      7X,'YCA')
 34 FORMAT (' ')
 35 FORMAT (' ',6(2X,E8.3))
 138  STOP
    END
*
SUBROUTINE EQB(DISS,K1,K2,CPA,CPB,CPC,CSA,CSB,CSC,
CSD,CSE,CTC,CAC)
*
*
* _____
*    EQUILIBRIUM SUBROUTINE TO CALCULATE CARBONIC SPECIES
*    CONCENTRATIONS
* _____
IMPLICIT REAL*8 (A-H,O-Z)
    REAL*8 K1,K2
    EPS=1.E-10
    V1=CPB+CPC-CSB-CSC
      H0=3.E-07
    X=1.+H0/K1+K2/H0
    F=V1+H0-(DISS/H0)-(CTC*(1.+K2/H0)/X)
    DF=1.+DISS/(H0**2.)+(CTC*K2/(X*H0*H0))+((1.+K2/H0)*(CTC/(X*X))
  1  *(1/K1-K2/(H0*H0)))
    H=H0-F/DF
    DO WHILE((ABS(H-H0)/H).GT.EPS)
    H0=H
    X=1.+H0/K1+K2/H0
    F=V1+H0-(DISS/H0)-(CTC*(1.+K2/H0)/X)
    DF=1.+DISS/(H0**2.)+(CTC*K2/(X*H0*H0))+((1.+K2/H0)*(CTC/(X*X))
  1  *(1/K1-K2/(H0*H0)))
    H=H0-F/DF
    END DO
    X=1.+H/K1+K2/H
    CSE = CTC/X
    CSD =  K2*CSE/H
    CAC=H*CSE/K1
    CSA=DISS/H
      CPA=H
    RETURN
      END
*
*
*
* _____
*    SUBROUTINE 'MULT' TO CALCULATE THE INTERFACIAL
*    CONCENTRATIONS AND IONIC FLUXES OF CATIONS
```

```fortran
*     _____
*
      SUBROUTINE MULT(YB,YC,TKAB,TKAC,XBO,XCO,
     1 DA,DB,DC,QC,ZA,ZB,ZC,ZCA,ZCB,ZCC,ZCD,ZCE,
     1 CAO,CBO,CCO,
     1  COA,COB,COC,COD,COE,CF,RB,RC,DR)
*
      IMPLICIT REAL*8(A-H, O-Z)
      REAL*8 NA,NB,NC,LAMB,LAMC
*
      IF(ZB.LT.1.0)THEN
      W = -1
      ELSE
      W = 1
      ENDIF
*
      YA = 1.-YB-YC
*
      CTO = CAO+CBO+CCO
      XBO = XBO*CF/CTO
      XCO = XCO*CF/CTO
      XAO=1.-XBO-XCO
*
      COA=COA/ABS(ZCA)
      COB=COB/ABS(ZCB)
      COC=COC/ABS(ZCC)
      COD=COD/ABS(ZCD)
      COE=COE/ABS(ZCE)
*
      ZY=(ZCA*ZCA*COA+ZCB*ZCB*COB+ZCC*ZCC*COC+ZCD*ZCD*COD
     1 +ZCE*ZCE*COE)/(ZCA*COA+ZCB*COB+ZCC*COC+ZCD*COD+ZCE*COE)
*
      NA = -ZA/ZY
      NB = -ZB/ZY
      NC = -ZC/ZY
*
      CTI = CTO
* CALCULATION OF THE INTERFACIAL CONCENTRATIONS
10    CONTINUE
      LAMB = YB*TKAB**(-1./ABS(ZA))*YA**(-ZB/ZA)*(QC/CTI)**(1.-ZB/ZA)
      LAMC = YC*TKAC**(-1./ABS(ZA))*YA**(-ZC/ZA)*(QC/CTI)**(1.-ZC/ZA)
*
*     NEWTON-RAPHSON SOLVER
      EPS = 1E-10
      XA = 0.1
```

124

```fortran
      F = XA+(LAMB*XA**(ZB/ZA))+(LAMC*XA**(ZC/ZA))-1.
      DF=1.+((ZB/ZA)*LAMB*XA**(ZB/ZA-1.))+((ZC/ZA)*LAMC*XA**(ZC/ZA-1.))
*
      XAI = XA-F/DF
      DO WHILE ((ABS(XAI-XA)/XAI).GT.EPS)
            XA = XAI
      F = XA+(LAMB*XA**(ZB/ZA))+(LAMC*XA**(ZC/ZA))-1.
      DF=1.+((ZB/ZA)*LAMB*XA**(ZB/ZA-1.))+((ZC/ZA)*LAMC*XA**(ZC/ZA-1.))
*
*

            XAI = XA-F/DF
      END DO
*

      XBI = LAMB*(XAI**(ZB/ZA))
      XCI = LAMC*(XAI**(ZC/ZA))
*
*
*   CALCULATION OF TOTAL INTERFACIAL CONCENTRATION CTI
*
      P1 = ABS(NA*DA*(XAI-XAO)) + ABS(NB*DB*(XBI-XBO)) +
    1 ABS(NC*DC*(XCI-XCO))
      P2 = ABS(DA*(XAI-XAO))+ABS(DB*(XBI-XBO))+ABS(DC*(XCI-XCO))
*

            P = P1/P2
*

      TN = (1.+NB)*DB*XBO + (1.+NC)*DC*XCO + (1.+NA)*DA*XAO
*

      TD = (1.+NB)*DB*XBI + (1.+NC)*DC*XCI + (1.+NA)*DA*XAI
*

      CTIN = (TN/TD)**(1./(P+1.))*CTO
*

            IF((ABS(CTIN-CTI)/CTIN).GT.EPS)THEN
            CTI=CTIN
            GO TO 10
*

            ELSE
*

            CTI = CTIN
            ENDIF
*

*   CALCULATION OF IONIC FLUXES
*
      BA = W*(XAI-XAO)/(CTI**(-P-1.)-CTO**(-P-1.))
      BB = W*(XBI-XBO)/(CTI**(-P-1.)-CTO**(-P-1.))
      BC = -(BA+BB)
*
```

125

```
        CAO=W*CAO/ZA
        CBO=W*CBO/ZB
        CCO=W*CCO/ZC
*
        AAA=(ZA*CAO-BA*CTO**(-P))/CTO
        AAB = (ZB*CBO-BB*CTO**(-P))/CTO
        AAC = W-(AAA+AAB)
*
        CAI = W*XAI*CTI/ZA
        CBI = W*XBI*CTI/ZB
        CCI = W*XCI*CTI/ZC
*
        RA1 = DA*((1.-NA/P)*(CAI-CAO)+NA*(AAA/ZA)*(1.+1./P)*(CTI-CTO))
        RB1 = DB*((1.-NB/P)*(CBI-CBO)+NB*(AAB/ZB)*(1.+1./P)*(CTI-CTO))
        RC1 = DC*((1.-NC/P)*(CCI-CCO)+NC*(AAC/ZC)*(1.+1./P)*(CTI-CTO))
*
*  CALCULATION OF EFFECTIVE DIFFUSIVITY
*
        SIGR = ABS(RA1)+ABS(RB1)+ABS(RC1)
        SIGD = ABS(CAI-CAO)+ABS(CBI-CBO)+ABS(CCI-CCO)
*
        DR = (SIGR/SIGD)
        RB = W*(ZB)*(RB1/DR)
        RC = W*(ZC)*(RC1/DR)
*
        CAO=W*ZA*CAO
        CBO=W*ZB*CBO
        CCO=W*ZC*CCO
*
        COA=ABS(ZCA)*COA
        COB=ABS(ZCB)*COB
        COC=ABS(ZCC)*COC
        COD=ABS(ZCD)*COD
        COE=ABS(ZCE)*COE
*
        XBO=XBO*CTO/CF
        XCO=XCO*CTO/CF
*
        RETURN
        END
*
*
*_____
*       SUBROUTINE 'MULT1' TO CALCULATE THE INTERFACIAL
*       CONCENTRATIONS AND IONIC FLUXES OF THE ANIONS
*_____
```

```
*
      SUBROUTINE MULT1(YB,YC,YD,YE,TKAB,TKAC,TKAD,TKAE,XBO,XCO,
    1 XDO,XEO,DA,DB,DC,DD,DE,QC,ZA,ZB,ZC,ZD,ZE,ZCA,ZCB,ZCC,
    1 CAO,CBO,CCO,CDO,CEO,
    1  COA,COB,COC,CF,RB,RC,RD,RE,DR)
*

      IMPLICIT REAL*8(A-H, O-Z)
      REAL*8 NA,NB,NC,ND,NE,LAMB,LAMC,LAMD,LAME
*

      IF(ZB.LT.1.0)THEN
      W = -1
      ELSE
*

      W = 1
      ENDIF
*

      YA = 1.-YB-YC-YD-YE
*

      CTO = CAO+CBO+CCO+CDO+CEO
      XBO = XBO*CF/CTO
      XCO = XCO*CF/CTO
      XDO = XDO*CF/CTO
      XEO = XEO*CF/CTO
      XAO=1.-XBO-XCO-XDO-XEO
*

      COA=COA/ABS(ZCA)
      COB=COB/ABS(ZCB)
      COC=COC/ABS(ZCC)
*

      ZY=(ZCA*ZCA*COA+ZCB*ZCB*COB+ZCC*ZCC*COC
    1 )/(ZCA*COA+ZCB*COB+ZCC*COC)
*

      NA = -ZA/ZY
      NB = -ZB/ZY
      NC = -ZC/ZY
      ND = -ZD/ZY
      NE = -ZE/ZY
*

      CTI = CTO
* CALCULATION OF THE INTERFACIAL CONCENTRASTIONS
 10   CONTINUE
      LAMB = YB*TKAB**(-1./ABS(ZA))*YA**(-ZB/ZA)*(QC/CTI)**(1.-ZB/ZA)
      LAMC = YC*TKAC**(-1./ABS(ZA))*YA**(-ZC/ZA)*(QC/CTI)**(1.-ZC/ZA)
      LAMD = YD*TKAD**(-1./ABS(ZA))*YA**(-ZD/ZA)*(QC/CTI)**(1.-ZD/ZA)
      LAME = YE*TKAE**(-1./ABS(ZA))*YA**(-ZE/ZA)*(QC/CTI)**(1.-ZE/ZA)
```

127

```
*
*      NEWTON-RAPHSON SOLVER
       EPS = 1E-10
       XA = 0.01
       F =
XA+(LAMB*XA**(ZB/ZA))+(LAMC*XA**(ZC/ZA))+(LAMD*XA**(ZD/ZA))
   1    +(LAME*XA**(ZE/ZA))-1.
   DF=1.+((ZB/ZA)*LAMB*XA**(ZB/ZA-1.))+((ZC/ZA)*LAMC*XA**(ZC/ZA-1.))
   1   +((ZD/ZA)*LAMD*XA**(ZD/ZA-1.))+((ZE/ZA)*LAME*XA**(ZE/ZA-1.))
*
       XAI = XA-F/DF
       DO WHILE ((ABS(XAI-XA)/XAI).GT.EPS)
           XA = XAI
       F =
XA+(LAMB*XA**(ZB/ZA))+(LAMC*XA**(ZC/ZA))+(LAMD*XA**(ZD/ZA))
   1    +(LAME*XA**(ZE/ZA))-1.
   DF=1.+((ZB/ZA)*LAMB*XA**(ZB/ZA-1.))+((ZC/ZA)*LAMC*XA**(ZC/ZA-1.))
   1   +((ZD/ZA)*LAMD*XA**(ZD/ZA-1.))+((ZE/ZA)*LAME*XA**(ZE/ZA-1.))
*
           XAI = XA-F/DF
       END DO
       XBI = LAMB*(XAI**(ZB/ZA))
       XCI = LAMC*(XAI**(ZC/ZA))
       XDI = LAMD*(XAI**(ZD/ZA))
       XEI = LAME*(XAI**(ZE/ZA))
*
*      CALCULATION OF TOTAL INTERFACIAL CONCENTRATION CTI
*
       P1 = ABS(NA*DA*(XAI-XAO)) + ABS(NB*DB*(XBI-XBO)) +
   1ABS(NC*DC*(XCI-XCO)) +ABS(ND*DD*(XDI-XDO))+ABS(NE*DE*(XEI-
XEO))
       P2 = ABS(DA*(XAI-XAO))+ABS(DB*(XBI-XBO))+ABS(DC*(XCI-XCO))+
   1 ABS(DD*(XDI-XDO))+ABS(DE*(XEI-XEO))
*
           P = P1/P2
TN = (1.+NB)*DB*XBO + (1.+NC)*DC*XCO + (1.+ND)*DD*XDO
   1     +(1.+NE)*DE*XEO + (1.+NA)*DA*XAO
*
       TD = (1.+NB)*DB*XBI + (1.+NC)*DC*XCI + (1.+ND)*DD*XDI
   1     +(1.+NE)*DE*XEI + (1.+NA)*DA*XAI
*
       CTIN = (TN/TD)**(1./(P+1.))*CTO
*
           IF((ABS(CTIN-CTI)/CTIN).GT.EPS)THEN
           CTI=CTIN
```

```
                 GO TO 10
*
                 ELSE
                 CTI = CTIN
                 ENDIF
*
*      CALCULATION OF IONIC FLUXES
*
       BA = W*(XAI-XAO)/(CTI**(-P-1.)-CTO**(-P-1.))
       BB = W*(XBI-XBO)/(CTI**(-P-1.)-CTO**(-P-1.))
       BC = W*(XCI-XCO)/(CTI**(-P-1.)-CTO**(-P-1.))
       BD = W*(XDI-XDO)/(CTI**(-P-1.)-CTO**(-P-1.))
         BE=-(BA+BB+BC+BD)
       CAO=W*CAO/ZA
       CBO=W*CBO/ZB
       CCO=W*CCO/ZC
       CDO=W*CDO/ZD
       CEO=W*CEO/ZE
*
       AAA=(ZA*CAO-BA*CTO**(-P))/CTO
       AAB = (ZB*CBO-BB*CTO**(-P))/CTO
       AAC = (ZC*CCO-BC*CTO**(-P))/CTO
       AAD = (ZD*CDO-BD*CTO**(-P))/CTO
         AAE=W-(AAA+AAB+AAC+AAD)
*
         CAI = W*XAI*CTI/ZA
       CBI = W*XBI*CTI/ZB
       CCI = W*XCI*CTI/ZC
       CDI = W*XDI*CTI/ZD
       CEI = W*XEI*CTI/ZE
*
         RA1 = DA*((1.-NA/P)*(CAI-CAO)+NA*(AAA/ZA)*(1.+1./P)*(CTI-CTO))
       RB1 = DB*((1.-NB/P)*(CBI-CBO)+NB*(AAB/ZB)*(1.+1./P)*(CTI-CTO))
       RC1 = DC*((1.-NC/P)*(CCI-CCO)+NC*(AAC/ZC)*(1.+1./P)*(CTI-CTO))
       RD1 = DD*((1.-ND/P)*(CDI-CDO)+ND*(AAD/ZD)*(1.+1./P)*(CTI-CTO))
       RE1 = DE*((1.-NE/P)*(CEI-CEO)+NE*(AAE/ZE)*(1.+1./P)*(CTI-CTO))
* CALCULATION OF EFFECTIVE DIFFUSIVITY
       SIGR = ABS(RA1)+ABS(RB1)+ABS(RC1)+ABS(RD1)+ABS(RE1)
       SIGD = ABS(CAI-CAO)+ABS(CBI-CBO)+ABS(CCI-CCO)+ABS(CDI-CDO)
     1 +ABS(CEI-CEO)
       DR = ABS(SIGR/SIGD)
*
         RB = W*(ZB)*(RB1/DR)
       RC = W*(ZC)*(RC1/DR)
       RD = W*(ZD)*(RD1/DR)
```

129

```
      RE = W*(ZE)*(RE1/DR)
*

      CAO=W*ZA*CAO
      CBO=W*ZB*CBO
      CCO=W*ZC*CCO
      CDO=W*ZD*CDO
      CEO=W*ZE*CEO
*

      COA=ABS(ZCA)*COA
      COB=ABS(ZCB)*COB
      COC=ABS(ZCC)*COC
*

      XBO=XBO*CTO/CF
      XCO=XCO*CTO/CF
      XDO=XDO*CTO/CF
      XEO=XEO*CTO/CF
*

      RETURN
      END
```

2

VITA

Ramesh Bulusu

Candidate for the Degree of

Master of Science

Thesis: DEVELOPMENT OF A COLUMN MODEL TO PREDICT
             MULTICOMPONENT MIXED BED ION EXCHANGE
             BREAKTHROUGH

Major Field: Chemical Engineering

Biographical:

   Personal Data: Born in Vyagreswaram, AP, India, September 15, 1971, the son
   of Sita and Sarma Bulusu.

   Educational: Graduated from Bharatiya Vidya Bhavan Public School,
          Hyderabad, AP, India, in May 1988; received Bachelor of Technology
          Degree in Chemical Engineering from Andhra University in May 1992;
          completed requirements for the Master of Science degree with a major in
          Chemical Engineering at Oklahoma State University in December 1994.

   Experience: Employed as a teaching assistant, School of Chemical
          Engineering, Oklahoma State University, January 1993 to May 1993.
          Employed as a research assistant, School of Chemical
          Engineering, Oklahoma State University, June 1993 to December 1994.

   Professional Memberships: Phi kappa Phi, AIChE